RHENIUM(I) COMPLEXES AND CANCER: SYNTHESIS AND CHARACTERISATION OF MONO- AND BI-METALLIC COMPLEXES

by

URSULA OOSTHUIZEN

A dissertation submitted to meet the requirements for the degree of

MAGISTER SCIENTIAE

In the

DEPARTMENT OF CHEMISTRY

FACULTY OF NATURAL AND AGRICULTURAL SCIENCES

at the

UNIVERSITY OF THE FREE STATE

Supervisor: Prof. Hendrik G. Visser

Co-Supervisor: Dr. Marietjie Schutte-Smith

April 2019

I would like to thank my Heavenly Father for giving me the strength and courage to complete this work. I am living proof that all things are possible through Him. I am truly blessed.

I would like to thank my supervisor, Prof Deon Visser for the time, continuous assistance and patience and the encouragement through tough times. Dr Marietjie Smith, thank you for the guidance and support. It is an honour to your student. I appreciate both of you a lot. Thank you.

I would like to express my gratitude to Lucy Kapp, my lab partner, for all your support, talks and friendship. I would like to thank my colleagues of the Analytical - and Inorganic Group. Dumisane Kama (Tom), Teboho Alexander (Orbett), Penny Mokolokolo and Francios Jacobs, the crystallographers for their time and help with the crystallographic part of my dissertation. Thank you to Dr Gilles Gasser and his group for the cytotoxicity testing of my samples.

To all of my friends and family THANK YOU for the support and prayers. Mom and Dad, thank you for the support and the opportunity. To my sister, Amoreen and Johan, thank you for your support, love and being there for me. I wouldn't be able to make a success of this work without the support of my family. I am grateful to have all of you part of my life. I love you all.

There are no secret to success. It is the result of preparation, hard work and learning from failure.

~ Colin Powell ~

TABLE OF CONTENT

Table of content

ABBREVIATION

DNA	Deoxyribonucleic acid
MLCT	Metal-to-ligand charge transfer
DSSC	Dye-sensitized solar cells
bpy	2,2'-Bipyridine
phen	1,10-Phenanthroline
dpq	Pyrazinophenanthroline
dppz	Dipyridophenazine
Phenhat	(1,10-Phenathroline [5,6-b] 1,4,5,8,9,12-hexaazatriphenylene)
Phendione/phenO_2	1,10-Phenanthroline-5,6-dione
TNBC	Triple negative breast cancer
damp	2-[(Dimethylamino) methyl] phenyl
PDT	Photodynamic therapy
PACT	Photoactivated chemotherapy
PS	Photosensitizer
OLED	Organic light-emitting diodes
EL	Electroluminescence
°	Degree
α	Alpha
π	Pi
λ	Wavelength
ε	Molar absorptivity coefficient
δ	Gamma
°C	Degree Celsius

ν_{CO}	C=O stretching frequency
fac	Facial
N,N′	Bidentate ligand with N,N′ donor atoms
O,O′	Bidentate ligand with O,O′ donor atoms
$[NEt_4]^+$	Tetraethyl ammonium cation
NMR	Nuclear Magnetic Resonance Spectroscopy
IR	Infrared Spectroscopy
PPh_3	Triphenylphosphine
PTA	1,3,5-Triaza-7-phosphaadamantane
DAPTA	3,7-Diacetyl-1,3,7-triaza-5-phosphabicyclo[3.3.1]nonane
UV/Vis	Ultraviolet/Visible Spectroscopy
$Phen(NH_2)_2$	1,10-Phenanthroline-5,6-diamine
ReAA	*fac*-$[NEt_4]_2[Re(CO)_3(Br)_3]$
XRD	X-ray Diffraction
CH_3OH	Methanol
DMSO	Dimethyl sulfoxide
DCM	Dichloromethane
ppm	(Unit of chemical shift) parts per million
M	$mol \cdot dm^{-3}$
CO	Carbonyl
TNBC	Triple negative breast cancer
MRI	Magnetic resonance imaging
GCC	Graphite conjugated catalysts
PLQY	Photoluminescence quantum yield

ABSTRACT

Organometallic compounds such as Re(I) complexes showed to be toxic to a few cancer cell lines, but lack the property of being selective towards cancer cells for the use as novel chemotherapeutic agents. Toxicity tests are preliminary tests performed on different cell lines such as HeLa, HepG2 or PT45 to determine whether the compounds could be used as potential PDT (photodynamic therapy) agents. PDT is the administration of non-toxic drugs or dyes also known as photosensitizers (PS) to patients.

The main aim of this studies were to synthesize two *N,N′*-bidentate ligands, 1,10-phenanthroline-5,6-dione (**phenO_2**) and 1,10-phenanthroline-5,5-diamine (**phen$(NH_2)_2$**) and this was done successfully with a yield of 52 % and 48 % respectively, as reported in Chapter 3. Re(I) tri- and dicarbonyl complexes with different monodentate ligands: PPh_3, PTA and DAPTA were synthesized for the evaluation of their luminescent properties and are reported in Chapter 5. PhenO_2 and phen$(NH_2)_2$ are used as bridging ligands for the formation of two dinuclear complexes, $[NEt_4][Re_2(CO)_6(phen(NH)_2)Br_2]$ and $[Re_2(CO)_6(phenO_2)Br_2]$. The *N,N′*-bidentate ligand, 1,10-phenanthroline, were coordinated to the Ru(III) metal centre which formed the precursor that was used for the synthesis of new bimetallic complexes with a combination of Pt(II) and Re(I) metals. All the compounds were successfully synthesized and characterised by NMR, IR, UV/Vis and elemental analysis as reported in Chapter 3.

The crystal structures of *fac*-$[Re(CO)_3(phen)(H_2O)][NO_3]\cdot 1.5H_2O$ (**3**), *fac*-$[Re(CO)_3(phen)(Br)]$ (**4**) and 5-amino-6-nitro-1,10-phenanthroline (**phen$(NH_2)(NO_2)$**) are collected and reported in Chapter 4. **3** and **4** crystallized in the $P\bar{1}$ space group while **phen$(NH_2)(NO_2)$** crystallized in the *Pbca* space group. The Re-CO bond distances of **3** are within the range of 1.864(15) Å to 1.914(13) Å and **4** within the range of 1.902(9) Å to 1.934(7) Å. The Re-N bond distances for **3** is 2.178(8) Å and 2.180(8) Å and for **4** the Re-N distances is 2.183(6) Å. The bite angle of **3** is 76.5(3) ° and the bite angle of **4** is 75.8(2) °. The N-H bond distances of **phen$(NH_2)(NO_2)$** are 0.89(3) Å and 0.93(4) Å, while the N-O bond distances are greater than the N-H distances with bond distances reported as 1.244(3) Å and 1.241(3) Å. The angles between the O-N-O and H- N-H substituents are 120.0 °.

Luminescent studies was performed on the Re(I) tri- and dicarbonyl complexes for the evaluation of their luminescent properties. The Re(I) tricarbonyl complexes with monodentate phosphine ligands, *fac*-$[Re(CO)_3(phen)(PPh_3)][NO_3]$, *fac*-$[Re(CO)_3(phen)(PTA)][NO_3]$ and

Abstract

fac-[Re(CO)$_3$(phen)(DAPTA)][NO$_3$], showed to absorb electrons from a wavelength of 265 nm to 266 nm. Their molar absorptivity coefficient ranges from 11490 to 31185 M^{-1} cm^{-1} while their emission wavelengths is at 610 nm. The Re(I) dicarbonyl complexes with bis-phosphine ligands, *cis*-*trans*-[Re(CO)$_2$(phen)(PPh$_3$)$_2$][NO$_3$], *cis*-*trans*-[Re(CO)$_2$(phen)(PTA)$_2$][NO$_3$] and *cis*-*trans*-[Re(CO)$_2$(phen)(DAPTA)$_2$][NO$_3$] showed luminescent properties at excitation wavelengths of 616 nm, 610 nm and 610 nm respectively. *cis*-*trans*-[Re(CO)$_2$(phen)(PTA)$_2$][NO$_3$] has the largest molar absorptivity coefficient (14465 M^{-1} cm^{-1}) of the three dicarbonyl complexes. *cis*-[Re(CO)$_2$(phen)(PPh$_3$)(Cl)], *cis*-[Re(CO)$_2$(phen)(PTA)(Cl)] and *cis*-[Re(CO)$_2$(phen)(DAPTA)(Cl)], the three dicarbonyl complexes with a monodentate phosphine ligands, have smaller molar absorptivity coefficients than all of the Re(I) compounds. These compounds also have greater emission wavelengths ranging from 620 nm to 630 nm.

Three novel bimetallic complexes, [Ru(phen)$_2$(*N,N′*-phenO$_2$-*O,O′*)-Re(CO)$_3$Br][PF$_6$]$_3$, [Ru(phen)$_2$(*N,N′*-phenO$_2$-*O,O′*)-PtCl$_2$][PF$_6$]$_3$ and [Re(CO)$_3$(*N,N′*-phenO$_2$-*O,O′*)-PtCl$_2$]Br with yields of 25 %, 96 % and 98 % respectively, were synthesized to evaluate their cytotoxicity against HeLa and RPE-1 cell lines. [Re(CO)$_3$(*N,N′*-phenO$_2$-*O,O′*)-PtCl$_2$]Br is the only complex that showed cytotoxic effects against the HeLa cell line with an IC_{50} value of 7.31 ± 0.07 μM.

CHAPTER 1: BACKGROUND AND AIM

1.1. Introduction:

Cancer is a disease that millions of people get diagnosed with every year, worldwide.[1] Based on recent available statistics, 10 million new cases, 6 million deaths and more than 22 million people living with cancer were reported during 2000 internationally. Globally, lung cancer is the cause of most deaths (1.2 million) while the incidence of breast cancer (1.05 million), stomach (876 000) and liver (564 000) cancer are slightly less. An increase in the statistical number of new cancer cases diagnosed are the reason for the big thrust in the development of new radiopharmaceuticals and agents for the treatment of cancer.[1]

1.2. Re and Tc radiopharmaceuticals:

Radiopharmaceuticals are used for the diagnosis and treatment of a variety of disease types.[2] ^{99m}Tc is the most common nuclide used for diagnostic imaging. [*fac*-$Re(CO)_3(H_2O)_3]^+$, an aqueous organometallic cation is used as a model in chemistry for [*fac*-$^{99m}Tc(CO)_3(H_2O)_3]^+$. There is an interest in this cation because of the possibility to develop compounds which contain the [*fac*- $^{186/188}Re(CO)_3]^+$ core for radiotherapeutic purposes.[2] ^{99m}Tc has been widely used as a γ-emitter over the past few years for diagnostic imaging while ^{186}Re and ^{188}Re have been considered for medical use as β^--emitters. The ^{188}Re isotope can be used in pharmaceuticals for tumour radiation therapy because of the combination of energies and the half-lives.[2] These pharmaceuticals are used in patients ineligible for external beam radiation therapy or in patients with inoperable tumours.

1.3. The use of different metal complexes for cancer treatment:

Metal-based compounds are good potential anti-cancer drugs due to their chemical modification capability and effectiveness against the origins of cancer.[3] Ruthenium complexes are powerful inhibitors to the growth of cancer cells and is used as an alternative to platinum complexes for the evolution of some anti-cancer drugs.[3] Complexes containing a platinum metal like cisplatin, carboplatin and oxaliplatin have been used for the treatment of different types of cancers, such as ovarian and colon cancer.[3] Platinum complexes can inhibit cancer cell

[1] D. Maxwell Parkin, *The Lancet Oncology*, **2001**, 2(10), 533-543.

[2] B. R. Franklin, R. S. Herrick, C. J. Ziegler, A. Cetin, N. Barone and L. R. Condon, *Inorganic Chemistry*, **2008**, 47, 5902-5909.

[3] J. Iida, E. T. Bell-Lincella, M. L. Purazo, Y. Lu, J. Dorchak, R. Clancy, J. Slavik, M. L. Cutlet and C. D. Shriver¸ *Journal of Translational Medicine*, **2016**, 14(48), 1-10.

growth, causing interstrand and intrastrand crosslinking of the DNA, inhibiting DNA repair or replication. However, platinum based anticancer drugs have side effects such a nephrotoxicity, neurotoxicity and drug resistance, which limits the effectiveness of these complexes. [3]

1.4. Photodynamic therapy (PDT) used in cancer treatment:

Photodynamic therapy is a non-invasive therapeutic procedure for the destruction of malignant cells. [4,5] During the procedure of administrating a photosensitizing agent, it is irradiated at a specific wavelength.[4] PDT or PACT (photoactivated chemotherapy) allow the spatiotemporal control of the cytotoxic effects to be maximized during cancer cell death and minimizes the damage to healthy cells.[6] PDT agents have a high selectivity and requires three components which include a photosensitizer (PS), molecular oxygen and visible or near infrared (NIR) light.[5] The PS is taken up in targeted cells and is harmless in the absence of light.[4] PDT use dye sensitizers like chlorins, bacteriochlorins and phthalocyanines and absorb light in the visible region.[7] In 1990, photofrin was the first approved sensitizer used for treating cancer with photodynamic therapy. Photofrin has the disadvantage of patient photosensitivity and it has a weak long-wavelength absorption of 630 nm.[8] Therefore the development of more improved photosensitizers are a main focus currently. Photosensitizer agents are pure compounds and have a low manufacturing cost as well as good stability.[4] A high absorption between 600 nm and 800 nm are required from these agents to provide enough energy for the excitation of oxygen to its singlet state. The development of better and improved PDT agents, requires the potential use of transition-metal complexes.[6] Most studies for potential PDT agents are done on ruthenium(II) polypyridyl compounds and luminescent platinum(II) and gold(III) compounds that can act as photosensitizers.[9]

Rhenium complexes have excellent photophysical, as well as rich spectroscopic properties and can potentially be used in PDT or PACT. Several rhenium(I) tricarbonyl compounds have the

[4] P. Agostinis, K. Berg, K. A. Cengel, T. H. Foster, A. W. Girotti, S.O. Gollnick, S. M. Hahn, M. R. Hamblin, A. Juzeniene, D. Kessel, M. Korbelik, J. Moan, P. Mroz, D. Nowis, J. Piette, B. C. Wilson and J. Golab, *CA J Clin*, **2011**, 61(4), 250-281.

[5] L. Benov, *Medical Priciples and Practice*, **2015**, 24, 14-28.

[6] S. C. marker, S. N. MacMillan, W. R. Zipfel, Z. Li, P. C. Ford and J. J. Wilson, *Inorganic Chemistry*, **2018**, 57, 1311-1331.

[7] A. B. Ormond and H. S. Freeman, *Materials*, **2013**, 6, 817-840.

[8] L. B. Josefsen and R. W. Boyle, *Metal-Based Drugs*, **2008**, 1-24.

[9] H. Abrahamse and M. R. Hamblin, *Biochemical Journal*, **2016**, 473, 347-364.

ability to induce cell death *in vitro* through phototoxic effects and the associated production of singlet oxygen.[6]

1.5. Aim of this study:

For this study, the main aim is to synthesize rhenium(I) tri- and dicarbonyl complexes and to successfully characterize these compounds. Photoluminescent studies for the determination and comparison of their luminescent properties will be performed. Bimetallic and dinuclear compounds will be synthesized, characterized and sent for cell studies to evaluate their use as potential PDT agents.

Summary of the aims of this study:

- Synthesis and characterization of two bidentate ligands (*N,N′* and *O,O′*): 1,10-phenanthrolin-5,6-dione (**phenO_2**) and 1,10-phenanthrolin-5,6-diamine (**phen$(NH_2)_2$**).
- Synthesis and characterization of $[Ru(phen)_2Cl]Cl \cdot 2H_2O$ and $[Ru(phen)_2(phenO_2)][PF_6]_3$.
- Synthesis and characterization of Re(I) tri- and dicarbonyl complexes coordinated to 1,10-phenanthroline and different phosphines such as PTA (1,3,5-triaza-7-phosphaadamantane), PPh_3 (triphenylphosphine) and DAPTA (3,7-diacetyl-1,3,5-triaza-5-phosphabicyclo[3.3.1]nonane.
- Synthesis and characterization of three novel bimetallic complexes with the combination of different metal centres: $[Ru(phen)_2(N,N'\text{-}phenO_2\text{-}O,O')\text{-}Re(CO)_3Br][PF_6]_3$, $[Ru(phen)_2(N,N'\text{-}phenO_2\text{-}O,O')\text{-}PtCl_2][PF_6]_3$ and $[Re(CO)_3(N,N'\text{-}phenO_2\text{-}O,O')\text{-}PtCl_2]Br$.
- Evaluation of photoluminescence properties of eleven Re(I) tri- and dicarbonyl complexes with different phosphine ligands.
- Cytotoxicity tests on $[Ru(phen)_2(N,N'\text{-}phenO_2\text{-}O,O')\text{-}Re(CO)_3Br][PF_6]_3$, $[Ru(phen)_2(N,N'\text{-}phenO_2\text{-}O,O')\text{-}PtCl_2][PF_6]_3$ and $[Re(CO)_3(N,N'\text{-}phenO_2\text{-}O,O')\text{-}PtCl_2]Br$ as well as the dinuclear complex $[Re_2(CO)_6(phenO_2)Br_2]$ for the potential use as PDT agents.

CHAPTER 2: LITERATURE STUDY

2.1. Cancer:

Cancer is one of the top killers in the world and is caused by the uncontrolled division of non-functional cells.[1] Chemotherapy is the method mostly used for the treatment of metastasis for a variety of cancer types. The toxicity, other side-effects as well as the safety and efficacy are some of the main concerns. Breast cancer is a common cancer type and cause death worldwide. TNBC (triple negative breast cancer) is an aggressive breast cancer subtype, in which cells don't have any estrogen, progesterone and HER2 receptors.[2] These cells may display a resistance against multi-drugs and make the treatment of its metastasis difficult. According to Popolin *et al.* TNBC can be treated with a combination of therapies such a surgery, radiation and chemotherapy.[2]

Most of the anti-cancer drugs in use today are organic molecules.[3] Cisplatin, oxaliplatin and carboplatin are approved metal-based chemotherapeutic drugs[2] (Figure 2.1). These complexes are all square planar platinum(II) complexes with two ammine ligands in a *cis* position.[4] These drugs are very efficient but cause some side effects[4] such as decreased immunity to infections, kidney problems and hearing loss.

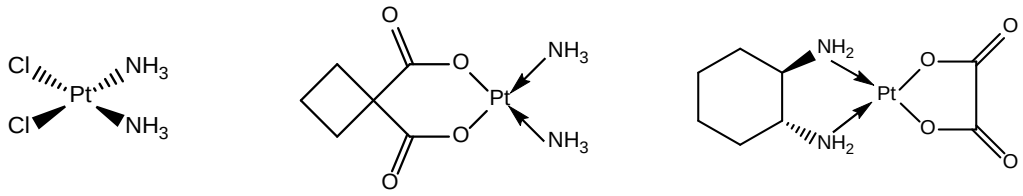

Figure 2.1: Structure of cisplatin, oxaliplatin and carboplatin.

Cisplatin's anticancer activity lies in the coordinative interaction with DNA. When cisplatin enters the cell, strong electrophiles are formed when the chlorido ligands are substituted with water and interact with the nucleophilic bases of the nucleic acids. Covalent bonds form with

[1] F. Hayat, Z. Rehman and M.H. Khan, *Journal of Coordination Chemistry*, **2017**, 702, 279-295.

[2] C. P. Popolin, J. P. B Reis, A. B. Becceneri, A. E. Graminha, M. A. P. Almeida, R. S. Corrêa, L. A. Colina-Vegas, J. Ellena, A. A. Batista and M. R Cominetti, *Public Library of Science*, **2017**, 1-21.

[3] L. Zeng, P. Gupta, Y. Chen, E. Wang, L. Ji, H. Chao and Z. Chen, *Chemical Society Reviews*, **2017**, 46, 5771-5804.

[4] B. W. J. Harper, E. Petruzella, R. Sirota, F. F. Faccioli, J. R. Aldrich-Wright, V. Gandin and D. Gibson, *Dalton Transactions*, **2017**, 47, 7005-7019.

monofunctional and bifunctional adducts, according to Deo *et al.*[5] These bonds induce a conformational change to the DNA and lead to apoptosis. Metallointercalators are typical anticancer metal complexes.[5] These intercalators facilitate electron deficient and planar aromatic rings with non-covalent interactions with DNA and is stabilized through π-π-stacking as well as dipole-dipole interactions. This result in the unwinding and extending of the DNA helix, for the metal complex to bind between the base pairs. For the above action, intercalation is needed and is defined as the insertion of a complex within two adjacent base pairs of the DNA.[5]

2.2. The development of new anticancer drugs:

Many efforts have been made for the development of new metal-based complexes which exhibit improved pharmacological properties and complexes that target cellular components other than DNA with different modes of action and a higher efficacy relative to cisplatin derivatives.[5] Novel non-classical platinum complexes that kill cancer cells and that are different from those of cisplatin will be of great use in future research according to Harper *et al.*[4] For the design of new anti-cancer drugs, DNA is an important target to stop replication. According to Hayat *et al.*, DNA-targeting drugs stop DNA- strands by seizing their replication and causing death of the cells.[1] Ru(III) polypyridyl complexes change the DNA binding behaviour. An example of this change in the DNA-binding behaviour exist in the presence of a methyl group in diamine ligands in a specific complex that will enhance the DNA-binding, compared to the unsubstituted ones. These substituents on the ligands cause a change in the stereo-configuration as well as the electron density which result in a change in the DNA-binding behaviour.[1]

Novel metal based compounds of titanium, copper, ruthenium, rhodium and tin have the potential of being used as chemotherapeutic agents and act differently as the platinum based drugs.[6] According to Devereux *et al.*, there are more active anti-cancer agents than cisplatin such as N,N′-donor ligands (1,10-phenanthroline and 1,10-phenanthroline-5,6-dione) and Cu(II), Mn(II) and Ag(I) carboxylate complexes.[6] These active complexes inhibit DNA synthesis in a concentration-dependant manner and does not involve intercalation. Ruthenium complexes are potential candidates to replace platinum based chemotherapy as stated by

[5] K. M Deo, B. J. Pages, D. L. Ang, C. P. Gordon and J. R. Aldrich-Wright, *International Journal of Molecular Sciences*, **2016**, 17, 1818.

[6] M. Devereux, D. O. Shea, A. Kellett, M. McCann, M. Walsh, D. Egan, C. Deegan, K. Kedziora, Q. Rosair and H. Műller-Bunz, *Journal of Inorganic Biochemistry*, **2007**, 101, 881-892.

Popolin *et al*. NAMI-A (imidazolium trans-[tetrachloro(dimethylsulfoxide)(1H-imidazole)ruthenium(III)) is an effective ruthenium complex for the imaging of lung cancer.[2] At this point, combination therapy are introduced using NAMI-A and hemcitabine and is in Phase I/II of clinical trials.[2] This therapy will be used for the treatment of larger cell lung carcinoma. Another Ru-based anticancer agent KP1019 also known as (trans-[tetrachlorobis(1H-indazole)-ruthenate(III)], as seen in Figure 2.2, is submitted for clinical trials.[2]

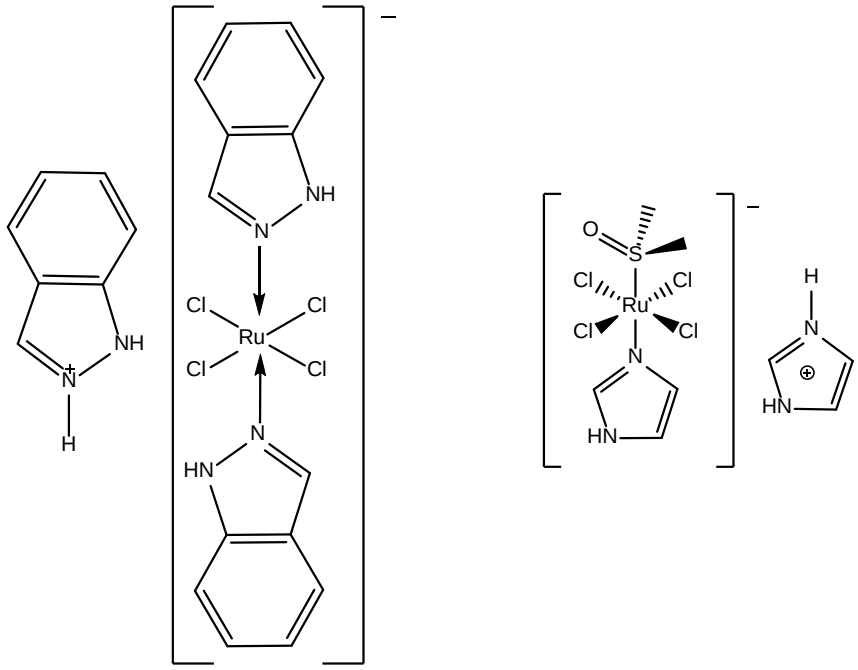

Figure 2.2: Schematic representation of KP1019 and NAMI-A Ru-based agent.

Genetic materials are transferred in cells within the patient by the means of gene therapy, another technique used for treating human diseases.[7] For the delivery of genetic material *in vivo* nanomaterials are used and can function as fluorescent tracking vectors.[7] These tracking nanomaterials can be labelled with organic dyes or metal complexes. Ru(II) polypyridyl metallodendrimer based vectors are used for tracking intracellular gene delivery.[7]

Gold complexes also show anticancer activity.[8] The mitochondria is the target site of gold complexes and not the DNA. Cytotoxicity against cancer cells has been shown for gold

[7] K. Qiu, B. Yu, H. Huang, P. Zhang, J. Huang, S. Zou, Y.Chen, L. Ji and H. Chao, *Scientific Reports*, **2015**, 1-11.

[8] S. Rafique, M. Idrees, A. Nasin, H. Akbar and A. Athar, *Biotechnology and Molecular Biology Reviews*, **2010**, 5(2), 38-45.

complexes coordinated to aromatic bipyridyl ligands.[8] It was proven that [$AuCl_2$(damp)] (damp = 2-[(dimethylamino)methyl] phenyl) gold(III) is an successful anti-tumour agent for humans (Figure 2.3). When gold nanoparticles is used for the combination of radiotherapy and chemotherapy, it enhances DNA damage and makes the treatment target specific.[8]

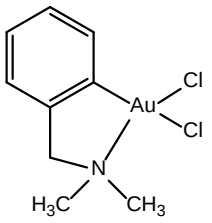

Figure 2.3: Schematic representation of [$AuCl_2$(damp)].

2.3. Bimetallic complexes:

Most dinuclear compounds are used as bimetallic catalysts and are required in industrial processes and for the understanding of surface catalysts.[9] The stability, selectivity and the catalytic properties are influenced when a second metal is added to a monometallic catalyst. Changes between the metals can cause electronic or geometric interactions.[9] Platinum is widely used in catalysis and more studies are being done on clusters containing platinum and transition metals like rhenium with a metal to metal bond.[9]

Only a few bimetallic complexes have been reported where rhenium(I) is coordinated to ruthenium(II).[10] Rhenium(I) carbonyl complexes are useful in showing the intense *ν*(CO) stretching frequencies and respond to the electronic distribution at the metal centre. As reported by Venlayudham *et al.,* the heterobimetallic Ru(II)/ Re(I) complexes are used as photo catalysts for CO_2 fixation.[10] Metal-based drugs have been used in medicine the past few years for the treatment of different diseases.[11] According to Fernandez-Moreira *et al.,* it has been proven that compounds containing more than one metallic fragment, will have an effect on the properties of the final complexes and the cytotoxic activities.[11] They overcome some cellular resistance when combining the different mechanistic properties of each metal fragment.

A bimetallic d^6-d^{10} probe has been designed, namely a Re(I)/ Au(I) complex, with the purpose of using the Re(I) fragment to supply the optical properties, Au(I) fragments for the therapeutic

[9] J. Xiao and R. J. Puddephatt, *Coordination Chemistry Reviews*, **1995**, 143, 457-500.

[10] M. Venlayudham and S. Rajagopal, *Inorganica Chimica Acta*, **2009**, 362, 5073-5079.

[11] V. Fernandez-Moieira and M. C. Gimeno, *Chemistry: A European Journal*, **2018**, 24, 3345-3353.

activities. By selecting different fragments, a suitable complex can be designed. The rhenium-tricarbonyl-bis-imine species were chosen for the emissive properties, while the gold phosphine species were chosen for the biological scaffold.[11] Ditopic ligands are used and carefully selected for connecting the bimetallic fragments.[11] Rhenium(I) diamine complexes can also be used as catalysts for CO_2 reduction and produce CO via a two-electron proton reduction coupled pathway.[12] These Re-diimine complexes have poor absorption in the visible light region. Bimetallic M-Re (where M is ruthenium or osmium), supramolecular compounds are formed for application in photocatalytic CO_2 reduction in the visible light region. The rhenium complex are attached via covalent bonds to the photosensitizers.[12] Some ruthenium(II) polyazine complexes are developed for anticancer agents and for the use in PDT due to their ability to absorb visible light.[19] According to Calderazzo *et al*., two complexes are obtained by reacting phendione with platinum(0) or palladium(II) precursors resulting in $[Pt(PPh_3)_2(C_{12}H_6N_2O_2\text{-}O,O')]$**(1)** and $[PdCl_2(C_{12}H_6N_2O_2\text{-}N,N')]$**(2)**.[13] Phendione showed interaction with the metal centres through the diiminic and/ or the quinonoid functionality. For the synthesis of bimetallic compounds, phendione could behave as a bridging ligand as mentioned in Paragraph 2.6. Calderazzo and coworkers, focused on synthesising organometallic compounds with the co-ordination of phendione with metals in group 4 and 5.[13]

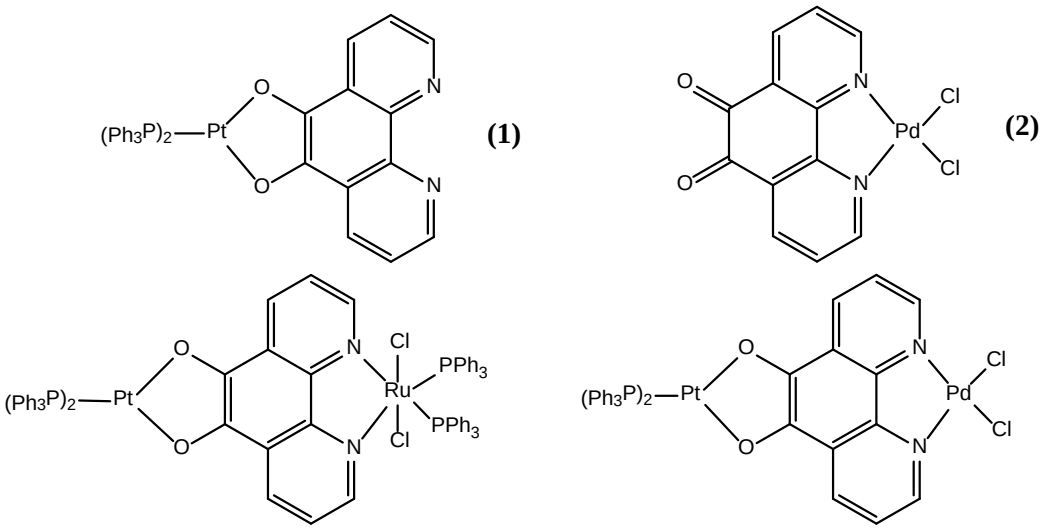

Figure 2.4: Representation of bimetallic complexes with phendione as the bridging ligand.

[12] X. Deng, J. Albero, L. Xu, H. Garcia and Z. Li, *Inorganic Chemistry*, **2018**, 57, 8276-8286.

[13] F. Calderazzo, F. Marchetti, G. Pampaloni and V. Passarelli, *Journal of the Chemical Society, Dalton Transactions,* **1999**, 4389-4396.

2.4. Photodynamic Therapy:

Photodynamic therapy (PDT) is a technique used in the medical industry for the treatment of diseases and different types of cancer. [14] These diseases include cancer, fungal infections, pathological myopia as well as dermatological diseases.[15] Chemotherapeutic agents are non-discriminating cytotoxic compounds and induce cell death obtained by the combination of photoactive compounds.[15] PDT (Photodynamic therapy) and PACT (Photoactivated chemotherapy) are two concepts for increasing the selectivity and minimizing the toxic side effects for drugs that are activated by light.[16] A nontoxic photosensitizer (PS) is administered to a patient during PDT. Molecular oxygen ($^3O_2$) are converted to more reactive oxygen species (ROS) by photosensitizers which is activated by light. For cancer diagnosis and treatment the application of metals are fixed and include examples such as Pt(II), which is used as a chemotherapeutic drug.

Anticancer therapeutic applications depends on the single therapeutic modality according to Quental and co-workers.[17] Over the past few years new and different strategies have been developed to minimize the disadvantages of the drugs. This involve the design of more selective and target-specific drugs or a combination of a few therapeutic aspects. These combinations can involve chemotherapy and photodynamic therapy.[17] Photodynamic therapy possesses a multi-process.[18] The first stage is the administration of the photosensitiser with a small amount of dark toxicity in the absence of light. When the correct amount of photosensitiser in the unhealthy *versus* the healthy tissue is reached, the photosensitisers are activated. For the activation of the PS, it is exposed to an adjusted dose of light and shone directly on the unhealthy tissue for a certain time. This ensures that the dose exposed to the

[14] C. Mari, V. Pierroz, R. Rubbiani, M. Patra, J. Hess, B. Spingler, L. Oehninger, J. Schur, I. Ott, L. Salassa, S. Ferrari and G. Gasser, *Chemistry: A European Journal*, **2014**, 20, 14421-14436.

[15] P. Ung, M. Clerc, H. Huang, K. Qui, M. Seitz, B. Boyd, B. Graham and G. Gasser, *Inorganic Chemistry*, **2017**, 56, 7960-7974.

[16] S.C. Marker, S. N. MacMillan, W. R. Zipfel, Z. Li, P. C. Ford and J. J. Wilson, *Inorganic Chemistry*, **2018**, 57, 1311-1331.

[17] L. Quental, P. Raposinho, F. Mendes, I. Santos, C. Navarro-Ranninger, A. Alvarez-Valdes, H. Huang, H. Chao, R. rubbiani, G. Gasser, A. G. Quiroga and A. Paulo, *Dalton Transactions*, **2017**, 46, 14523-14536.

[18] L. B. Josefsen and R. W. Boyle, *Metal Based Drugs*, **2008**, 1-24.

damage tissue is small enough to limit the damage to the neighbouring healthy tissue. The activated form of PS is a toxic response, released in the tissue causing cell death.[18]

Ruthenium-Platinum supramolecular complexes have been developed as PDT agents and for the improvement of the optical excitation in therapeutic section.[19] The ruthenium light absorbers of the bimetallic complexes, Ru-Pt, couple directly to the platinum site, and has an impact on the photophysical properties of the system. These Ru-Pt complexes can be a target for metal-based PDT agents to maintain the photo cleaving properties and the binding to the DNA.[19] These bimetallic complexes contains a positive charge which increase the solubility in water and improve the electrostatic interactions between the Ru-Pt systems.

A few polymetallic complexes were synthesized and tested. The results obtained showed that the polymetallic compounds are more cytotoxic than monometallic compounds as stated by Wenzel *et al.*[20] For the improvement of the activity of antitumor agents, two cytotoxic metals like gold(I) or platinum(II), are combined and can interact with multiple biological targets. Wenzel and co-workers synthesised a bimetallic compound with Au(I)-Pt(II) (Figure 2.5) to study their antiproliferative activities *in vitro* in human cancer cells. The results obtained showed that the gold(I)-platinum(II) complex has increased antiproliferative effects compared to monometallic gold(I) compounds.

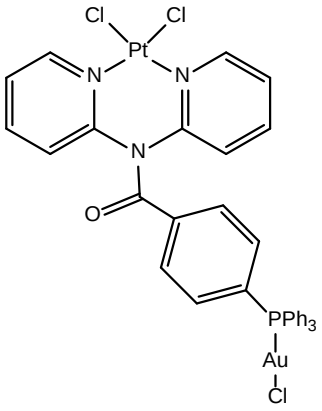

Figure 2.5: Illustration of the Au(I)-Pt(II) bimetallic complex.

[19] S. L. H. Higgins, T. A. White, B. S. J. Winkel and K. J. Brewer, *Inorganic Chemistry*, **2011**, 50, 463-470.

[20] M. Wenzel, E. Bigaeva, P. Richard, P. Le Gendre, M. Picquet, A. Casini and E. Bodio, *Journal of Inorganic Biochemistry*, **2014**, 141, 10-16.

Another study of two heterobimetallic compounds were prepared by Massai et al. and are more favourable for in vitro pharmacological uses towards cancer cells.[21] The individual use of both gold and ruthenium are either more selective or more cytotoxic. For the incorporation of the gold and a second metal may have an advantage for their potential of being anticancer derivatives.[21] Massai and co-workers combined with ruthenium(II)-p-cymene-phosphane and gold(I)-phosphane-chloride fragments to form novel chemotherapeutics. Ruthenium(II)-p-cymene-phosphane have the potential of being cytotoxic, while the gold(I)-phosphane-chloride compound have cytotoxic properties (Figure 2.6).[21]

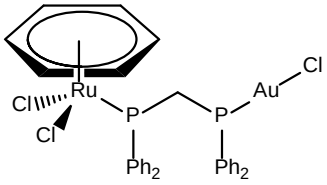

Figure 2.6: Schematic representation of [$RuCl_2$(p-cymene)(μ-dppm)AuCl].

2.5. Ruthenium(II) complexes:

Ru, Os, Re and Ir are a few examples of transition metals and when coordinated to polypyridyl ligands their photo physical and electrochemical properties are studied.[23] With these properties they are perfect candidates for the use as dyes as they can absorb light in the visible wavelength regions. They also have luminescent properties, are rich in redox chemistry and have long-lived metal-to-ligand charge transfer (MLCT) excited states and cause strong absorbance.[22,23] These properties are due to the high brightness and high efficiency emissions with a low-driving voltage, and make them appealing luminophores for luminescent devices.[24]

Ruthenium complexes are considered the best substitute for Pt-based complexes. Saturated Ru(II) polypyridyl complexes have anticancer activity, strong DNA binding and its photochemical and photophysical properties can be changed with advantageous applications in

[21] L. Massai, J. Fernández-Gallardo, A. Guerri, A. Arcangeli, S. Pillozzi, M. Contel and L. Messori, *Dalton Transactions*, **2015**, 44, 11067-11076.

[22] A. Delgadillo, P. Roma, A. M. Leiva and B. Loeb, *Helvetica Chimica Acta*, **2003**, 86, 2110-2121.

[23] S. P. Foxon, C. Green, M. G. Walker, A. Wragg, H. Adams, J. A. Weinstein, S. C. Parker, A. J. H. M. Meijer and J. A. Thomas, *Inorganic Chemistry*, **2012**, 51, 463-471.

[24] H. Shahroosvand, S. Rezaei, E. Mohajerani, M. Mahmoudi, M. A. Kamyabi and S. Nasiri, *The Royal Society of Chemistry*, 1-13.

biochemistry, physics and chemistry.[1] Ruthenium is one of the transition metals in group 8 and has two oxidation states, Ru(II) and Ru(III). Ru(IV) compounds can exist, but are unstable. The kinetic stability of Ru(III) complexes are much lower than Ru(II) complexes. Ru(III) complexes can be reduced to Ru(II) complexes as reported by Zeng *et al*.[3] According to Zeng *et al*. the design of any new drug candidate requires the following to ensure the effectiveness of the drug:

i) Constructing complexes with selective and specific targets;

ii) exploiting the potential targets as well as the mechanism;

iii) evaluation of the structure-activity relationship;

iv) exploiting prodrugs that can be activated by light and

v) exploiting the drug accumulation and activation at the tumour tissues with nano drug-delivery systems.

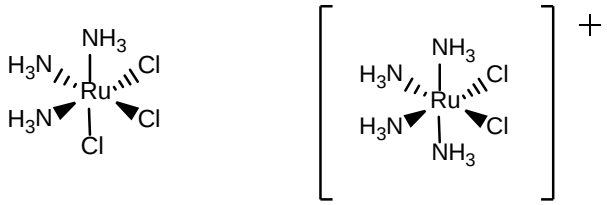

Figure 2.7: Schematic structures of Ru(III) complexes that exhibit anticancer activity.

For the design of new anticancer drugs, the interest in Ru(II) complexes has expanded and some have been tested against cancer cell lines.[3] According to Lazarević *et al.*[25] Ru(III) complexes such as *fac*-[$RuCl_3(NH_3)_3$] and *cis*-[$RuCl_2(NH_3)_4$]Cl (Figure 2.7) showed promising results towards anticancer activity. [25] Ruthenium(II) complexes with polypyridyl ligands contain photophysical, photochemical and electrochemical properties.[26]

[25] T. Lazarević, A. Rilak and Z. D. Burgarčić, *European Journal of Medicinal Chemistry*, 2017, 1-24.

[26] K.Snehadrinarayan, S. Debabrata, J.W. Bats and M. Schmittel, *Inorganic Chemistry*, **2012**, 51, 7075-7086.

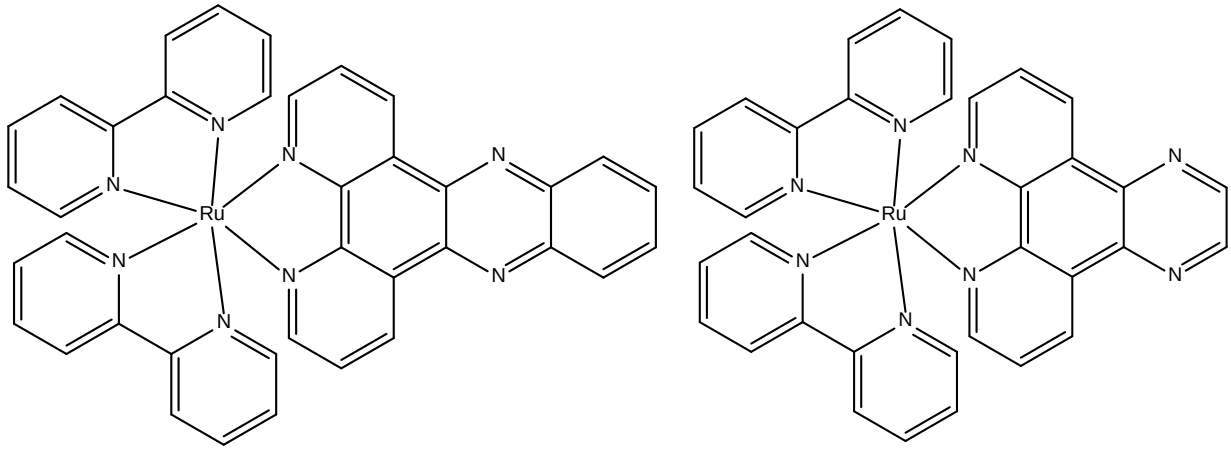

Figure 2.8: Schematic representation of Ru(II) polypyridyl complexes used as chemosensors.

Some phosphorescent Ru(II) polypyridine complexes can act as chemo sensors and has photo physical properties which include large Stokes shifts, visible excitation wavelengths and long excited state lifetimes.[27] These complexes can be easily prepared, because it is cationic in nature and have thermal and photochemical stability, which are good properties for potential photosensitizers.[28] Ruthenium polypyridine complexes are used in different fields such as fluorescent probes for biomolecules, light emitting diodes or photosynthetic centres. Ru(II) polypyridyl complexes with ligands such as 2, 2'-bipyridine (bpy) or 1,10-phenanthroline (phen) have properties that make these complexes attractive for the evolution of photoactive devices, dye-sensitized solar cells (DSSC), photo induced switches and luminescent sensors.[26]

Ruthenium di-nuclear complexes with N-heterocyclic bridging ligands revealed to be multi-electron acceptors and more or less 4 electrons can be gathered when 2 dppz (dipyridophenazine) of pyzphen (pyrazinophenanthroline) portions are combined back-to-back.[29] A number of studies have been done by changing the properties which include the redox and excited state of Ru(II) polypyridine complexes by altering the ligands.[30] This type of

[27] K. Snehadrinarayan, S. Debabrata, J. W. Bats and M. Schmittel, *Inorganic Chemistry*, **2001**, 211, 163-175.

[28] P. Parakh, S. Gokulakrishnan and H. Prakash, *Separation and Purification Technology*, **2013**, 109, 9-17.

[29] S. Ott, R. Faust, *Research Gate-Synthesis*, **2005**, 18, 3135-3139.

[30] A. A. Bhuiyan, S. Kudo, C. Wade and R.F. Davis, *Journal of the Arkansas Academy of Science*, **2009**, 63, 44-49.

modification can produce favourable redox- and excited state properties, but will create a problem when determining which ligand will be used in an advantageous manner.

Tris-chelate complexes are the most studied complexes and are useful in elucidating chemical principles, for developing photochemical reagents and in the design of novel chemotherapeutics.[31] The focus of Ru(II) complexes is on the ability of these complexes to selectively bind or interact with DNA.[32] To understand the nature of the interaction between the complex and the DNA, the investigation of the structure of these complexes is very important. Divalent ruthenium polypyridine complexes is used as efficient photo catalysts for solar-energy conversion. Ruthenium polypyridyl complexes were investigated for the use in artificial photosynthesis by Bhuiyan *et al.*[30] According to Bhuiyan *et al*., ruthenium polypyridyl complexes have the potential for the use as photo initiators in electron transfer studies.[53] Different ruthenium(II) complexes, homoleptic and heteroleptic were tested with different ligands to see how the properties are affected. Ru(II) polypyridine complexes are used in semiconductor oxide electrodes like TiO_2 electrodes to improve the light-to-electricity-conversion yield of the cell.[22]

2.6. Rhenium(I) complexes:

In Re(I) complexes ([*fac*-$Re(CO)_3$(N,N′)(X)]) a neutral bidentate diamine ligand regulates the opto-electric properties of the complexes, where X represents a halogen and N,N′, a bidentate diamine ligand (Figure 2.9). Some disadvantages of Re(I) compounds are low photoluminescence quantum yields, single emissive colours and an inferior electroluminescent efficiency. [33] These type of complexes are also helpful for photosensitizers to generate singlet oxygen ($^1O_2$) and for the use of photodynamic therapy (PDT) as reported by Lee and coworkers.[33] Rhenium(I) tricarbonyl complexes have carbon monoxide (CO) ligands and are advantageous of being photoactivatable for the release of the CO molecules and deliver the CO ligand to the target site, destroying cancer cells at the same time, if the cells are irradiated.[33]

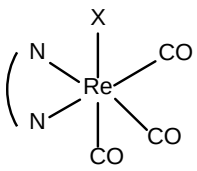

N,N′ = diamine bidentate ligand

X = Halogen

[31] I. Turel, A. Golobic, J. Kljun, P. Samastur, U. Batista and K. Specic, *Acta Chimica Slovenica*, **2015**, 62, 337-345.

[32] G. Yang and L. N. Ji, *Transition Metal Chemistry*, **1998**, 23, 273-276.

[33] L. C-C Lee, K-K Leung and K-W. Lo, *Dalton Transactions*, **2017**, 46, 16357-16380.

Figure 2.9: Schematic representation of the octahedral Re(I) tricarbonyl complexes with N,N′ diamine bidendate ligands.

The coordination chemistry of technetium-99m and rhenium is more or less the same and therefor the same ligands coordinated to Re(I), can be coordinated to ^{99m}Tc and result in $[^{99m}Tc(CO)_3]^+$ core with radio imaging and radiopharmaceutical reagents.[33] ^{99m}Tc and ^{186} Re/ ^{188} Re is subjects for radiolabelling with biological interest due to the short lived radionuclides.[34] ^{99m}Tc is a radionuclide used for imaging as diagnostic nuclear medicine because ^{99m}Tc is available from ^{99}Mo/^{99m}Tc generator with relative low cost.[35] The life-time of ^{99m}Tc is long enough for the necessary preparation of different radiopharmaceuticals and short enough to minimize the dose of radiation to the patient. Radiopharmaceuticals are drug containing radionuclide and is used for diagnosis and treatment of some disease.[35,36]

The electron configuration of Re(I) are a d^6 specie in the outer shell and have a low spin coordination sphere in the metal-ligand complexes which makes the metal ion kinetically inert for ligand substitution and result in a weaker metal-DNA interaction.[38] Recently Re(I) complexes showed to have active properties against suspended cancer cell lines such as breast cancer.**Error! Bookmark not defined.**,[37] Re(I) polypyridine complexes were designed for targeting biomolecules like DNA and proteins but is used as cellular probes with applications such as bio imaging and cytotoxicity. The ligand coordinated to the complex plays an important role as it control the way it will interact with the DNA. This interaction occurs via intercalation, external electrostatic binding or by groove binding.**Error! Bookmark not defined.**

[34] F. Minutolo and J. A. Katzenellenbogen, *Journal of American Chemistry Society*, **1998**, 120, 4514-4515.

[35] S. Jurisson, D. Berning, W. Jia and D. Ma, *Chemical Reviewes*, **1993**, 93, 1137-1156.

[36] M. Kaplanis, G. Stamatakis, V. D. Papakonstantinou, M. Paravatou-Petsotas, C. A. Demopoulos and C. A. Mitsopoulou, *Journal of Inorganic Biochemistry*, **2014**, 135, 1-9.

[37] P. Collery, A. Mohsen, A. Kermagoret, S. Corr, G. Bastian, A. Tomas, M. Wei, F. Santoni, N. Guerra, D. Desmaële and J. d' Angelo, *Investigational New Drugs*, **2015**, 33, 848-860.

According to Ranasinghe *et al.,* Re(I) metal complexes have the potential for better biochemical applications with longer lifetimes, high photo stability and large Stokes shifts.[38] Re(I) complexes with these properties as mentioned above are ideal compounds for *in vitro* and *in vivo* visualization during biological processes and the excitation of visible light will minimize the UV damage of the cell by these complexes.[38] As reported by Leonidova *et al*. Re(I) tricarbonyl *N,N′*-bis(quinolinoyl) complexes and their derivatives can couple to targeting vectors and are developed as luminescent probes.[39] These probes are coupled to different biological molecules like biotin, glucose or β-breaker peptide derivatives. These complexes also consist of imaging properties and some have therapeutic potentials. Many rhenium complexes are very efficient triplet photosensitizer (PS) as stated by Leonidova *et al.* and could be an outstanding $^1O_2$ generator in cells.[39] *fac*-$[Re(CO)_3(N,N')X]^+$ core (*N,N′* = any bidentate ligand like phenanthroline of bipyridine; X = monodentate ligand) are used mostly as Re(I) lumophores. [40]

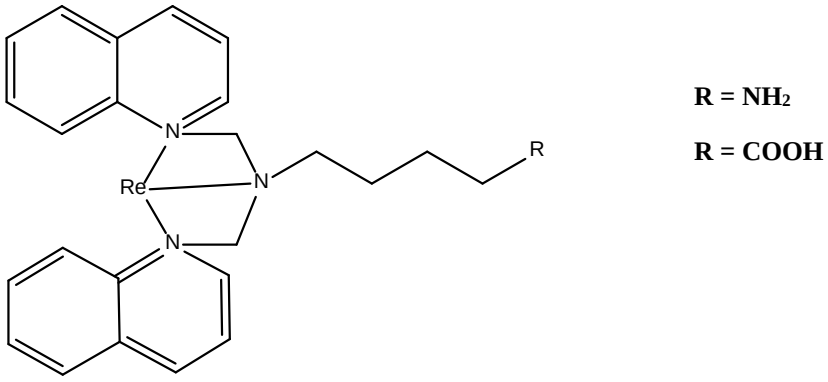

Figure 2.10: Structure of Re complexes and their derivatives.

Complexes with bisquinoline amine ligands are used for imaging and are used as the basis of Tc(I) analogues. These analogues are used as diagnostic and therapeutic radiopharmaceuticals. The general *fac*-$[Re(CO)_3(N,N')X]$ complex are stable and displays luminescence properties which are required for imaging according to Coogan and co-workers.[40] Re(I) and Tc(I) consist of a d^6 low-spin electron configuration and are kinetically stable with a decrease in the toxicity.

[38] K. Ranasinghe, S. Handunnetti, I. C. Perera and T. Perera, *Chemistry Central Journal*, **2016**, 10(71), 1-10.

[39] A. Leonidova, V. Pierroz, R. Rubbiani, J. Heier, S. Ferrari and G. Gasser, *Dalton Transactions*, **2014**, 43, 4287-4294.

[40] M. P. Coogan and V. Fernádez-Moreira, *Chemical Communications*, **2014**, 50, 384-399.

According to Coogan *et al.* most rhenium complexes have low toxicity while other complexes are cytotoxic, depending on the coordinated ligands and not the metal itself. [40]

Carbon monoxide (CO) are lately used as cytoprotective and homeostatic molecules in medicine and have beneficial therapeutic effects.[41] CO are clinically used in medical agents for inflammation, cardiovascular diseases and for organ transplantations. A few applications of Re(I) carbonyl complexes as versatile dyes are singlet oxygen generation, photosensitization of light driven CO_2 reduction and long range electron transfer through proteins.[42] Not all rhenium dyes display light absorbance in the visible spectrum range. Ultraviolet or blue light is often required for a transition from the filled Re d-orbital to an empty ligand π* orbital.[42] By changing the diamine ligand by adding an electron withdrawing group, causes a shift in the absorbance of the complex. These groups lower the energy of the metal-to-ligand charge transfer transition and stabilize the π* orbital.[42]

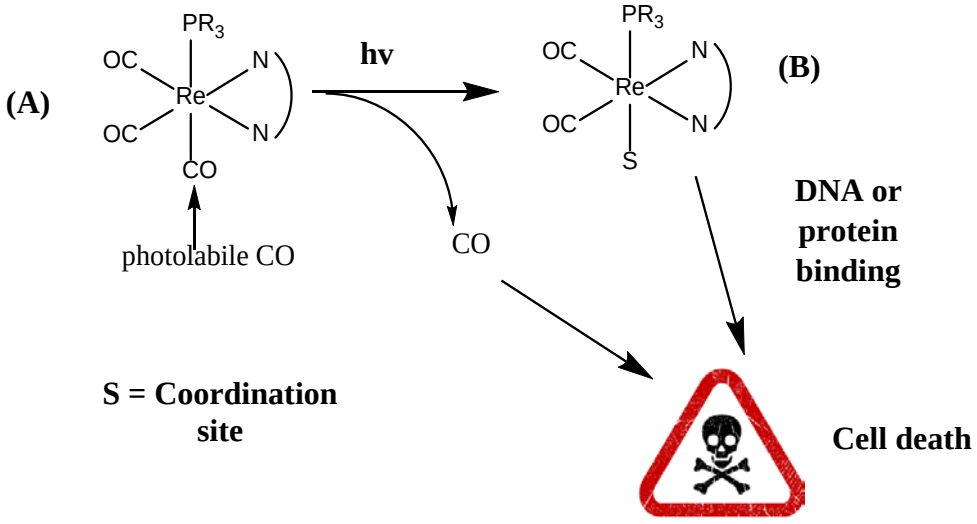

Scheme 2.1. Illustration of a photoreaction releasing one equivalent of CO.[43]

Most of rhenium(I) tricarbonyl complexes are inert to photo substitution reactions. [43] Introducing a phosphine ligand to the inner sphere of coordination result in the following complex $[Re(N,N')(CO)_3(PR_3)]^+$ and one CO ligand are photolabile and are brightly

[41] F. Zobi, O. Blacque, R. A. Jacobs, M. C. Schaub and A. Y. Bogdanova, *Dalton Transactions*, **2012**, 41, 370-378.

[42] D. A. Kurtz, K. R. Brereton, K. P. Ruoff, H. M. Tang, G. A. N. Felton, A. J. M. Miller and J. L. Dempsey, *Inorganic Chemistry*, **2018**, 5389-5399.

[43] S. C. Marker, S. N. MacMillan, W. R. Zipfel, Z. Li, P. C. Ford and J. J. Wilson, *Inorganic Chemistry*, **2018**, 57, 1311-1331.

luminescent as seen in Scheme 2.1. When $[Re(CO)_3(N,N')(PR_3)]^+$ is irradiated with UVA light, the CO ligand trans to the phosphine, dissociates and forms a new dicarbonyl complex. (Scheme 2.1.B) According to Marker *et al.* they reported these complexes as photoactivated anticancer agents.[43] The rhenium(I) dicarbonyl complex contains a labile coordination site and act as a photoproduct. This complex will interact with biological targets such as DNA.[43] Marker and co-workers synthesized Re(I) compounds with phosphine ligands and had the ability of being UVA light active at 365 nm, with toxicity against several cancer cell lines. The depth of light for biological penetration are 365 nm and are too shallow for the use of *in* vivo applications.[43] Smithback and co-workers synthesized novel mixed-ligand Re(I) dicarbonyl compounds and these compounds have long-lived excited states which are synthesized with different paths as seen in Scheme 2.2.[44]

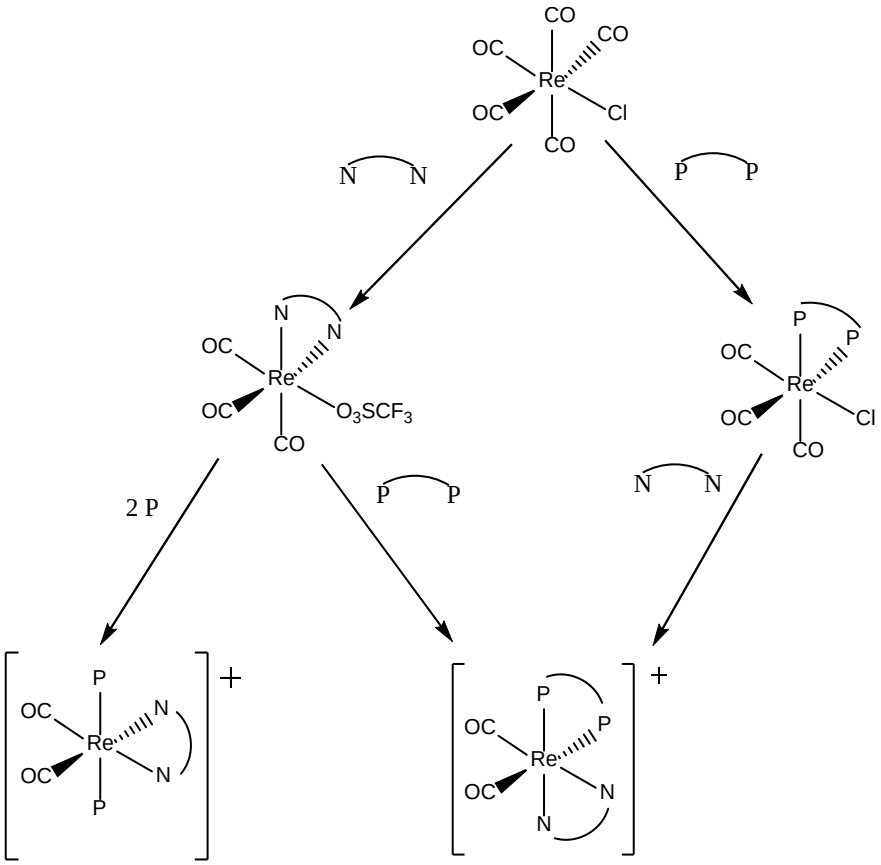

Scheme 2.2: Direct synthesis of Re(I) dicarbonyl compounds with phosphine-diimine ligands.[44]

[44] J. L. Smithback, J. B. Helms, E. Schutte, S. M. Woessner and B. P. Sullivan¸ *Inorganic Chemistry*, **2006**, 45(5), 2163-2174.

2.7. 1,10-Phenanthroline:

Transition metal complexes with polypyridyl ligands, like bipyridine or 1,10-phenanthroline are used for the structural studies of nucleic acids.[45] Most of the organic molecules do not possess the properties of these metal complexes, for example catalytic activity, redox activity and photophysical properties. Polypyridine complexes that are covalenty attached to nucleic acids were first seen in the field of artificial nucleases. Complexes with transition metals such as copper or iron with 1,10-phenanthroline, has the ability to cleave nucleic acids. As stated by Gislason *et al.,* the use of transition metal complexes with polypyridine ligands are used as probes in nucleic acid research and, in conjugation with DNA, to form structures for nanotechnological application.

1,10-Phenanthroline (phen) as well as its derivatives play an important role as building blocks for the synthesis of metallic-dendrimers, molecular scaffolding for supramolecular construction and as a ligand for the synthesis of ring opening metathesis polymerization (ROMP).[46] The heterocyclic ligand, phen, also known as a N-heterocyclic chelating ligand, is a tricyclic molecule and belongs to the phenanthrene family. Phen, illustrated in Figure 2.11 below, is believed to be a α-di-iminic ligand or a bidentate ligand.

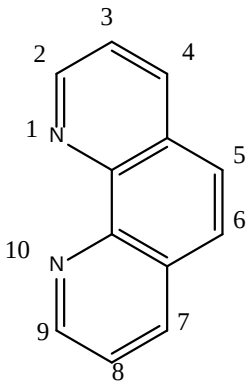

Figure 2.11: Structure of 1,10-phenanthroline.

Pyrazinophenanthroline (dpq) and dipyridophenazine (dppz) derivatives of phen, have lower π* orbitals and are superior electron acceptors compared to phen. [29]

[45] K. Gislason and S. T. Sigurdsson, *European Journal of Organic Chemistry*, **2010**, 4713-4718.

[46] H. Hadadzadeh, M. M. Olmstead, A. R. Rezvani, N. Safari and H. Saravani, *Inorganica Chimica Acta*, **2006**, 359, 2154-2158.

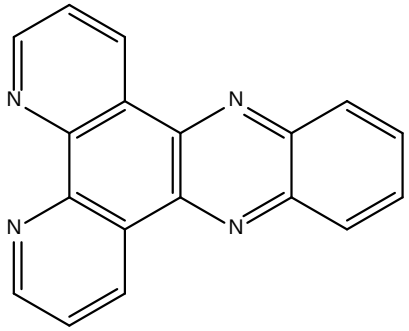

dppz

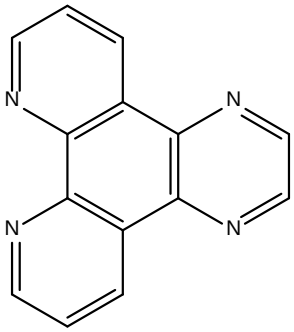

dpq

Figure 2.12: Structures of dipyridophenazine and pyrazinophenanthroline ligands.

1,10-Phenanthroline and the derivatives thereof play an important role in the molecular scaffolding of supramolecules.[47] The 1,10-phenanthroline ligand has metal-chelating properties and its derivatives can be utilized as analytical reagents for the development of bio-organic probes.[48] Phenanthroline and bipyridine are both chelating ligands and have been used in different areas of coordination chemistry as well as analytical chemistry. Six-membered aromatic nitrogen heterocyclic molecules have a low energy π* orbital and acts as a good π-acceptor of metal d-orbital electron density in metal-ligand back bonding and is very poor π-donors. Five membered aromatic nitrogen heterocyclic molecules have the ability to occur as an anionic ligand by the protonation of the acidic N-H groups in the free ligand.

Triphenylphosphine and tertiary phosphines are strong field ligands and affect the orbital state of the metal center by increasing the splitting between them.[49] Compared to pyridine ligands containing a nitrogen, phosphine ligands form stronger bonds with the metal ion. Photostable supramolecular compounds are created from mixed ligand polypyridyl phosphine Ru(II) complexes as stated by Litke *et al.*[49] These complexes have a high absorption ability in the visible spectral range and have a higher photochemical stability.

$[Ni(phen)_2]^+$, a tetrahedral complex were reported as a potent inhibitor for polymerase I Escherichia coli by DNA cleavage, as stated by Deo *et al.*[50] The octahedral complex,

[47] S. Bodige and F.M. Mac Donnell, *Tetrahedron Letters*, **1997**, 38, 8159-8160.

[48] A. Angeloff, J. Daran, J. Bernadou and B. Meunier, *European Journal of Inorganic Chemistry*, **2000**, 1985-1996.

[49] S. V. Litke and A. Yu. Ershov, *Optics and Spectroscopy*, **2011**, 11(4), 522-528.

[50] K. M. Deo, B. J. Pages, D. L. Ang, C. P. Gordon and J. R. Aldrich-Wright, *International Journal of Molecular Sciences*, **2016**, 17, 1818.

$[Ru(phen)_3]^{2+}$ can intercalate and unwind DNA very effectively, while $[Ru(bpy)_2(dppz)]^{2+}$ enhances luminescence upon the intercalation with DNA and is used as a luminescent DNA probes.[50] Figure 2.13 illustrates the structures of these three complexes.

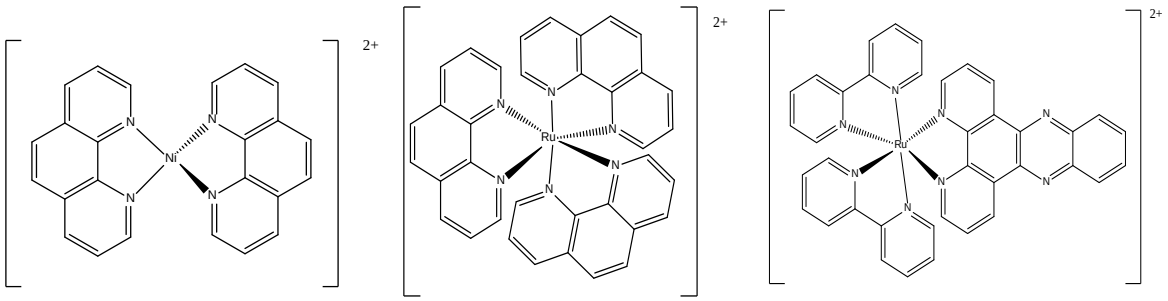

$[Ni(phen)_2]^+$ **$[Ru(phen)_3]^{2+}$** **$[Ru(bpy)_2(dzzp)]^2$**

Figure 2.13: Structures of different metal-based complexes with phen and phen derivatives.

A number of mixed ligand Ru(II) complexes were synthesised with phenanthroline ligands such as 5-methylphenanthroline (Figure 2.14) to investigate the impact of on the photophysical properties.[51]

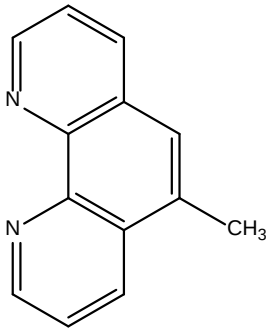

Figure 2.14: Structure of 5-methylphenanthroline.

According to Bhuiyan *et al.,* during thermal stability tests, quaternary amine groups are stable towards hydrolysis. Ruthenium complexes can initiate electron transfer reactions between proteins and these complexes require a high charge and water solubility. An increase in the charge of the complexes are obtained by modifying the ligand for example, the addition of a quaternary amine to a benzylic position. This enhances the water solubility at the same time.[51]

[51] A. A. Bhuiyan, R. Dossey, T. J. Anderson, F. Millett and B. Durham, *Journal of Coordination Chemistry,* **2008**, 61(13), 1-10.

Lanthanide complexes coordinated to ligands like phen and bpy was studied and was found to strongly absorbs ultraviolet light.[52]

Phenanthroline can be used in two possible ways:

i) As a monohydrate compound and

ii) as an anhydrous compound.

Phenanthroline can dissolve fully in ethanol, acetone, ether and benzene. Phenanthroline and bipyridine coordinate through the two nitrogen atoms in a bidentate fashion to the metal centres. The delocalized π-orbitals provide an empty π*-orbitals. These ligands will form a 5-memebered ring when coordinated to metals. In most cases phen and bpy is used to stabilize metal complexes in a lower oxidation state. Phenanthroline contains a strong ligand field, causing spin pairing.[53] Phenanthroline has been used as a ligand in cationic ionophores and for homogeneous catalytic reactions.[54] 1,10-Phenanthroline complexes with, copper(I) or ruthenium(II) were designed to ensure photo induced energy or electron transfer processes could occur for the application in the field of photonic devices.[54] Different isomers of phenanthroline exist, depending on the position of the two nitrogen atoms, and are considered to be α-di-imines.[53] In Figure 2.15, some isomers of phenanthroline are illustrated.

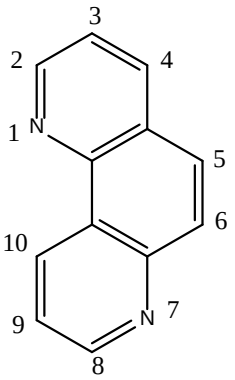

1,7-Phenanthroline

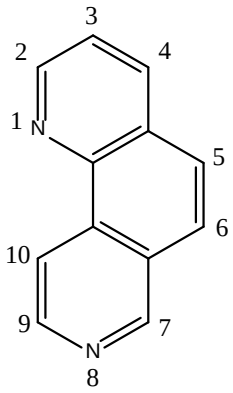

1,8-Phenanthroline

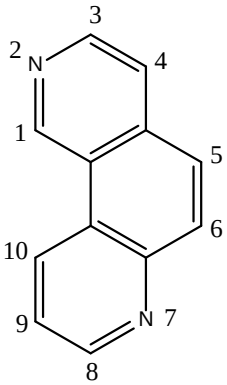

2,7-Phenanthroline

[52] C. Xu, *Monatshefte für chemie*, **2010**, 141, 631-635.

[53] R. Cogan, **2009, '***Synthesis, Characterisation and Anti-Candida Activity of Inorganic and Organic Derivatives of 1,10-phenanthroline'*, Master dissertation, Dublin Institute of Technology, Marlborough St Dublin I.

[54] B. Chesneau, A. Passelande and P. Hudhomme, *American Chemical Society*, **2009**, 11(3), 649-652.

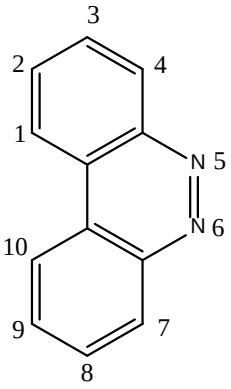

5,6-Phenanthroline

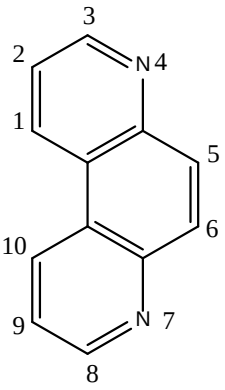

4,7-Phenanthroline

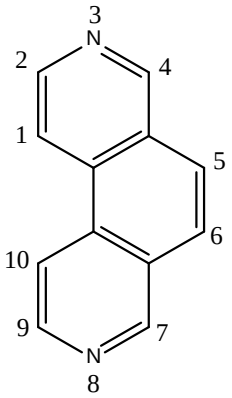

3,8-Phenanthroline

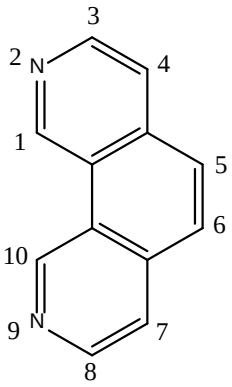

2,9-Phenanthroline

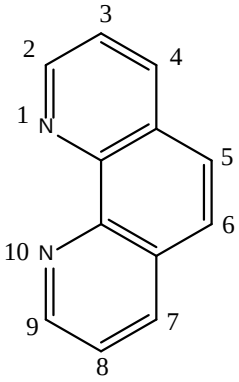

1,10-Phenanthroline

Figure 2.15: Structures of different phenanthroline isomers.

Positions 2, 4, 7 and 9 on the phenanthroline backbone are assigned to be nucleophilic substitution areas, due to the electron withdrawing effect of the two nitrogen atoms. Both the 4th and 7th N-positions are neighbouring quaternary carbons and experience strong electron withdrawing effects during nucleophilic substitution. Positions 3, 5, 6 and 8 are electrophilic because of their higher electron density.[53] Phenanthroline has a rigid planar framework. When divalent metal ions like Cu^{2+}, Zn^{2+} and Ru^{2+} are chelated to phenanthroline, cytotoxicity has been reported. Some metal complexes that contain a phenanthroline ligand has been reported with anti-cancer, anti-fungal and anti-bacetrial properties. Phen, bpy and their substituted derivatives, rearrange the functioning of biological systems in the metal free state and as a ligand coordinated to a transition metal.[53]

The chelating ligand 1,10-phenanthroline and phendione (1,10-phenanthroline-5,6-dione) represent a novel class of anti-fungal agents. The structure of 1,10-phenanthroline-5,6-dione is illustrated in Figure 2.16.

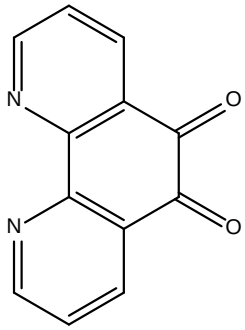

Figure 2.16: Structures of 1,10-phenanthroline-5,6-dione.

2.8. Phendione as ligand in medicine:

1,10-Phenanthroline-5,6-dione (Figure 2.16) has the ability to form stable complexes with metal ions.[46] Similarly as phenanthroline in structure, phendione contains an additional two carbonyl groups attached to positions 5 and 6. Phendione is a chelate ligand and have two coordination functionalities: i) Quinoid functionality that is redox reactive and ii) a di-iminic functionality that is a Lewis base. Phendione can interact with other compounds or metal centres through these functionalities.[53]

Molecules or compounds formed between a ligand and metal ion is known as coordination complexes.[55] The metal ions are Lewis acids while ligands are Lewis bases. Most of the time, ligands has a lone pair of electrons and donates the electrons to the empty d-orbital of the metal.[55] According to coordination chemistry, o-quinones have useful features like the formation of stable complexes with all metals and they can change oxidation states when coordinated directly to a metal ion.[55]

According to R.Cogan *et al.* if the phendione contains oxygen bonds, Lewis acids are used for the coordination of the metal to the ligand.

[55] N. Samadi and M. Salamati, *Bulletin of the Chemistry Society of Ethiopia*, **2014**, 28(3), 373-382.

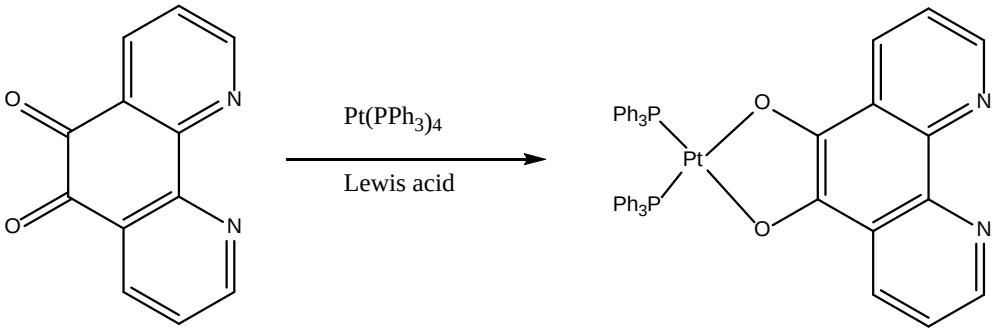

Scheme 2.3: Reaction between phendione and $Pt(PPh_3)_4$.

The low-valent $Pt(PPh_3)_4$ undergo oxidative addition to the dioxolene site and the catecholate complex are formed and seen in Scheme 2.3.[48]

Due to the quinonoid function it is redox active and will act as a Lewis base with regards to the diiminic nitrogen atoms.[55] The complex are used as a 'quinone equivalent' with a metal in the lowest oxidation state, only when the transition metal coordinate through the two nitrogen atoms.

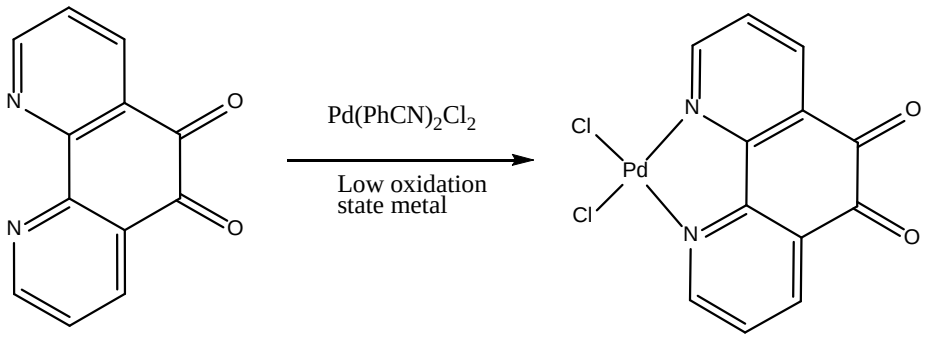

Scheme 2.4: Reaction between phendione and $Pd(PhCN)_2Cl_2$.

$Pd(PhCN)_2Cl_2$ will selectively react with the N-donor center for the formation of the complex illustrated in Scheme 2.4. [55]

The isomers of phendione is depended on the position of the two nitrogen atoms. 4,7-Phenanthroline, also known as Phanquinone (Figure 2.17) is used in the treatment of Alzheimer's disease and has limited to no side effects.[53]

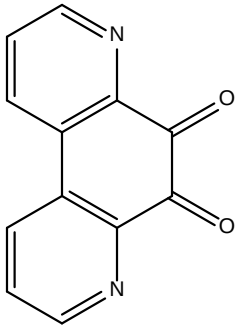

Figure 2.17: Structure of Phanquinone.

The addition of water to the quinone functions in $[Ru(phen)_2(phendione)]^{2+}$ and $[Ru(phendione)_3]^{2+}$ (phendione = 1,10-phenanthroline-5,6-dione) can activate fluorescence at 605 nm as stated by Poteet *et al.*[56] (Figure 2.18). The formation of a germinal diol, eliminate the quinone-based non-radiative decay pathway and produce a long-lived ^{3}MLCT state.

Hydration of the quinone moiety occurs and as the diol species is formed, it eliminates the quinone-based non-radiative decay path. Poteet *et al.* stated that this hydration step could affect the electrochemical activity of the ligands.[56]

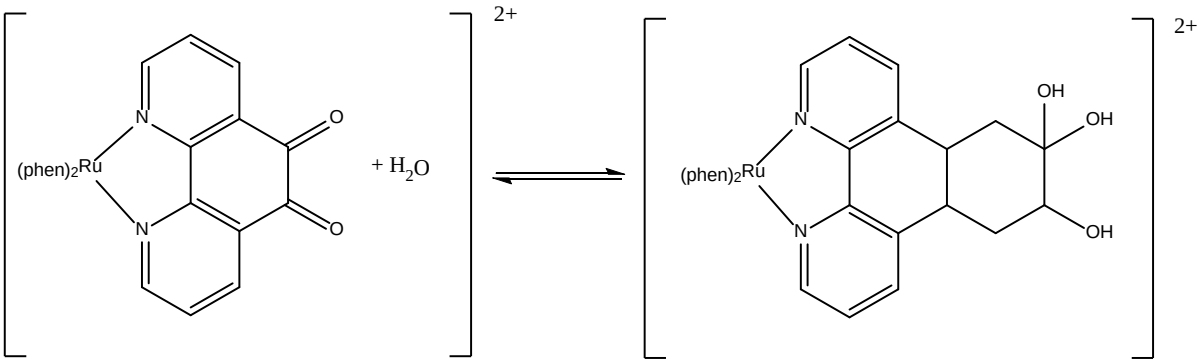

No emission **Bright emission at 605 nm**

Complex 1 **Complex 2**

Figure 2.18: Schematic representation of the reaction with the addition of water.

Complex 1 has been studied and reported a photoinduced DNA cleavage activity of this complex and showed luminescence properties in water and is due to the ground state effect.[56]

[56] S. A. Poteet and F. M. MacDonnell, *Dalton Transaction*, **2013**, 42, 13305-13307.

2.9. 1,10-phenanthroline-5,6-diamine:

Phendiamine is one of the phenanthroline derivatives with substitutents on positions five and six.[57] These derivatives have not been studied extensively due to the fact that the five and six substituted moieties don't have the ability to act as multidentate ligands as stated by Young.[57] Figure 2.19 represents possible ligands with the functionalized position five and six that can be synthesised. As seen in Figure 2.19, these ligands can act as bridging ligands. To synthesize these ligands, strong oxidative conditions are introduced.

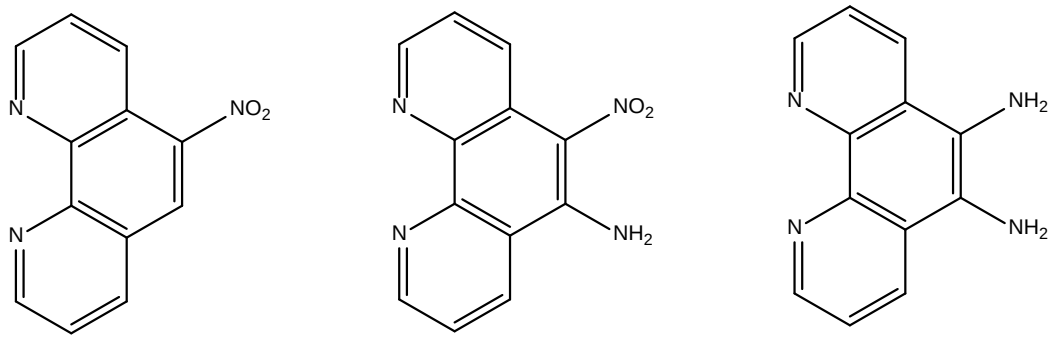

(a) **(b)** **(c)**

Figure 2.19: Illustration of modified 1,10-phenanthroline derivatives on position five and/or six.

For the synthesis of (a) nitric- as well as sulphuric acid are used at 170°C with no bromine present, (b) is then formed by amination and then (c) is synthesized by hydrogenation of (b).[57] (Scheme 2.5)

[57] C. Young, *Bulky Metal Complexes as model nanoscale catalysts*, **2012**, 1-155.

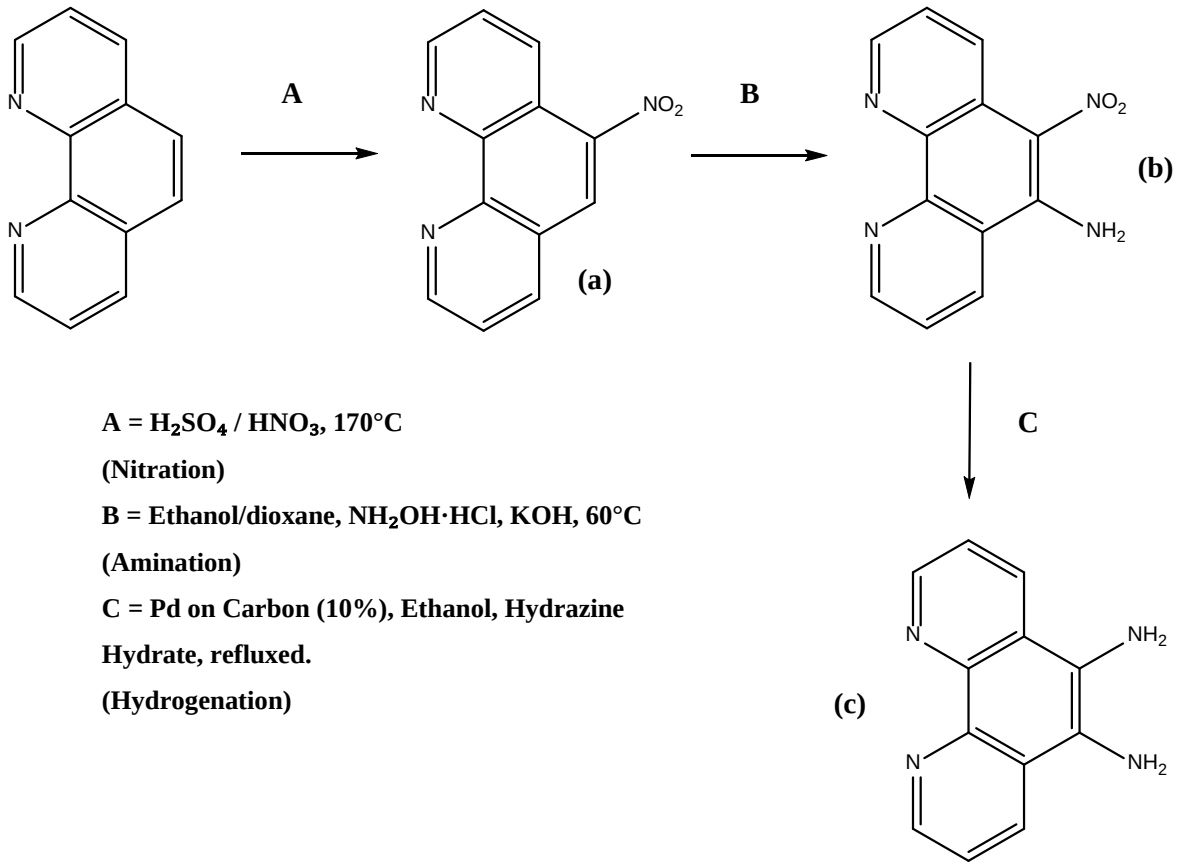

Scheme 2.5: Represents the synthesis method for phendiamine.[57]

Phendiamine (5,6-diamino-1,10-phenanthroline) can either coordinate to bridge two metal centers or it can be condensed with quinones.[58] With the condensation of phendiamine and phendione, a bridging ligand, tpphz (tetrapyrido[3,2-a:2',3'',2''-h:2''', 3'''-j] phenazine will be formed as stated by Bodige *et al.*[58]

2.10. Photoluminescence properties:

Ruthenium, iridium, platinum, copper and gold are d^6, d^8 and d^{10} species and can be used as luminescent transition metal complexes.[59] These metal complexes have been studied for their strong luminescence at ambient temperature and because of their solid state. Heavy-metal complexes with phosphorescent properties are used as bioimaging probes, which are a new research field. These complexes have applications in targeted bioimaging, two-photon

[58] S. Bodige and F.M. MacDonnell, *Tetrahedron Letters*, **1997**, 38(47), 8159-8160.

[59] M. Wallesch, D. Volz, D. M. Zink, U. Schepers, M. Nieger, T. Baumann and S. Bräse, *Chemistry: A European Journal*, **2014**, 20, 6578-6590.

bioimaging as well as time-resolved bio imaging *in vitro* and *in vivo*.[60] Luminescent probes for bio imaging requires excitation and emission wavelengths with brightness and photo stability.[60] The cytotoxicity of phosphorescent heavy-metal complexes originate from the toxic effects on the metabolism of the complex and the survival and proliferation of cells. The cytotoxicity of these phosphorescent heavy-metal complexes are dependent on the chemical structure and the lipophilicity are correlated by the cytotoxicity. With a high lipophilicity, a higher cytotoxicity of the complex are reported.[60]

DNA, peptides and proteins can covalently be attached to biotin resulting in biotinylated biomolecules which can be recognized by avidin conjugated markers as fluorescent labels and detection procedures is carried out when avidin is used as a bridge and biotin as the fluorophore conjugated reporter.[61] Using fluorescent biotin reagents are less common, while most of the biotin-fluorophore conjugates like fluorescein or pyrene when bound to avidin, lose their fluorescence property. As reported by Lo *et al.* when using luminescent biotin-transition metal complexes with photo physical properties like large stokes shifts and long emission lifetimes, the problem could be solved. [61]

Some interesting Cu(I) complexes with N, O, P or S coordinating ligands have been reported by Wallesch *et al.*[59] Soft Cu(I) ions are more stable when coordinated to soft atoms like phosphine-oxide or phosphine ligands. Commercially available nitrogen and phosphorus containing ligands are favourable due to their soft electron donor properties.[59] When adding electron-donating of withdrawing groups to the ligand, the colour of emission changes because the electronic structure of the complex changes.[59] Amines, amides and carbazolides are hard N donors and causes Cu(I) complexes to be easily oxidized by air, while nitriles or pyridines also known as soft N donors form more stable compounds. Cu(I) complexes with P and N ligands are used as successful emitters in material sciences.[59]

Gold(I) complexes are known for their photoluminescence and aurophilic interactions.[62] Differences in the adsorption as well as the emission properties between binuclear and mononuclear Au(I) complexes with phosphine ligands was studied by Zhang and co-workers.[62] They focused on the relationship between aurophilic attractions and the luminescent behaviour. Metal-localized transitions have been allocated by the lowest energy emission of the binuclear

[60] Q. Zhao, C. Huang and F. Li, *Chemical Society Reviews*, **2011**, 40, 2508-2524.

[61] K. K. Lo, W. Hui and D. C. Ng, *Journal of American Chemical Society*, **2002**, 124(32), 9344-9345.

[62] H. X. Zhang and C. M. Che, *Chemistry: A European Journal*, **2001**, 7(22), 4887-4893.

gold(I) complex with bridging phosphine ligands. Aurophilic attraction is used to explain the red shift in photoluminescence from mono- to binuclear complexes.[62] According to Zhang *et al.*, gold(I) complexes like $[Au_2(dppm)_2]^{2+}$, $[Au_2X_2(dppm)]$ (were X= dppm, Br, Cl or I) and $[AuCl(PPh_3)]$ show an intra- and intermolecular weak Au'-Au' bonding attraction with stabilized energy. The phosphine ligands in these gold(I) complexes are electron donors and neutralize the positive charge on the gold atoms through the Au-P bonding interactions.[62]

Luminescent Re(I) tricarbonyl polypyridine complexes with the general formula $[Re(CO)_3(N,N')(L)]^n$ (N,N′ = 2,2'-bipyridine, 1,10-phenanthroline and 1,10-phenanthroline-5,6-dione; n = +1, 0; and L= Cl, MeOH or Br) are used as cellular imaging reagents and are beneficial over triplet emitters. The bidentate ligand, (N,N′-ligand), control the photophysical properties of these complexes.[63] The experimental and theoretical properties of luminescent rhenium(I) complexes is recently more investigated, especially the mononuclear neutral, $[Re(CO)_3(N,N')(L)]$ or the cationic complex, $[Re(CO)_3(N,N')(L)]^+$. For these complexes, the neutral and cationic (where L = halide and amine or phosphine) respectively, possesses pseudo-octahedral structure.[63] These complexes can undergo radiative decay at room temperature according to Kamecka *et al.*[64] They also reported that the metal-to-ligand charge-transfer (MLCT) emission of rhenium(I) polypyridines provide new luminescent biotin derivatives with different emissions as the normal biotin-fluorophores.[61] *fac*-$[Re(N,N')(CO)_3(py\text{-}CH_2\text{-}NH\text{-}biotin)][PF_6]$ (Figure 2.20) where N,N′ = 1,10-phenanthroline, 3,4,7,8-tetramethyl-1,10-phenanthroline or 2,9-dimethyl-4,7-diphenyl-1,10-phenanthroline were prepared from *fac*-$[Re(N,N')(CO)_3(CH_3CN)](CF_3SO_3)$ and py-CH_2-NH-biotin, refluxing in THF. Upon photoexcitation of these complexes, they have intense and long-lived yellow luminescence.[61]

[63] L. C-C. Lee, K-K. Leung and K. K-W. Lo¸ *Dalton Transactions,* **2017**, 46, 16357-16380.

[64] A. Kamecka, K. Prachnio and A. Kapturkiewicz, *Journal of Luminescence*, **2018**, 203, 409-419.

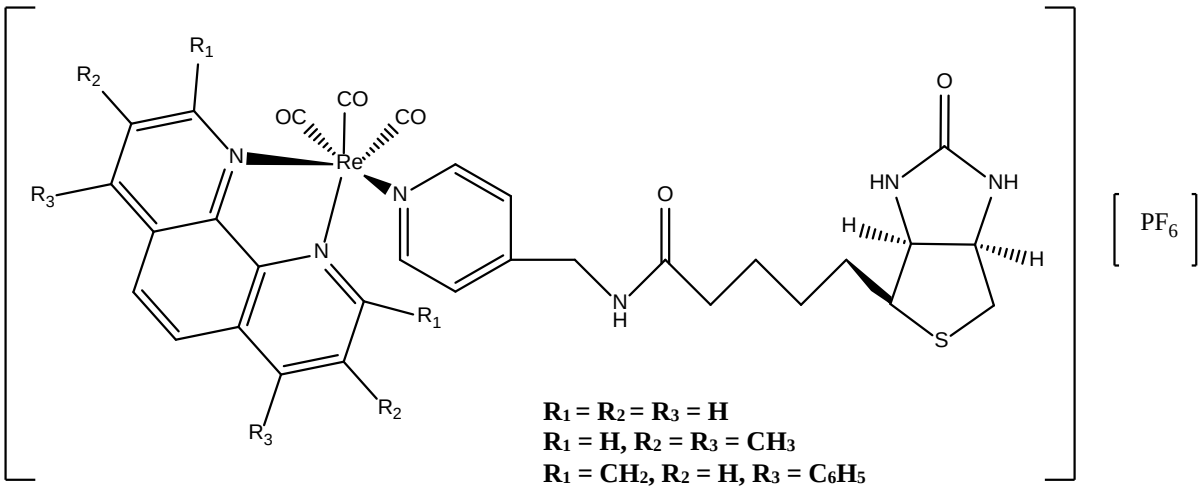

Figure 2.20: Schematic representation of [Re(N,N)(CO)$_3$(py-CH$_3$-NH-biotin)][PF$_6$].[10]

Polypyridyl ruthenium complexes are studied because of their photoluminescence properties and in the visible light region the molar absorption coefficients are very large.[65] These complexes insert and stack themselves between the base pairs of the double helix of DNA. The insertion can develop into photochemical probes of the DNA structure and can be used as potential anticancer drugs. [65] When [Ru(phen)$_2$dppz]$^{2+}$ (dppz = dipyrido-[3,2-a:2',3'-c]phenazine) is in an aqueous solution, no photoluminescence properties are observed, but when it is intercalated into adjacent DNA base pairs, it becomes luminescent due to the dppz ligand. This complex is known as a "DNA light-switch" as reported by Chen and co-workers.[65,66] A light switch effect can also be observed when the {Ru(phen)$_2$} moiety is coordinate to a phen part of the PHENHAT (1,10-Phenathroline [5,6-b] 1,4,5,8,9,12-hexaazatriphenylene) ligand (Figure 2.21). There are no effect of the light switch observed when the moiety are coordinated to the "HAT" part of the same ligand.[66]

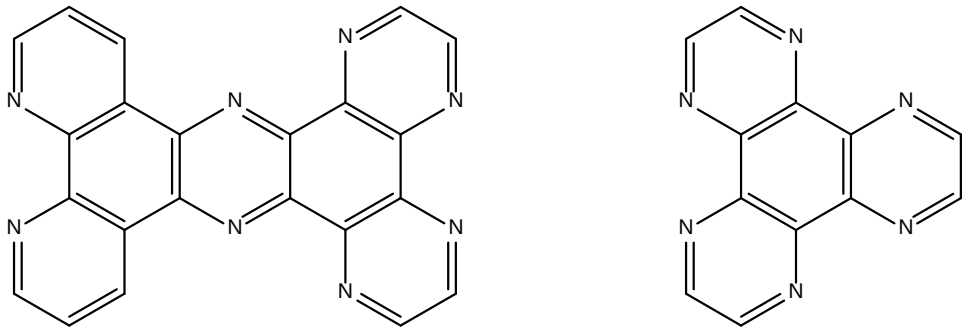

Figure 2.21: Structures of PHENHAT and HAT ligands.[65]

[65] P.L. Chen, H. Chao, J. Xu, L. Wang and H. Li, *Transition Metal Chemistry*, **2009**, 34, 773-778.

Heavy-metal complexes with a d^6, d^8 and d^{10} electron configuration have strong spin-orbit coupling and result in intense phosphorescent emission according to Zhao *et al.*[66] These emissions are useful due to the radiative decay times. Re(I), Ru(II) and Rh(III) heavy-metal complexes with a d^6 electron structure and Pt(II) complexes with a d^8 structure are very important components with phosphorescent emission properties at room temperature. Heavy-metal complexes have rich excited state properties and are very attractive due to many applications in different fields like organic-light-emitting diodes, chemical sensors and bio imaging probes.[66] Excitation with green or blue light for cell imaging are satisfactory but for whole body small animal imaging the optimal excitation wavelength are required. This optimal wavelength of the fluorophore is in the range of 650-950 nm, deep red or near infrared region. Using this wavelength range, good tissue penetration and low auto fluorescence are obtained as stated by Zhao and co-workers.[66] The brightness is also important for bio imaging probes. If the agent has a bright emission, less excitation intensity is needed, and it results in deeper penetration due to the higher signal-to-noise ratio. [66] d^6 Metal ions such as Re(I) and Ru(II) with α,α'-diimine ligands form complexes with a variety of excited states and due to changes in the energy or structure, inversion of the lowest configurations are achieved according to Striplin *et al.*[67] Coordinated complexes with 1,10-phenanthroline (phen) and a d^6 metal-ion like Re(I) contains $3\pi\pi^*$, 3dd (LF) and $3d\pi^*$ (MLCT) excited terms within the wavenumber of the lowest (emitting) excited configuration. These terms can be achieved indirectly with radiationless decay from higher singlet states.[67]

2.11. OLEDs:

Iridium(II) complexes have been used as phosphorescent emitters in OLEDs because these complexes have a high photoluminescence efficiency, thermal stability, strong spin-orbit coupling effects and flexible colour tunability.[68] When comparing Ir(II) phosphorescent emitters with Re(I) or Ir(II) complexes have disadvantages like low photoluminescence quantum yield (PLQY) and single emissive colors. Re(I) complexes have a few advantages such as easy synthesis and short phosphorescent lifetime.[68] During the study Hu and co-workers developed a neutral tricarbonyl Re(I) complex with TDAP ligand (TDAP =

[66] Q. Zhao, C. Huang and F. Li, *Chemical Society Review*, **2011**, 40, 2508-2524.

[67] D. R. Striplin and G. A. Crosby, *Coordination Chemistry Reviews*, **2001**, 211, 163-175.

[68] Y. Hu, G. Zhao, Y. Dong, Y. Lü, X. Li and D. Zhang, *Dyes and Pigments*, **2017**, 137, 569-575.

[1,2,5]thiadiazolo[3,4-f][1,10-phenanthroline]). The Re-TDAP complex has a short luminescent life-time with high thermal stability, according to Hu *et al.*[68]

Cu(I)-diimine-diphosphine systems have great emission properties and higher dissociation for solar energy capture systems, OLEDs and chemosensors. α-Diimine ligands (Figure 2.22) are used to constru Cu(I)-diimine-diphosphine systems because of their good chelating ability. The most popular α-diimines are 2,2'-bipyridine and 1,10-phenanthroline.[58]

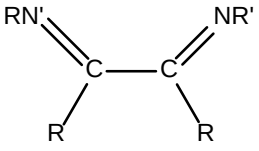

HN=C(R)-(R)C=NH

Figure 2.22: Illustration of α-diimine structures.[60]

More studies are performed on organic light-emitting diodes to improve the display technology with an increased efficiency, flexibility as well as long lifetimes.[69] Electrical energy are converted into light using OLEDs and allow the electrons to be transported from the opposed electrodes. Facile balanced charge transport and a high conversion efficiency of the excitons to light are required for a successful OLED. When producing OLEDs, the brightness of the device is one of the most important considerations and for this reason metal complexes with phosphorescent properties are favoured over fluorescent organic materials as stated by Lundin *et al.*[69]

The dopant used can also affect the wavelength, the broadness of the emission and efficiency of devices.[69] In this case the OLED can be tuned by selecting the most appropriate metal centre and ligands. Re(I) polypyridyl complexes are highly emissive and is used as emitting dopants in different OLED structures. Heterocycles such as 1,3,4-oxadiazole are used as electron-transporting groups because of their electron deficiency and good thermal stability.[69]

Organic EL (electroluminescence) devices have been developed and focus on the optimization of EL cell structures.[70] The quantum- and conversion efficiency, lifetime as well as the emission colours have been improved by different types of EL cell structures. More recently, EL devices use transition metal complexes like zinc bisquinoline and ruthenium containing polyester complexes. The synthesis and properties of novel, trifunctional light-emitting

[69] N. I. Lundin, A. G. Blackman, K. C. Gordon and D. L. Officer, *Angewandte Chemie International Edition*, **2006**, 45, 2582-2584.

[70] X. Gong, P. K. Ng and W. K. Chan, *Advanced Materials*, **1998**, 10(16), 1337-1340.

molecules with rhenium(I) and ruthenium(II) bipyridine complexes was done by Gong and co-workers.[70] These complexes contain light-emitting and electron transporting functional groups in one molecule. Re(I) and Ru(II) bipyridine complexes have long-lived excited states that is caused by metal-ligand charge transfer (MLCT) transitions and is used in photo catalysis and electro-chemiluminescence.[70]

2.12. Summary:

Ruthenium contains an octahedral geometry and has interchangeable oxidation state of Ru(II) and Ru(III), resulting in the ability for different ligands coordination and combinations. Ruthenium compounds are beneficial to biological studies and have been used as anticancer agents. Ruthenium complexes with polypyridyl ligand have great photophysical and tunable absorption properties.

Rhenium(I) carbonyl complexes have been used in different application such as singlet oxygen generation, biological labelling and possesses long-lived excited states. Recently more research has been done on the luminescent properties of these Re(I) complexes for the diagnosis of cancer in the human body.

The anticancer agent, cisplatin is a platinum based complex and is used for treating cancer. Cisplatin exhibit different side-effects and the activity are obtained by the coordinative interaction with DNA. Recently dinuclear complexes were studied for treating cancer and with less side-effects, but with more efficient properties for treating cancer. Both ruthenium and rhenium have outstanding properties and qualities on its own, but when combining these two metals as well as platinum or palladium, a new field of study will exist. Bimetallic complexes can be used for the treatment of cancer, PDT and can reduces the side-effects.

CHAPTER 3: SYNTHESIS AND CHARACTERIZATION OF LIGANDS AND METAL COMPLEXES

3.1. Introduction:

d^6 Transition metal complexes with luminescent properties are used in probes of macromolecular structures and as photosensitizers for the conversion of solar energy and electron transfer reactions.[1] *fac*-$[Re(CO)_3(L)(X)]$ (where X can be any ion such as Cl, Br or CN and L any α-diimine ligand) is an important class of luminescent complexes. In the study of Sacksteder *et al.* their idea was to design customized luminescent metal complexes for the use as probes, and to study the luminescent properties where X is a substituted pyridine. They wanted to determine how the substituted pyridine would affect the energy states and the energy degradation paths. [1] With the variation of the substituted pyridine, the basicity can be manipulated which can result in larger changes in luminescent properties. They however only observed a small effect with the variation in the pyridine ligands.[1]

The favorable properties of the *fac*-$[M(CO)_3]^+$ core are unexplored with N,N-bidentate ligand systems and in this study the coordinative ability of *fac*-$[Re^1(CO)_3]^+$ was investigated to determine their luminescent behavior. The N,N′-bidentate ligands used in this study are 1,10-phenanthroline (phen), 1,10-phenanthroline-5,6-dione ($phenO_2$) and 1,10-phenanthroline-5,6-diamine ($phen(NH_2)_2$). These ligands were coordinated to the rhenium metal as well as a monodentate ligand in the sixth position. Phosphine ligands were chosen as the monodentate ligands due to their ability to coordinate with the low valent ^{99m}Tc/Re carbonyl complexes and form strong bonds.[2] The phosphines used in this study are triphenylphosphine (PPh_3), 1,3,5-triaza-7-phosphaadamantane (PTA) and 3,7-diacetyl-1,3,7-triaza-5-phosphabicyclo[3.3.1]nonane (DAPTA). Two dinuclear Re(I) complexes were synthesized with 1,10-phenanthroline-5,6-dione

[1] L. Sacksteder, A. P. Zipp, E. A. Brown, J. Streich, J. N. Demas and B. A. DeGraff, *Inorganic Chemistry*, **1990**, 29(21), 4335-4340.

[2] A. E. Manicum, M. Schutte-Smith, O. T. Alexander, L. Twigge, A. Roodt and H.G. Visser, *Inorganic Chemistry Communications*, **2019**, 101, 93-98.

($phenO_2$) and 1,10-phenanthroline-5,6-diamine ($phen(NH_2)_2$). Bimetallic compounds are used as PDT agents due to their potential of being therapeutic and diagnostic agents also known as theranostic agents. In this study $phenO_2$ are used as the bridging ligand with different metal centers such as Re(I), Ru(III) and Pt(II). Three bimetallic complexes were successfully synthesized.

3.2. Apparatus and chemicals used:

All reagents used in the synthesis and preparation of the compounds were of analytical grade and purchased from Merck, or Sigma Aldrich, South Africa. Rhenium pentacarbonyl bromide was purchased from Strem Chemical, Newburyport, USA.

The rhenium(I) tricarbonyl complexes, ligands as well as the bimetallic complexes in this study were synthesized and characterized by Nuclear Magnetic Resonance Spectroscopy (NMR), Infrared Spectroscopy (IR), Ultraviolet/Visible Spectroscopy (UV/Vis) and some complexes and ligands by single crystal X-ray diffraction and LECO. The ^{13}C, ^{1}H and ^{31}P NMR spectra were recorded on Bruker 300, 400 and 600 MHz nuclear magnetic resonance spectrometers. Different deuterated solvents were used as indicated in the synthetic procedures. Infrared spectra of the complexes and ligands were recorded at room temperature on a Bruker Tensor 27 Fourier transform spectrometer (ATR), utilizing a He-Ne laser at 632.6 nm, in the range of 4000 to 600 cm^{-1}, coupled to a computer.

The following bidentate ligands, illustrated in Figure 3.1, were used in this study as *N,N′*-donor - and *O,O′*-donor ligands. All these ligands were synthesized except for phen that was bought from Sigma Aldrich.

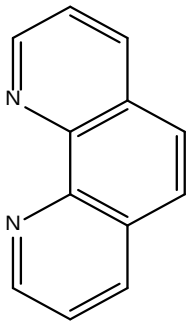

1,10-phenanthroline [phen]

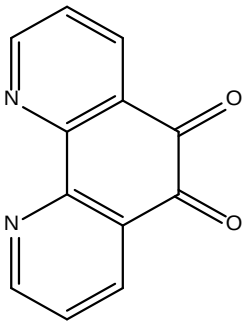

1,10-phenanthroline-5,6-dione [$phenO_2$]

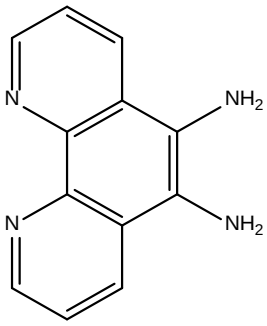

1,10-phenanthroline-5.6-diamine [$phen(NH_2)_2$]

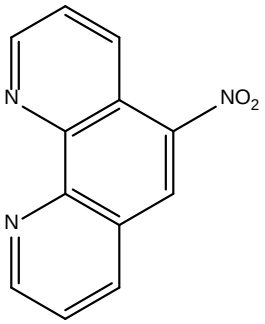

5-nitro-1,10-phenanthroline
[phen(NO_2)]

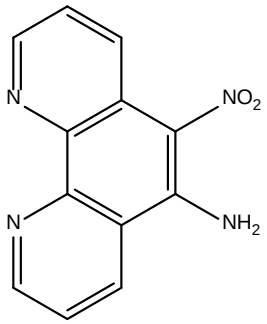

6-amino-5-nitro-1,10-phenanthroline
[phen(NH_2)(NO_2)]

Figure 3.1: Illustration of the *N,N′*-donor and *O,O′*-donor bidenatate ligands.

Triphenylphosphine, 1,3,5-triaza-7-phosphaadamantane and 3,7-diacetyl-1,3,7-triaza-5-phosphabicyclo[3.3.1]nonane that were used as phosphine ligands are illustrated in Figure 3.2 below.

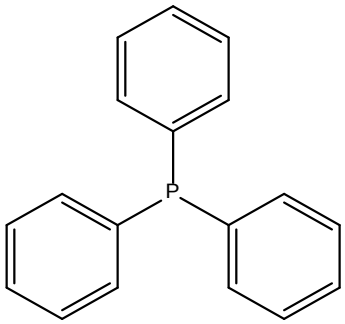

Triphenylphosphine
[PPh_3]

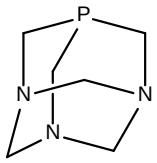

1,3,5-triaza-7-phosphaadamantane
[PTA]

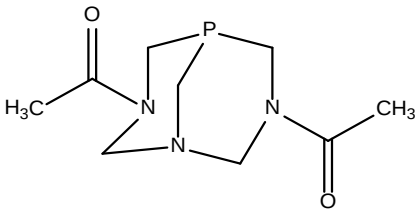

3,7-diacetyl-1,3,7-triaza-5-phosphabicyclo[3.3.1]nonane
[DAPTA]

Figure 3.2: Schematic representation of the *N,N′*-bidentate ligands and the monodentate phosphine ligands used in this study.

The following ligands were successfully synthesised:

- 1,10-phenanthroline-5,6-dione – [phenO_2],
- 1,10-phenanthroline-5.6-diamine – [phen$(NH_2)_2$],
- 5-nitro-1,10-phenanthroline – [phen(NO_2)],
- 6-amino-5-nitro-1,10-phenanthroline – [phen$(NH_2)(NH_2)$],

while two Ruthenium complexes were synthesized.

- $[Ru(phen)_2Cl_2]Cl \cdot 2H_2O$ – [1] and
- $[Ru(phen)_2(phenO_2)][PF_6]_2$ - [2].

The following six Re(I) tricarbonyl complexes were synthesized:

- $[Re(CO)_3(Br)_3]$ – [ReAA],
- $[Re(CO)_3(phen)(H_2O)][NO_3]$ – [3],
- $[Re(CO)_3(phen)(Br)]$ – [4],
- $[Re(CO)_3(phenO_2)(Br)]$ – [5],
- *fac*-$[Re(CO)_3(phen)(PPh_3)][NO_3]$ – [6],
- *fac*-$[Re(CO)_3(phen)(PTA)][NO_3]$ – [7] and
- *fac*-$[Re(CO)_3(phen)(DAPTA)][NO_3]$ – [8].

Six Re(I) dicarbonyl complexes were synthesized:

- *cis*-$[Re(CO)_2(phen)(PPh_3)_2][NO_3]$ – [9],
- *cis*-$[Re(CO)_2(phen)(PTA)_2][NO_3]$ – [10],
- *cis*-$[Re(CO)_2(phen)(DAPTA)_2][NO_3]$ – [11],
- *cis*-$[Re(CO)_2(phen)(PPh_3)(Cl)]$ – [12],
- *cis*-$[Re(CO)_2(phen)(PTA)(Cl)]$ – [13] and
- *cis*-$[Re(CO)_2(phen)(DAPTA)(Cl)]$ – [14].

Two dinuclear complexes are synthesized:

- $[NEt_4]_2[Re_2(CO)_6(\mu\text{-phen}(NH_2)_2)Br_2]$- [15] and
- $[Re_2(CO)_6(\mu\text{-phen}O_2)Br_2]$ – [16].

The following bimetallic complexes were successfully synthesized:

- $[Ru(phen)_2(N,N'\text{-phen}O_2\text{-}O,O')\text{-}Re(CO)_3Br][PF_6]_3$– [17],
- $[Ru(phen)_2(N,N'\text{-phen}O_2\text{-}O,O')\text{-}PtCl_2][PF_6]_3$ – [18] and

- $[Re(CO)_3(N,N'\text{-phen}O_2\text{-}O,O')\text{-}PtCl_2]Br$ – [19].

3.3. Synthesis of ligands:

3.3.1. 1,10-Phenanthroline-5,6-dione – [phenO_2]:

3.3.1.1. Method 1:

1,10-Phenanthroline (5.04 g, 27.9 mmol) was added to a solution of 60 % sulfuric acid (64 ml). After the solid compound was dissolved, potassium bromate (5.16 g, 30.8 mmol) was added over a period of half an hour. The mixture was stirred at room temperature for 20 hours. The mixture was poured over ice and was carefully neutralized to pH 7 using a saturated solution of sodium hydroxide. The solution was then filtered, extracted with CH_2Cl_2 and evaporated to dryness. The crude product was recrystallized from methanol to provide the desired product.

Yield: 0.3g (5.1%).

The yield was too low to proceed with further characterization.

3.3.1.2. Method 2:

A mixture of 1,10-phenanthroline (1.0 g, 5.54 mmol) and KBr (6.79 g, 57.1 mmol) was added to 22.4 ml of H_2SO_4 (98 %) previously cooled at liquid nitrogen temperature. The mixture was slowly allowed to warm to room temperature and a thick orange paste was obtained. 12.3 ml of concentrated HNO_3 were added dropwise at room temperature. The resulting red solution was heated at 90 °C for 3 hours and poured into water (273.4 ml). The solution was neutralized with Na_2CO_3 and extracted with CH_2Cl_2. The yellow extract was dried on $MgSO_4$ and the solvent removed in vacuum. The orange-yellow solid was recrystallized from ethanol.

Yield: 0.637 g (52 %).

IR (ATR, cm^{-1}): ν_{CO} = 1609, 1560.

^{1}H NMR (300 MHz, Acetone-*d6*): δ 9.0 (dd, *J* = 1.84, 4.64 Hz, 2H), 8.4 (dd, *J* = 1.84, 7.85 Hz, 2H) and 7.7 (dd, *J* = 4.64, 7.85 Hz, 2H).

^{13}C NMR (600 MHz, Acetone-*d6*): δ 155, 150, 138, 136, 125, 124.

UV/Vis: ε (λ_{max} = 295 nm) = 4999 M^{-1} cm^{-1}.

3.3.3. 5-Nitro-1,10-phenanthroline – [phen(NO_2)]:

1,10-Phenanthroline (5.0 g, 27.7 mmol) was dissolved in concentrated H_2SO_4 (7.5 ml). A mixture of concentrated H_2SO_4 (15 ml) and concentrated HNO_3 (15 ml) was slowly added to ensure the temperature did not exceed 170 °C. The solution was refluxed at 170 °C for 3 hours. The solution was then poured onto ice and neutralized to pH 6 using a 30 % KOH solution. The precipitate was then filtered off, washed with cold water and dried to produce a pale yellow solid.

Yield: 5.093 g (81.44 %).

IR (ATR, cm^{-1}): 1589, 1504, 1447, 1421, 1353, 1105, 905, 832, 806, 732, 615.

^{1}H NMR (300 MHz, Methanol-*d4*): δ 9.2 (dd,dd, *J* = 1.69, 4.47 Hz, *J* = 1.57, 4.34 Hz, 2H), 9.0 (dd, *J* = 1.59, 8.65 Hz, 1H), 8.9 (s, 1H), 8.7 (dd, *J* = 1.70, 8.14 Hz, 1H), 7.9 (dt, *J* = 4.37, 8.70 Hz, *J* = 4.43, 8.14 Hz, 2H).

^{13}C NMR (400 MHz, Methanol-*d4*): δ 153, 151, 149, 146, 138, 136, 132, 126, 125, 124.

UV/Vis: ε (λ_{max} = 303 nm) = 4185 M^{-1} cm^{-1}.

3.3.4. 6-Amino-5-nitro-1,10-phenanthroline – [phen(NH_2)(NO_2)]:

5-Nitro-1,10-phenanthroline (3.49 g, 15.5 mmol) was dissolved in 100 ml of an ethanol/dioxane (3:2) mixture. The solution was heated to 60 °C until all the solids were dissolved. Is was rapidly cooled to 4 °C which resulted in a fine suspension. Powdered hydroxyl amine hydrochloride (6.84 g, 9.84 mmol) was then added. Followed by the dropwise addition of KOH (7.27 g, 129.5 mmol) in methanol (100 ml). The solution was stirred at 4 °C for one hour and then heated to 60 °C for one hour. The solution was then poured onto ice and resulted in the formation of a yellow solid. The solid was filtered and washed with methanol and water.

Yield: 0.5441 g (14 %).

IR (ATR, cm^{-1}): 1626, 1523, 1486, 1433, 1383, 1302, 1260, 1172, 1095, 827, 796, 734, 670.

^{1}H NMR (300 MHz, DMSO-*d6*): δ 9.2 (dd, *J* = 1.35, 4.26 Hz, 1H), 9.1 (dd, *J* = 1.36, 8.44 Hz, 1H), 8.8 (dd, *J* = 1.47, 4.27 Hz, 1H), 8.7 (dd, *J* = 1.48, 8.58 Hz, 1H), 8.6 (s,2H), 7.9 (dd, *J* = 4.27, 8.46 Hz, 1H) and 7.7 (dd, *J* = 4.15, 8.46 Hz, 1H).

^{13}C NMR (600 MHz, DMSO-*d6*): δ 154, 148, 147, 144, 140, 137, 134, 131, 125, 124, 123, 121.

UV/Vis: ε (λ_{max} = 419 nm) = 19985 M^{-1} cm^{-1}.

3.3.5. 1,10-Phenanthroline-5,6-diamine – [phen(NH_2)$_2$]:

6-Amino-5-nitro-1,10-phenanthroline (0.20 g; 0.83 mmol) and Pd on carbon (10 %) was placed in ethanol (100 ml) and brought to reflux. Hydrazine hydrate (0.84 ml, 17.2 mmol) in ethanol (20 ml) was then added dropwise over fifteen minutes. The solution was then refluxed for two hours and filtered through a bed of Celite. 80 % of the ethanol was removed under vacuum and the final product was precipitated by the addition of excess pentane.

Yield: 0.0844 g (48 %).

IR (ATR, cm^{-1}): 1602, 1565, 1483, 1432, 1409, 1348, 1304, 1112, 1058, 1004, 798, 730, 694.

^{1}H NMR (300 MHz, Methanol-*d4*): δ 8.8 (dd, *J* = 1.65, 4.29 Hz, 2H), 8.5 (dd, *J* = 1.50, 8.49 Hz, 2H), 7.7 (dd, *J* = 4.28, 8.47 Hz, 2H), 4.7 (s, 4H).

^{13}C NMR (600 MHz, Methanol-*d4*): δ 145, 141, 129, 124, 123, 122.

UV/Vis: ε (λ_{max} = 265 nm) = 21259 M^{-1} cm^{-1}.

3.4. Synthesis of Ruthenium compounds:

3.4.1. [Ru(phen)$_2$Cl$_2$]Cl·2H$_2$O – [1]:

An ethanolic solution of 1,10-phenanthroline (0.90 g, 5.01 mmol) was added from a dropping funnel to an ethanolic solution of $RuCl_3 \cdot 3H_2O$ (0.50 g, 2.45 mmol) being stirred magnetically in an ice bath. The mixture was allowed to stir for 3 hours at room temperature. A reddish-brown homogeneous solution was obtained and the solvent was removed with vacuum. The reddish-brown powder was collected and washed three times with acetone to remove any unreacted 1,10-phenanthroline. The product was recrystallized from ethanol to remove unreacted $RuCl_3 \cdot 3H_2O$.

Yield: 0.836 g (56 %).

IR (ATR, cm^{-1}): 1596, 1540, 1427, 1223, 1145, 843, 715.

^{1}H NMR (300 MHz, Methanol- *d4*): δ 9.3 (d, *J* = 4.61 Hz, 2H), 8.9 (dd, *J* = 1.39, 8.14 Hz, 2H), 8.3 (s, 2H), 8.2 (dd, *J* = 4.85, 8.21 Hz, 2H).

^{13}C NMR (600 MHz, Methanol-*d4*): δ 146, 139, 137, 129, 126, 124.

UV/Vis: ε (λ_{max} = 269 nm) = 12059 M^{-1} cm^{-1}.

EA: calculated: C: 47.74 %, H: 3.34 % and N: 9.28 %; found: C: 47.71 %, H: 3.35 % and N: 9.26 %.

3.4.2. $[Ru(phen)_2(phenO_2)][PF_6]_3$ – [2]:

$[Ru(Phen)_2Cl_2]Cl \cdot 2H_2O$ (0.128 g, 0.24 mmol) was reacted with a suspension of 1,10-phenanthroline-5,6-dione (0.10 g, 0.50 mmol) in ethanol (30 ml) and the resulting suspension was refluxed for 4 hours at 78 °C. The addition of an ethanolic solution of NH_4PF_6 resulted in the precipitation of the product and recrystallized by vapour diffusion of diethyl ether into an acetonitrile solution of the complex. The product was filtered off, washed with ethanol and air-dried.

Yield: 0.105 g (65 %).

IR (ATR, cm^{-1}): ν_{CO} **=** 1698.

^{1}H NMR (300 MHz, Acetone-*d6*): δ 9.2 (dd, *J* = 1.67, 4.56 Hz, 2H), 8.7 (dd, *J* = 1.17, 8.28 Hz, 2H), 8.6 (dd, *J* = 1.59, 8.21 Hz, 2H), 8.1 (dd, *J* = 1.17, 5.24, 2H), 8.07 (s, 2H), 7.9 (dd, *J* = 4.62, 8.19 Hz, 2H) and 7.7 (dd, *J* = 5.25, 8.40 Hz, 2H).

^{13}C NMR (600 MHz, Methanol-*d4*): δ 151, 147, 142, 138, 135, 130, 128, 127, 126, 124, 123.

UV/Vis: ε (λ_{max} = 428 nm) = 32027 M^{-1} cm^{-1}.

EA: calculated: C: 39.29 %, H: 2.00 %, N: 3.80 %; found: C: 39.30 %, H: 1.98 %, N: 3.79 %.

3.5. Synthesis of Rhenium compounds:

3.5.1. $[NEt_4]_2[Re(CO)_3(Br)_3]$ - (ReAA):

ReAA was synthesized according to Alberto.[3] The $(NEt_4)Br$ (5.25 g, 0.025 mol) was dried and grounded to a powder. 2,5,8-Trioxanone diglyme (150 ml) was added to the $(NEt_4)Br$ under dry nitrogen and slurried on an oil bath at 80 °C for 30 minutes. The system was evacuated and purged with N_2 several times. The solid $Re(CO)_5Br$ (5 g, 12.31 mmol) was added to the mixture and stirred for 15 hours at 115 °C. The whole system needs stirring and ventilation because of the continuous evolution of CO gas. The reaction mixture was cooled to room temperature, filtered and dried. The

[3] R. Alberto, R. Schibli, R. Waibel, U. Abram and A. P. Schubiger, *Coordination Chemistry Reviews*, **1999**, 190-192, 901-919.

solid was stirred in small amount of ethanol for 5 minutes, filtered and washed with cold DCM and dried.

Yield: 7.92 g (84 %).

IR (ATR, cm^{-1}): ν_{CO} = 1995, 1845.

UV/Vis: (λ_{max} = 263 nm) = 9703 M^{-1} cm^{-1}.

EA: calculated: C: 24.96 %, H: 5.24 %, N: 3.64 %; found: C: 24.93 %, H: 5.22 %, N: 3.65 %.

3.5.2.1. *fac*-[$Re(CO)_3(phen)(H_2O)][NO_3$] – [3]:

ReAA (0.100 g, 0.13 mmol) was dissolved in 20 ml of water (pH 2-nitric acid) by stirring for a few minutes until all solids dissolved at room temperature. $AgNO_3$ (0.066 g, 0.39 mmol) was added to the solution and stirred for 24 hours at room temperature. The precipitate, AgBr, was filtered off. 1,10-phenanthroline was dissolved in 5 ml of methanol, added to the filtrate and stirred for another 24 hours at room temperature. The precipitate was filtered and dried.

Yield: 0.0616 g (84 %).

IR (ATR, cm^{-1}): ν_{CO} = 2019, 1891.

^{1}H NMR (300 MHz, Acetone-*d6*): δ 9.6 (dd, *J* = 1.40, 5.10 Hz, 2H), 9.1 (dd, *J* = 1.37, 8.32 Hz, 2H), 8.4 (s, 2H), 8.2 (dd, *J* = 5.15, 8.31 Hz, 2H).

^{13}C NMR (600 MHz, Methanol-*d4*): δ 154, 147, 140, 131, 128, 127.

UV/Vis: ε (λ_{max} = 265 nm) = 32595 M^{-1} cm^{-1}.

3.5.2.2 *fac*-[$Re(CO)_3(phen)(Br)$] - [4]:

ReAA (0.108 g, 0.14 mmol) was dissolved in 20 ml of methanol and stirred for a few minutes until all solids dissolved at room temperature. 1,1-Phenanthroline (0.034 g, 0.188 mmol) was added to the solution and stirred for 24 hours at room temperature. The yellow precipitate, was filtered off and dried.

Yield: 0.0636 g (86 %).

IR (ATR, cm^{-1}): ν_{CO} = 2014, 1926, 1887.

^{1}H NMR (400 MHz, Chloroform-*d6*)): δ 9.4 (dd, *J* = 1.42, 5.16 Hz, 2H), 8.6 (dd, *J* = 1.39, 8.24 Hz, 2H), 8.0 (s, 2H), 7.9 (dd, *J* = 5.10, 8.23 Hz, 2H).

^{13}C NMR (600 MHz, Methanol-*d4*): δ 154, 147, 140, 131, 128, 127.

UV/Vis: ε (λ_{max} = 265 nm) = 16202 M^{-1} cm^{-1}.

3.5.3. *fac*-[Re(CO)$_3$(phenO$_2$)Br] - [5]:

ReAA (0.2001 g, 0.259 mmol) was dissolved in 20 ml of methanol by stirring for a few minutes until all solids dissolved at room temperature. 1,10-Phenanthroline-5,6-dione (0.0537 g, 0.26 mmol) was added to the solution and stirred for 24 hours at room temperature. The methanol was removed by vacuum and precipitate was washed with ethanol and dried.

Yield: 0.1003 g (69 %).

IR (ATR, cm^{-1}): ν_{CO} = 2024, 1937, 1878.

^{1}H NMR (600 MHz, Acetone-*d6*): δ 9.4 (dd, *J* = 1.51, 5.43Hz, 2H), 8.8 (dd, *J* = 1.51, 7.94Hz, 2H), 8.1 (dd, *J* = 5.49, 7.94Hz, 2H).

^{13}C NMR (600 MHz, Acetone-*d6*): δ 175, 157, 155, 138, 131, 129.

UV/Vis: ε (λ_{max} = 298 nm) = 6766 M^{-1} cm^{-1}.

3.5.4. *fac*-[Re(CO)$_3$(phen)(PPh$_3$)][NO$_3$] – [6]:

fac-[Re(CO)$_3$(phen)(H$_2$O)][NO$_3$] (0.053 g, 0.1 mmol) was dissolved in methanol (10 ml) and a methanol solution of PPh$_3$ (0.026 g, 0.1 mmol) (5 ml) was added. The solution was stirred for 24 hours at 50 °C. The light yellow solution was filtered and the precipitate was dried.

Yield: 0.045 g (52 %).

IR (ATR, cm^{-1}): ν_{CO} = 2022, 1906, 1878.

^{1}H NMR (300 MHz, Methanol-*d4*): δ 9.6 (dd, *J* = 1.35, 5.06 Hz, 2H), 9.0 (dd, *J* = 1.40, 8.26 Hz, 2H), 8.4 (s, 2H), 8.2 (dd, *J* = 5.14, 8.29 Hz, 2H), 7.4 (m, 9H) and 7.3 (m, 6H).

^{13}C NMR (400 MHz, Methanol-*d4*): δ 156, 141, 133, 132, 129, 128, 135, 130, 129.

^{31}P NMR (400 MHz, Acetone-*d6*): δ 24.4.

UV/Vis: ε (λ_{max} = 265 nm) = 11490 M^{-1} cm^{-1}.

3.5.5. *fac*-[Re(CO)$_3$(phen)(PTA)][NO$_3$] – [7]:

fac-[Re(CO)$_3$(phen)(H$_2$O)][NO$_3$] (0.053 g, 0.1 mmol) was dissolved in methanol (10 ml) and a methanol solution of PTA (0.157 g, 0.1 mmol) (5 ml) was added. The solution was stirred for 24 hours at 50 °C. The methanol was removed by rotary evaporation and the precipitate was dried.

Yield: 0.033 g (51 %).

IR (ATR, cm^{-1}): ν_{CO} = 2014, 1927, 1888.

^{1}H NMR (600 MHz, Deuteriumoxide-*d1*): δ 9.44 (d, *J* = 5.15 Hz, 2H), 8.83 (d, *J* = 8.11 Hz, 2H), 8.19 (s, 2H), 8.00 (dd, *J* = 5.21, 8.30 Hz, 2H), 4.29 (dd, *J* = 13.22, 25.58 Hz, 6H), 4.18 (d, *J* = 12.96 Hz, 2H) and 4.11 (d, *J* = 13.09 Hz, 4H).

^{13}C NMR (400 MHz, Methanol-*d4*): δ 155, 146, 140, 132, 128, 127, 71, 54.

^{31}P NMR (400 MHz, Acetone-*d6*): δ -15.4.

UV/Vis: ε (λ_{max} = 265 nm) = 13146 M^{-1} cm^{-1}.

3.5.6. *fac*-[Re(CO)$_3$(phen)(DAPTA)][NO$_3$] – [8]:

fac-[Re(CO)$_3$(phen)(H$_2$O)][NO$_3$] (0.054 g, 0.1 mmol) was dissolved in methanol (15 ml) and a methanol solution of DAPTA (0.023 g, 0.1 mmol) (5 ml) was added. The solution was stirred for 24 hours at 50 ºC. The methanol was removed by rotary evaporation and the yellow precipitate was dissolved in methanol and was left to crystallize.

Yield: 0.517 g (70 %).

IR (ATR, cm^{-1}): ν_{CO} = 2015, 1927, 1888.

^{1}H NMR (400 MHz, Chloroform-*d*): δ 9.4 (d, *J* = 17.43 Hz, 2H), 8.6 (dd, *J* = 7.97, 20.10 Hz, 2H), 8.1 (d, *J* = 8.47 Hz, 2H), 7.9 (t, *J* = 6.67 Hz, 2H), 5.7 (d, *J* = 14.23 Hz, 2H), 5.5 (t, *J* = 15.59 Hz, 2H), 4.9 (d, *J* = 14.23 Hz, 2H), 4.4 (q, *J* = 12.20 Hz, 4H), 3.9 (d, *J* = 14.23 Hz, 2H) and 3.8 (d, *J* = 7.46 Hz, 4H).

^{13}C NMR (600 MHz, Chloroform-*d*): δ 170, 154, 139, 128, 126, 67, 62, 53, 46, 42, and 21.

^{31}P NMR (400 MHz, Acetone-*d6*): δ 1.75.

UV/Vis: ε (λ_{max} = 265 nm) = 31185 M^{-1} cm^{-1}.

3.6. Synthesis of dicarbonyl complexes:

3.6.1. *cis*-[Re(CO)$_2$(phen)(PPh$_3$)$_2$][NO$_3$] – [9]:

fac-[Re(CO)$_3$(phen)(H$_2$O)][NO$_3$] (0.188 g, 0.346 mmol) and PPh$_3$ (0.182 g, 0.692 mmol) were placed in a round bottom flask with 8 ml of 1,2-dichlorobenzene. The solution was purged with N_2 for 20 minutes. The reaction mixture was refluxed under N_2 for 3-5 hours. A clear-orange solution was obtained, it was cooled to room temperature, and hexane were added to precipitate the yellow-orange product. The product was suction filtered and washed with hexane and diethyl ether before air-dried.

Yield: 0.128 g (44 %).

IR (ATR, cm^{-1}): ν_{CO} = 2014, 1927, 1887.

^{1}H NMR (300 MHz, Acetone-*d6*): δ 9.5 (dd, *J* = 1.35, 5.15 Hz, 2H), 9.0 (dd, *J* = 1.36, 8.22 Hz, 2H), 8.4 (s, 2H), 8.1 (dd, *J* = 5.14, 8.27 Hz, 2H), 7.4 (m, 9H) and 7.3 (m, 6H).

^{13}C NMR (600 MHz, DMSO-*d6*): δ 155, 152, 146, 141, 139, 131, 129, 128, 125.

^{31}P NMR (400 MHz, Acetone-*d6*): δ -92.9.

UV/Vis: ε (λ_{max} = 266 nm) = 12961 M^{-1} cm^{-1}.

3.6.2. *cis*-[Re(CO)$_2$(phen)(PTA)$_2$][NO$_3$] – [10]:

fac-[Re(CO)$_3$(phen)(H$_2$O)][NO$_3$] (0.188 g, 0.346 mmol) and PTA (0.109 g, 0.692 mmol) were placed in a round bottom flask with 8 ml of 1,2-dichlorobenzene. The solution was purged with N_2 for 20 minutes. The reaction mixture was refluxed under N_2 for 3 to 5 hours. An orange solution was obtained, the solution was cooled to room temperature, and hexane were added to precipitate the product. The product was washed with hexane and diethyl ether before air-dried.

Yield: 0.153 g (53 %).

IR (ATR, cm^{-1}): ν_{CO} = 2014, 1928, 1891.

^{1}H NMR (300 MHz, Acetone-*d6*): δ 9.5 (dd, *J* = 1.32, 5.14 Hz, 2H), 8.9 (dd, *J* = 1.47, 8.35 Hz, 2H), 8.4 (s, 2H), 8.2 (dd, *J* = 5.09, 8.49 Hz, 2H), 4.6 (s, 6H) and 4.4 (dd, *J* = 3.38, 21.00 Hz, 5H).

^{13}C NMR (600 MHz, Acetone-*d6*): δ 156, 152, 146, 140, 129, 127, 72, 48.

^{31}P NMR (400 MHz, Acetone-*d6*): δ -80.24.

UV/Vis: ε (λ_{max} = 262 nm) = 14465 M^{-1} cm^{-1}.

3.6.3. *cis*-[Re(CO)$_2$(phen)(DAPTA)$_2$][NO$_3$] – [11]:

fac-[Re(CO)$_3$(phen)(H$_2$O)][NO$_3$] (0.184 g, 0.346 mmol) and DAPTA (0.159 g, 0.692 mmol) were placed in a round bottom flask with 8 ml of 1,2-dichlorobenzene. The solution was purged with N_2 for 20 minutes. The reaction mixture was refluxed under N_2 for 3 to 5 hours. An orange solution was obtained and the solution was cooled to room temperature, hexane were added to precipitate the product. The product was washed with hexane and diethyl ether before air-dried.

Yield: 0.128 g (45 %).

IR (ATR, cm^{-1}): ν_{CO} = 2015, 1926, 1888.

^{1}H NMR (400 MHz, Acetone-*d6*): δ 9.47 (dd, *J* = 1.4, 5.1 Hz, 2H), 8.98 (dd, *J* = 1.4, 8.3 Hz, 2H), 8.36 (s, 2H), 8.13 (dd, *J* = 5.1, 8.3 Hz, 2H), 5.57 (d, *J* = 13.5, 3H), 5.37 (d, *J* = 13.3 Hz, 1H), 5.03 (ddd, *J* = 17.4, 15.5, 1.9 Hz, 3H), 4.90 (dd, *J* = 14.2 Hz, 2H), 4.75 (d, *J* = 14.2 Hz, 1H), 4.56 (d, *J* = 13.8 Hz, 3H), 4.34 (dd, *J* = 1.7, 15.3 Hz, 3H), 4.01 (d, *J* = 13.6 Hz, 3H), 3.87 (td, *J* = 13.1, 28.4, 2.6 Hz, 3H), 3.58 (d, *J* = 10.7Hz, 6H) and 3.31 (t, *J* = 15.8 Hz, 4H).

^{13}C NMR (600 MHz, Acetone-*d6*): δ 169, 154, 140, 131, 128, 127, 67, 62, 46, 42, 37, 22.

^{31}P NMR (400 MHz, Acetone-*d6*): δ 9.17.

UV/Vis: ε (λ_{max} = 265 nm) = 8279 M^{-1} cm^{-1}.

3.6.4. *cis*-[Re(CO)$_2$(phen)(PPh$_3$)(Cl)] – [12]:

TMAO (0.013 g, 0.177 mmol) was dissolved in a mixture of DCM (48 ml) and methanol (2 ml).

A solution of *fac*-[Re(CO)$_3$(phen)(PPh$_3$)] (0.068 g, 0.118 mmol) and NEt$_4$Cl (0.307 g, 1.85 mmol) in DCM (39 ml) was refluxed at 50 °C. The TMAO solution was added dropwise over a period of 1 hour to the reaction mixture observing a colour change from light yellow to dark red. The solution was refluxed for 24 hours. The DCM/methanol solvent was removed by rotary evaporation and the remaining solid was suspended in 20 ml of methanol. The solid was isolated by centrifugation and suspended in 5 to 10 ml of methanol (3 times). The red solid was collected as the product.

Yield: 0.0341 g (55 %).

IR (KBr, cm^{-1}): ν_{CO} = 2014, 1923, 1884.

^{1}H NMR (400 MHz, DMSO-*d6*): δ 9.45 (dd, *J* = 1.31, 5.10 Hz, 2H), 9.01 (dd, *J* = 1.35, 8.24 Hz, 2H), 8.35 (s, 2H), 7.66-7.54 (m, 15H).

^{13}C NMR (600 MHz, DMSO-*d6*): δ 154, 140, 134, 133, 132, 131, 129, 128, 127.

^{31}P NMR (400 MHz, DMSO-*d*6): δ 25.54.

UV/Vis: ε (λ_{max} = 266 nm) = 5641 M^{-1} cm^{-1}.

3.6.5. *cis*-[Re(CO)$_2$(phen)(PTA)(Cl)] – [13]:

TMAO (0.0239 g, 0.318 mmol) was dissolved in a mixture of DCM (105 ml) and methanol (4 ml). A solution of *fac*-[Re(CO)$_3$(phen)(PTA)] (0.173 g, 0.258 mmol) and NEt$_4$Cl (0.672 g, 4.056 mmol) in DCM (85 ml) was refluxed at 50 °C. The TMAO solution was added dropwise over a period of 1 hour to the reaction mixture observing a colour change from light yellow to dark red. The solution was refluxed for 24 hours. The DCM/methanol solvent was removed by rotary evaporation and the remaining solid was suspended in 20 ml of methanol. The solid was isolated by centrifugation and suspended in 5 to 10 ml of methanol 3 times. The red solid was collected as the product.

Yield: 0.0932 g (53 %).

IR (ATR, cm^{-1}): ν_{CO} = 2013, 1924, 1883.

^{1}H NMR (400 MHz, DCM-*d2*): δ 9.39 (dd, *J* = 1.4, 5.1 Hz, 2H), 8.75 (dd, *J* = 1.4, 8.2 Hz, 2H), 8.17 (s, 2H), 7.99 (dd, *J* = 5.1, 8.22 Hz, 2H), 4.67 (q, *J* = 13.2, 24.5, 37.1 Hz, 2H), 4.41 (s, 2H), 4.33 (d, *J* = 13.1 Hz, 4H) and 4.15 (dd, *J* = 0.99, 12.5 Hz, 4H).

^{13}C NMR (600 MHz, DMSO-*d6*): δ 154, 146, 140, 131, 128, 127, 71.

^{31}P NMR (400 MHz, DCM- *d*2): δ -13.65.

UV/Vis: ε (λ_{max} = 268 nm) = 2399 M^{-1} cm^{-1}.

3.6.6. *cis*-[Re(CO)$_2$(phen)(DAPTA)(Cl)] – [14]:

TMAO (0.0082 g, 0.109 mmol) was dissolved in a mixture of DCM (35 ml) and methanol (2 ml).

A solution of *fac*-[Re(CO)$_3$(phen)(DAPTA)] (0.064 g, 0.0858 mmol) and NEt$_4$Cl (0.227 g, 1.368 mmol) in DCM (28 ml) was refluxed at 50 °C. The TMAO solution was added dropwise over a period of 1 hour to the reaction mixture observing a colour change from light yellow to dark red. The solution was refluxed for 24 hours. The DCM/methanol solvent was removed by rotary evaporation and the remaining solid was suspended in 20 ml of methanol. The solid was isolated by centrifugation and suspended in 5 to 10 ml of methanol (3 times). The red solid was collected as the product.

Yield: 0.03266 g (55 %).

IR (ATR, cm^{-1}): ν_{CO} = 2015, 1926, 1886.

^{1}H NMR (400 MHz, Chloroform-*d*): δ 9.42 (dd, *J* = 1.31, 5.07 Hz, 2H), 8.62 (dd, *J* = 1.48, 8.28 Hz, 2H), 8.09 (d, *J* = 5.94 Hz, 2H), 7.94 (dd, *J* = 5.07, 8.37 Hz, 2H), 5.70 (d, *J* = 14.06 Hz, 1H), 5.48 (t, *J* = 15.94, 15.96 Hz, 1H), 5.13 (s, 2H), 4.83 (dd, *J* = 13.96, 30.21 Hz, 3H), 4.40 (t, J = 13.69, 15.90 Hz, 3H), 4.20 (d, *J* = 14.13 Hz, 1H), 4.01 (m, 1H), 3.90 (d, *J* = 14.57 Hz, 1H) and 3.80 (m, 3H).

^{13}C NMR (600 MHz, DMSO-*d6*): δ 169, 154, 146, 140, 128, 127, 52, 44, 42, 23, 22.

^{31}P NMR (400 MHz, Chloroform-*d*): δ 1.82.

UV/Vis: ε (λ_{max} = 269 nm) = 4041 M^{-1} cm^{-1}.

3.7. Synthesis of dinuclear complexes:

3.7.1. $[NEt_4]_2[Re_2(CO)_6(\mu\text{-phen}(NH)_2)Br_2]$ – [15]:

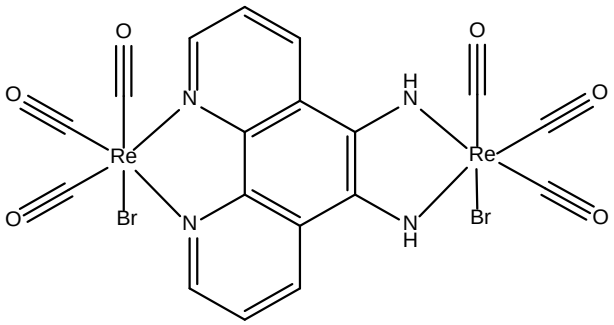

Figure 3.3: Illustration of the $[NEt_4]_2[Re_2(CO)_6(\mu\text{-phen}(NH_2)_2)Br_2]$ dinuclear complex.

ReAA (0.206 g, 0.268 mmol) was added to 1,10-phenanthroline-5,6-diamine (0.0268 g, 0.127 mmol) in water (30 ml) and stirred at 70 °C for 2 days. A colour change are observable from dark blue to purple. The volume was reduced to a third, precipitate was filtered off and continued to be stirred and the isolation of the product resulted in the formation of more product.

Yield: 0.0159 g (23 %).

IR (ATR, cm^{-1}): ν_{CO} = 2021, 1948, 1921, 1901.

^{1}H NMR (600 MHz, Acetone-*d6*): δ 9.4 (dd, *J* = 1.49, 5.42 Hz, 2H), 9.0 (dd, *J* = 1.49, 8.03 Hz, 2H) and (dd, *J* = 5.51, 8.03, 2H).

^{13}C NMR (600 MHz, Acetone-*d6*): δ 156, 135, 128.

UV/Vis: ε (λ_{max} = 258 nm) = 2426 M^{-1} cm^{-1}.

EA: calculated: C: 34.93 %, H: 4.14 %, N: 7.19 %; found: C: 34.95 %, H: 4.11 %, N: 7.22 %.

3.7.2. $[Re(CO)_3Br(\mu\text{-}phenO_2)Re(CO)_3Br]$ – [16]:

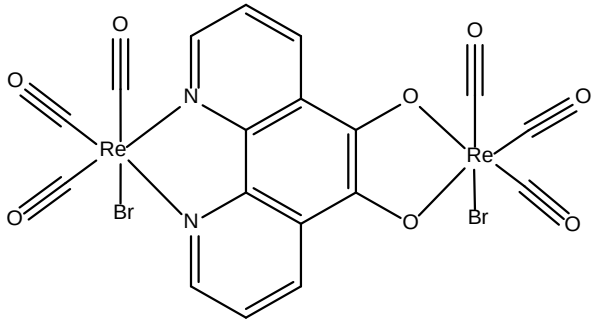

Figure 2.4: Illustration of the $[Re_2(CO)_6(\mu\text{-}phenO_2)Br_2]$ dinuclear complex.

ReAA (0.206 g, 0.268 mmol) was added to 1,10-phenanthroline-5,6-dione (0.0268 g, 0.127 mmol) in toluene (30 ml) and refluxed at 90 °C for 2 days. A colour change are observable from yellow to orange. The orange precipitate was filter off and dried.

Yield: 0.0159 g (23 %).

IR (ATR, cm^{-1}): ν_{CO} = 2021, 1948, 1921, 1901.

^{1}H NMR (600 MHz, Acetone-*d6*): δ 9.4 (dd, *J* = 1.49, 5.42 Hz, 2H), 9.0 (dd, *J* = 1.49, 8.03 Hz, 2H) and (dd, *J* = 5.51, 8.03, 2H).

^{13}C NMR (600 MHz, Chloroform-*d*): δ 138, 129, 128, 127, 125.

UV/Vis: ε (λ_{max} = 293 nm) = 7815 M^{-1} cm^{-1}.

EA: calculated: C: 23.75 %, H: 0.66 %, N: 3.08 %; found: C: 23.74 %, H: 0.70 %, N: 3.05 %.

3.8. Synthesis of Bi-metallic complexes:

3.8.1. $[Ru(phen)_2(N,N'\text{-}phenO_2\text{-}O,O')\text{-}Re(CO)_3Br][PF_6]_3$ – [17]:

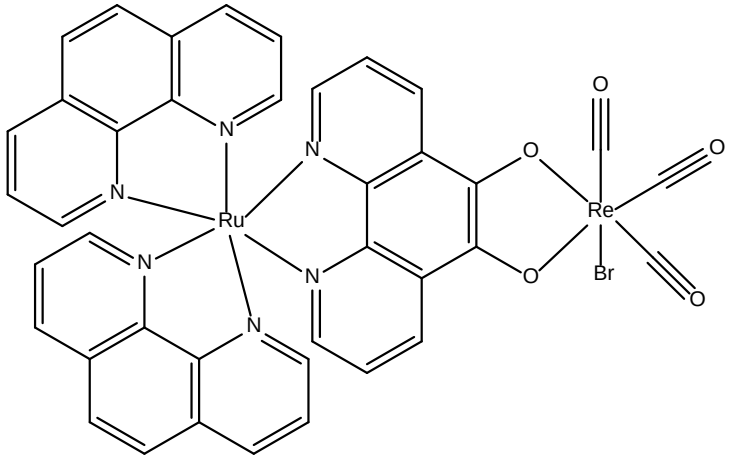

Figure 3.5: Illustration of $[Ru(phen)_2(N,N'\text{-}phenO_2\text{-}O,O')\text{-}Re(CO)_3Br][PF_6]_3$.

$[Ru(phen)_2(phenO_2)][PF_6]_3$ (0.0346 g, 0.0313 mmol) was reacted with ReAA (0.0268 g, 0.0348 mmol) in methanol (30 ml) and stirred at room temperature for 48 hours. A colour change was observed from brown to black. The solvent was removed by rotary evaporation and the product was recrystallized with acetone:ethanol (2:1). Crystals that were not suitable for single crystal x-ray diffraction were obtained.

Yield: 0.0342 g (25 %).

IR (ATR, cm^{-1}): ν_{CO} = 2017, 1884.

^{1}H NMR (600 MHz, Deuteriumoxide-*d2*): δ 9.15 (d, *J* = 3.6 Hz, 4H), 8.50 (dd, *J* = 1.1, 8.3 Hz, 4H), 8.15 (s, 4H), 7.51 (dd, *J* = 5.3, 8.3 Hz, 4H), 8.89 (d, *J* = 8.5 Hz, 2H), 8.09 (dd, 5.0, 7.9 Hz, 2H), 8.03 (dd, *J* = 1.1, 5.2 Hz, 2H).

UV/Vis: ε (λ_{max} = 427 nm) = 6010 M^{-1} cm^{-1}.

EA: calculated: C: 32.16 %, H: 1.52 %, N: 5.77 %; found: C: 32.13 %, H: 1.56 %, N: 5.79 %.

3.8.2. $[Ru(phen)_2(N,N'\text{-}phenO_2\text{-}O,O')\text{-}PtCl_2][PF_6]_3$ – [18]:

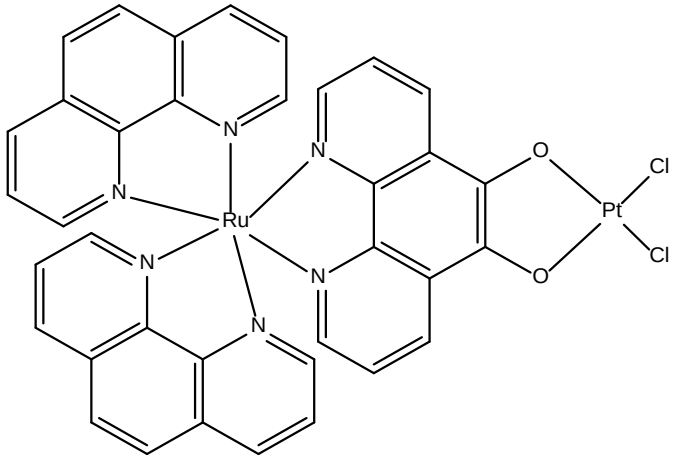

Figure 3.6: Illustration of $[Ru(phen)_2(N,N'\text{-}phenO_2\text{-}O,O')\text{-}PtCl_2][PF_6]_3$ complex.

$[Ru(phen)_2(phenO_2)][PF_6]_3$ (0.0692 g, 0.0625 mmol) was dissolved in methanol (30 ml) and K_2PtCl_4 (0.0288 g, 0.0695 mmol) and refluxed for 24 hours at 80 °C. After the completion of the reaction, the methanol was removed and the product was collected and dried.

Yield: 0.0603 g (96 %).

IR (ATR, cm^{-1}): ν_{CO} = 1695.

^{1}H NMR (600 MHz, Chloroform-*d*): δ 9.35 (dd, *J* = 1.3, 5.0 Hz, 2H), 8.50 (dd, *J* = 1.2, 8.1 Hz, 2H), 8.44 (d, *J* = 7.2 Hz, 4H), 8.17 (s, 4H), 8.05 (s, 4H), 7.97 (d, *J* = 4.2 Hz, 2H) and 7.86 (m, 4H).

UV/Vis: ε (λ_{max} = 311 nm) = 2217 M^{-1} cm^{-1}.

EA: calculated: C: 31.50 %, H: 1.62 %, N: 6.12 %; found: C: 31.47 %, H: 1.59 %, N: 6.16 %.

3.8.3. $[Re(CO)_3(N,N'\text{-}phenO_2\text{-}O,O')\text{-}PtCl_2]Br$ – [19]:

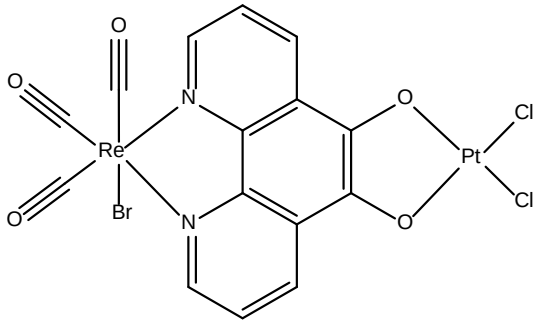

Figure 3.7: Illustration of the $[Re(CO)_3(N,N'\text{-}phenO_2\text{-}O,O')\text{-}PtCl_2]Br$ complex.

fac-[Re(CO)$_3$(phenO$_2$)(Br)] (0.035 g, 0.0625 mmol) was dissolved in methanol (30 ml) and K_2PtCl_4 (0.0288 g, 0.0695 mmol) were added. The reaction mixture were stirred at 50 °C for 5 days till a colour change from orange to brown were observed. The methanol was removed and the product was collected and dried.

Yield: 0.0492 g (98 %).

IR (ATR, cm^{-1}): ν_{CO} = 2021, 1881, 1693.

^{1}H NMR (600 MHz, Chloroform-*d*): δ 9.33 (dd, *J* = 1.5, 5.4 Hz, 2H), 8.75 (dd, *J* = 1.5, 7.9 Hz, 2H) and 7.89 (dd, *J* = 5.4, 7.9 Hz, 2H).

^{13}C NMR (600 MHz, Chloroform-*d*): δ 158, 155, 140, 139, 130, 129.

UV/Vis: ε (λ_{max} = 419 nm) = 3245 M^{-1} cm^{-1}.

EA: calculated: C: 21.80 %, H: 0.73 %, N: 3.39 %; found: C: 21.76 %, H: 0.74 %, N: 3.40 %.

3.9. Discussion:

In this chapter, the synthesis of the bidentate ligands, 1,10-phenanthrolin-5,6-dione (phenO$_2$) and 1,10-phenathroline-5,6-diamine (phen(NH$_2$)$_2$) as well as a few Re(I) tri- and dicarbonyl complexes was successfully synthesized. Three bimetallic compounds with phenO$_2$ as the bridging ligand was successfully synthesized as well as the two Re(I) dinuclear compounds with phenO$_2$ and (phen(NH$_2$)$_2$ as bridging ligand. The Re(I) compounds were mainly synthesized for photoluminescence evaluation studies and this is reported in Chapter 5. Ru(III) compounds were synthesized for the formation of bimetallic complexes and to study the toxicity of these complexes as reported in Chapter 6. Bimetallic compounds have two metal centres, where each metal alone have good therapeutic and diagnostic properties respectively. The combination of two metal centres give rise to compounds with altering properties.

PhenO$_2$ was successfully synthesized according to Zheng *et al.*[4], Calderazzo *et al.* [5] *and* Ocakoglu *et al.*[6] Two different methods were used for the synthesis of phenO$_2$. The first method are time

[4] R. H Zheng, H. C. Guo, H. J. Jiang, K. H. Xu, B. B. Lu, W. L. Sun and Z. Q. Shen, *Chinese Chemical Letters*, **2010**, 21, 1270-1272.

[5] F. Calderazzo, F. Marchetti, G. Pampaloni and V. Passarelli, *Journal of the Chemical Society and Dalton Transactions*, **1999**, 4389-4396.

[6] K. Ocakoglu, C. Zafer, B. Cetinkaya and S. Icli, *Dyes and Pigments*, **2007**, 75, 385-394.

consuming and resulted in very low yields [4], while the second method gave higher yields and was not time intensive.[5,6]

1,10-phenanthroline-5,6-diamine (phen(NH_2)$_2$) were synthesized according to C. Young[7] in a three step synthetic procedure. In the first step phen is functionalized with a nitro group on the 5th position using sulfuric- and nitric acid with potassium bromide, refluxing the mixture at 170 °C. After the isolation of 5-nitro-1,10-phenanthroline, it was refluxed in methanol and dioxane at 60 °C and then cooled to 4 °C resulting in a yellow orange precipitate, 5-nitro-6-amino-1,10-phenanthroline. The 5-nitro-6-amino-1,10-phenanthroline is converted to phendiamine, by adding Pd on carbon and hydrazine hydrate and refluxing the mixture in ethanol. Crystals were grown in methanol and ethanol, but were not suitable for single crystal X-ray diffraction.

Rhenium(I) tri- and dicarbonyl complexes were synthesized with different N,N-bidentate ligands, 1,10-phenanthroline and 1,10-phenanthroline-5,6-dione. Tricarbonyl carbon atom peaks requires a long relaxation time to obtain the carbon peaks of the rhenium(I) complexes on the ^{13}C NMR spectrometer. Bearing in mind the financial implication and the long time to obtain the carbon peaks of the carbonyl ligands, it was decided not to repeat it and we used IR to confirm the presence of the carbonyl ligands.

UV/Vis evaluations of Re(I) compounds are obtained in methanol at 25 °C and the absorption wavelengths of these compounds vary from 262 nm to 298 nm (Table 3.1). The molar absorptivity coefficient were calculated and no trend is observed as expected between the monophosphine and bisphosphine compounds.

The IR stretching frequencies of the carbonyl ligands of the synthesized Re(I) tri- and dicarbonyl complexes are tabulated in Table 3.1. The carbonyl stretching frequencies range from 2013 – 1878 cm^{-1}. The carbonyl stretching frequencies of the Re(I) tricarbonyl complexes are similar to the Re(I) dicarbonyl complexes and no definite difference is observed between them. These carbonyl ligands are coordinated to the metal center and when the density on the metal center decrease, a decrease in the electron back donation from the metal to the anti-bonding orbitals of the carbon atoms are observed. The decrease causes weak Re-CO bonds and strengthens the C≡O bond with an increase in the carbonyl stretching frequency. The phosphine ligands used in this study are arranged in the order of decreasing π-acceptor and increasing σ-donor properties as well as the

[7] C. Young, **2012**, 'Bulky metal complexes as model nanoscale catalysts', Dissertation for Philosophiae Scientae, University of the Free State, Bloemfontein.

trans influence: PPh_3 > PTA > DAPTA. A decrease in the carbonyl stretching frequency are expected due to the increase in electron density of the phosphine ligands: $\nu_{CO}(PPh_3) < \nu_{CO}(PTA) < \nu_{CO}(DAPTA)$. No specific trend is seen between **6**, **7**, **8** and **9**, **10** and **11** with regards to the π-acceaptor, σ-donor and *trans* influence properties of the phosphine ligands. Both the monophosphine and bisphosphine complexes have similar ν_{CO} frequencies. The same is seen in **12**, **13** and **14**, where no trend is observed, with only a slight difference in ν_{CO}.

Table 3.1: Summary of the molar absorptivity, carbonyl stretching frequencies (ν_{CO}/cm^{-1}), wavelenghts (nm) and the ^{31}P NMR chemical shifts δ (ppm) of the Re(I) synthesized compounds.

	Complex Name	Molar absorptivity coefficient (ε) (M^{-1} cm^{-1})	Carbonyl stretching frequencies (ν_{CO}/cm^{-1})	λ_{max} (nm)	^{31}P NMR Chemical shift δ (ppm)
3	***fac*-[Re(CO)$_3$(phen)(H$_2$O)][NO$_3$]**	32595	2019, 1891	265	-
5	***fac*-[Re(CO)$_3$(phenO$_2$)][Br]**	6766	2024, 1937, 1878	298	-
6	***fac*-[Re(CO)$_3$(phen)(PPh$_3$)][NO$_3$]**	11490	2022, 1906,1878	265	24.4
7	***fac*-[Re(CO)$_3$(phen)(PTA)][NO$_3$]**	13146	2014, 1927, 1888	265	-15.4
8	***fac*-[Re(CO)$_3$(phen)(DAPTA)][NO$_3$]**	31185	2015, 1927, 1888	265	1.75
9	***cis-trans*-[Re(CO)$_2$(phen)(PPh$_3$)$_2$][NO$_3$]**	12961	2014, 1927, 1887	266	-92.9
10	***cis-trans*-[Re(CO)$_2$(phen)(PTA)$_2$][NO$_3$]**	14465	2014, 1928, 1891	262	-80.24
11	***cis-trans*-[Re(CO)$_2$(phen)(DAPTA)$_2$][NO$_3$]**	8279	2015, 1926, 1888	265	9.17
12	***cis*-[Re(CO)$_2$(phen)(PPh$_3$)(Cl)]**	5641	2014, 1923, 1883	266	25.54
13	***cis*-[Re(CO)$_2$(phen)(PTA)(Cl)]**	2399	2013, 1924, 1883	268	-13.65
14	***cis*-[Re(CO)$_2$(phen)(DAPTA)(Cl)]**	4041	2015, 1926, 1886	269	1.82

The ^{31}P NMR chemical shifts of the complexes are given in Table 3.1 and shows single peaks for each complex. The chemical shifts obtained from ^{31}P NMR give important information about the electronic environment experienced by the nuclei. More electron donating phosphines would appear at a lower chemical shift while more electron withdrawing phosphines have a higher chemical shift. The electronic effect and the steric size of PR_3 ligands are adjusted when changing

the R group of phosphine ligands. By placing more electron withdrawing groups on the phosphorus atom causes a decrease in the sigma donating capacity of the phosphine ligand. The ^{31}P shifts of the tricarbonyl complexes (**6**, **7**, and **8**) are different form the dicarbonyl complexes (**9**, **10** and **11**) due to the presence of more than one phosphine ligand, but expected a trend of PPh_3 < PTA < DAPTA. The ^{31} P chemical shifts of **7**, **8** and **9** as well as **12**, **13** and **14** are seen as PTA < DAPTA < PPh_3, and are suspected that this result are due to steric hindrance of the phosphine ligands. **9**, **10** and **11** are the only compounds following the trend as expected (PPh_3 < PTA < DAPTA). The chemical shifts of **9**, **10** and **11** differs a lot from **6**, **7** and **8**. For **12**, **13**, and **14** the chemical shift are more of less the same than **6**, **7** and **8** although **12**, **13** and **14** are dicarbonyl compounds but contains only one phosphine ligand with a Cl ligand and therefor a trend between **6**, **7**, and **8** and **12**, **13** and **14** are observed.

Photochemical ligand substitution reactions were done twice in different solvents, water and acetonitrile. Rhenium(I) tricarbonyl complex was synthesised according 3.5.2. This complex showed that the carbonyl stretching frequencies were at 2024 cm^{-1} and 1925 cm^{-1}. During this reaction the *fac*-$[Re(CO)_3(phen)(PPh_3)][NO_3]$ were dissolved in acetonitrile and induced by excitation with 350 nm UV-A light for 24 hours for the removal of a CO ligand. Infrared spectrums were taken every 2 hours for 8 measurements to see if any CO ligands were lost. After 2 hours ν_{CO} = 2022 cm^{-1} and 1915 cm^{-1}. After 6 hours of exposure to the UV-A light the ν_{CO} = 2025 cm^{-1} and 1923 cm^{-1} showed a shift in the stretching frequencies but no indication of the loss or removal of one CO ligand. After 24 hours, the IR as well as the NMR indicated that the complex decomposed showing four phosphorus peaks and the stretching frequencies of the CO ligands decreased. The reaction was repeated in water and induced with the UV-A light at 350 nm for 24 hours. After 24 hours no indication of the loss of any CO ligands are observed and therefore a synthesis reaction was done using trimethylamine N-oxide (TMAO) and tetraethyl ammonium chloride (NEt_4Cl) for the release of the CO ligand and the coordination of Cl ligand.[8]

Three novel bimetallic compounds, $[Ru(phen)_2(N,N'\text{-}phenO_2\text{-}O,O')\text{-}Re(CO)_3Br][PF_6]_3$, $[Ru(phen)_2(N,N'\text{-}phenO_2\text{-}O,O')\text{-}PtCl_2][PF_6]_3$ and $[Re(CO)_3(N,N'\text{-}phenO_2\text{-}O,O')\text{-}PtCl_2]Br$ were synthesized and characterized by NMR, IR and elemental analysis. These compounds was synthesized for the aim of being used as PDT agents. The complexes were send for testing their

[8] S. C. Marker, S. N. MacMillan, W. R. Zipfel, Z. Li, P. C. Ford and J. J. Wilson, *Inorganic Chemistry*, **2018**, 57, 1311-1331.

cytotoxicity against a variety of cell lines and the results are reported in Chapter 6. Results were obtained from Wenzel *et al.* who synthesized polymetallic compounds and showed that these complexes are more cytotoxic than monometallic compounds.[9] When two cytotoxic metals like platinum and ruthenium are combined for the formation of bimetallic compounds, they could interact with multiple biological targets.[9]

3.10. Conclusion:

The synthesis and characterisation of the ligands, Ru(III) compounds, Re(I) tri- and dicarbonyl complexes, bimetallic- and dinuclear compounds was reported using IR, UV/Vis, NMR and elemental analysis. The crystallographic data of three compounds are obtained and reported in Chapter 4. Photoluminescence evaluations (PL) was successfully obtained on the Re(I) compounds as reported in Chapter 5 as well as the cytotoxicity results of the bimetallic compounds in Chapter 6.

[9] M. Wenzel, E. Bigaeva, P. Richard, P. Le Gendre, M. Picquet, A. Casini and E. Bodio, *Journal of Inorganic Biochemistry*, **2014**, 141, 10-16.

CHAPTER 4: THE CRYSTALLOGRAPHIC STUDY OF A N,N′-BIDENTATE LIGAND AND RHENIUM(I) COMPLEXES

4.1. Introduction:

Crystallography is the science employed to examine the solid state molecular arrangement of various crystalline compounds. The properties of the inner structure of the crystal are used for the determination of the arrangement of the atoms. Crystallographers can make use of neutron, X-ray or electron diffraction techniques for the characterization and identification of solid materials. The biochemical and pharmaceutical fields depend on crystallography in order to patent absolute structures and all possible isomers. The composition and structures of proteins and biological materials can also be studied with crystallography.

The synthesis of the N,N′-bidentate ligands and the Re(I) complexes were reported in Chapter 3. The following crystals suitable for X-ray diffraction were obtained:

- 5-Amino-6-nitro-1,10-phenanthroline (**phen(NH_2)(NO_2)**),
- *fac*-[$Re(CO)_3(phen)(H_2O)][NO_3]\cdot 1.5H_2O$ (**3**) and
- *fac*-[$Re(CO)_3$(phen)Br] (**4**).

A thorough search of the Cambridge Structure Database revealed that data for 3 was already deposited, but none available for **4** and **phen(NH_2)(NO_2)**.[1] A schematic representation of the synthetic pathway the ligand and the two Re(I) crystals obtained are illustrated in Scheme 4.1 and Scheme 4.2. The crystallographic data of the crystals are summarized in Table 4.1 and Table 4.2.

[1] Cambridge Structural Database (CSD), Version 5.32, Feb 2011 update., F.H. Allen, *Acta Crystallographica*, **2002,** B58, 380.

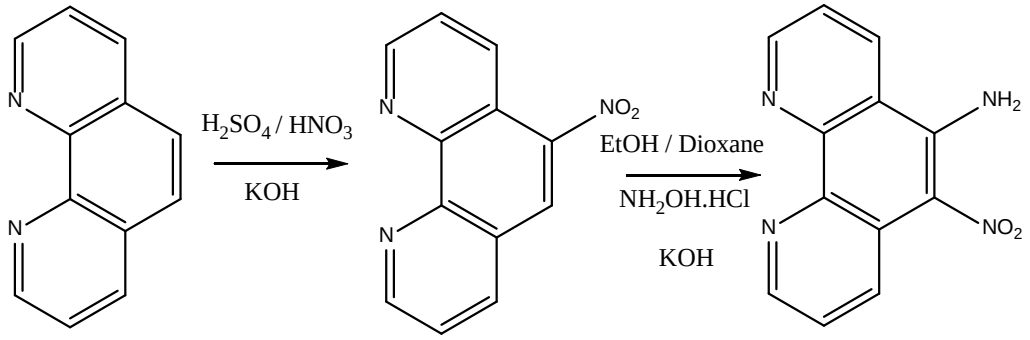

Scheme 4.1: Schematic representation of the formation of 5-amino-6-nitro-1,10-phenanthroline (phen(NH_2)(NO_2)).

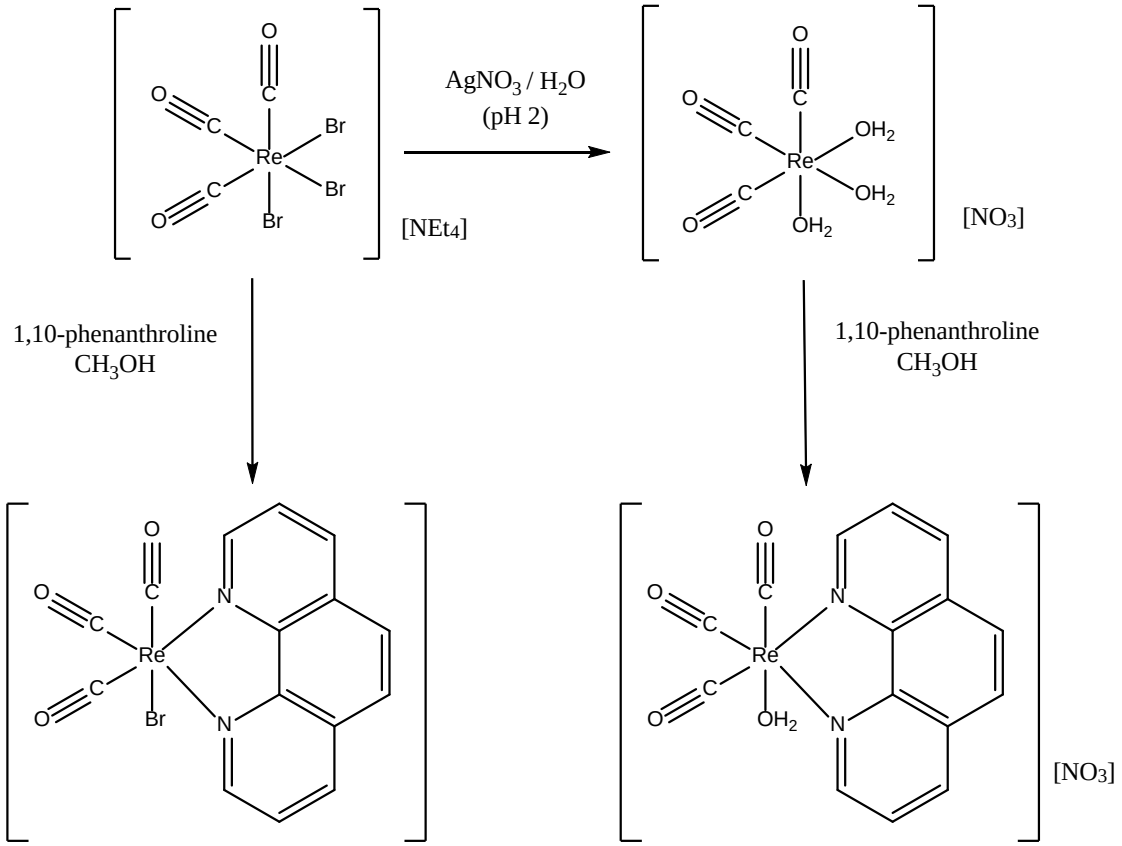

Scheme 4.2: A schematic representation of the synthesis pathways of the 3 and 4.

4.2. Experimental:

Data for all three crystals were collected on a Bruker X8 Apex II 4K diffractometer. The apparatus are equipped with graphite monochromated Mo *K*a radiation sourcwith a wavelength of 0.71073 Å with ω- and ϕ scans at 100K. The crystals were solved using the SIR-97[2] package

[2] A. Altomare, M. C. Burla, M. Camalli, G. L. Cascarano, C. Giacovazzo, A. Guagliardi, A. G. G. Moliterni, G. Polidori and R. Spanga *Journal of Applied Crystallography*, **1999**, 32, 115-119.

and refined with WinGX[3] and SHELXL-97[4]. The molecular graphics were completed with DIAMOND[5] and SADABS[6] software were used with a multi-scan technique to obtain the absorption corrections. All the structures were drawn with thermal ellipsoids with a 50 % probability level and all the non-hydrogen atoms were refined anisotropically. The atomic coordinates, bond distances, angles, anisotropic displacement parameters, torsion angles as well as the hydrogen coordinates of both crystals were reported in this chapter and shown in the supplementary data (Appendix A and B).

There was no time available to repeat these data collections within the time span allowed for this MSc study. Thus, less accurate data sets at 100K were obtained, yielding corresponding less accurate structures, a low completeness and accompanying high R factors throughout. Therefore, R_{int} and refinement agreement indexes, as well as very high goodness-of-fit values, artificial residual electron density peaks, both positive and negative, were obtained. In spite of this draw-back, all complex geometries could be unequivocally obtained as reported herein.

[3] L. J. Farrugia, *Journal of Applied Crystallography*, **1999**, 32, 837-838.

[4] G. M. Sheldrick, SHELXL97, Program for the refinement of crystal structures, University of Göttingen, Germany, **1997**.

[5] K. Brandenburg, H. Putz, DIAMOND, Release 3.0c, Crystal Impact GbR, Bonn, Germany, **2006**.

[6] Bruker, SADABS, Version 2004/1, Bruker AXS Inc., Madison Wisconsin, USA, **1998**.

Table 4.1: Crystallographic data of 5-amino-6-nitro-1,10-phenanthroline (phen(NH_2)(NO_2)) and *fac*-[$Re(CO)_3$(phen)(H_2O)][NO_3]·1.5H_2O (3).

Crystallographic data	**phen(NH_2)(NO_2)**	**3**
Empirical formula	$C_{12}H_8N_4O_2$	$ReC_{15}H_{13}N_3O_{8.5}$
Formula weight (g·mol^{-1})	240.22	557.49
Crystal system	Orthorhombic	Triclinic
Space group	*Pbca*	$\bar{P}$ 1
a (Å)	14.265(8)	10.9974(58)
b (Å)	8.060(4)	13.3905(68)
c (Å)	17.564(9)	14.3337(70)
α (°)	90	107.178(15)
β (°)	90	98.343(14)
γ (°)	90	112.58 (13)
Volume (A^3)	2019.4(19)	1780.15(212)
Z	8	4
ρ_{calc} (g·cm^{-3})	1.580	1.95
Crystal colour	Yellow	Yellow
Crystal morphology	Cuboid	Plate
Crystal size (mm)	0.370 x 0.120 x 0.090	0.220 x 0.157 x 0.047
μ (mm^{-1})	0.113	6.879
F (000)	992	1068.0
θ range (°)	3.987 to 27.998	4.027 to 28.445
Index ranges	$-18 \le h \le 18$ $-7 \le k \le 10$ $-22 \le l \le 23$	$-14 \le h \le 14$ $-17 \le k \le 17$ $-13 \le l \le 17$
Reflections collected	13477	13106
Unique reflections	2426	7090
Reflections with I > 2σ (1)	1204	4328
Rint	0.0933	0.0573
Completeness to theta (°, %)	25.242, 99.6	26.000, 84.4
Data / restraints / parameters	2426 / 0 / 172	7090 / 164 / 499
GooF	1.027	0.978
R [I > 2σ (1)]	R_1 = 0.0579 ; wR_2 = 0.1323	R_1 = 0.0525 ; wR_2 = 0.1253
R (all data)	R_1 = 0.1332 ; wR_2 = 0.1758	R_1 = 0.1004 ; wR_2 = 0.1453
ρ_{max}; ρ_{min} (e A^{-3})	0.355, -0.391	2.372, -1.817

* Phen = 1,10-phenanthroline

Table 4.2: Crystallographic data of *fac*-[Re(CO)$_3$(phen)Br] (4).

Crystallographic data	**4**
Empirical formula	$ReC_{15}H_{12}N_2O_3Br$
Formula weight (g·mol^{-1})	530.34
Crystal system	Triclinic
Space group	$\bar{P}$ 1
a (Å)	8.010(4)
b (Å)	9.955(5)
c (Å)	9.965(5)
α (°)	73.945(11)
β (°)	76.423(13)
γ (°)	76.358(13)
Volume (A^3)	729.8(6)
Z	2
ρ_{calc} (g·cm^{-3})	2.413
Crystal colour	Yellow
Crystal morphology	Cuboid
Crystal size (mm)	0.284 x 0.280 x 0.120
μ (mm^{-1})	11.075
F (000)	492
θ range (°)	4.298 – 27.995
Index ranges	$-10 \leq h \leq 10$ $-12 \leq k \leq 10$ $-13 \leq l \leq 13$
Reflections collected	4776
Unique reflections	3522
Reflections with I > 2σ (1)	2607
Rint	0.0364
Completeness to theta (°, %)	25.242, 84.8
Data / restraints / parameters	2925 / 0 / 199
GooF	1.054
R [I > 2σ (1)]	R_1 = 0.0388 ; wR_2 = 0.1010
R (all data)	R_1 = 0.0442 ; wR_2 = 0.1041
ρ_{max}; ρ_{min} (e A^{-3})	2.739, -2.498

4.3. Crystal structure of 5-amino-6-nitro-1,10-phenanthroline (phen(NH_2)(NO_2)):

The N,N′-bidentate ligand, 5-amino-6-nitro-1,10-phenanthroline was synthesized according to the synthetic procedure in Paragraph 3.3.4 in Chapter 3. Yellow cuboidal crystals were obtained from chloroform. The ligand crystallized in the *Pbca* space group. The molecular structure of **phen(NH_2)(NO_2)** is presented in Figure 4.1.

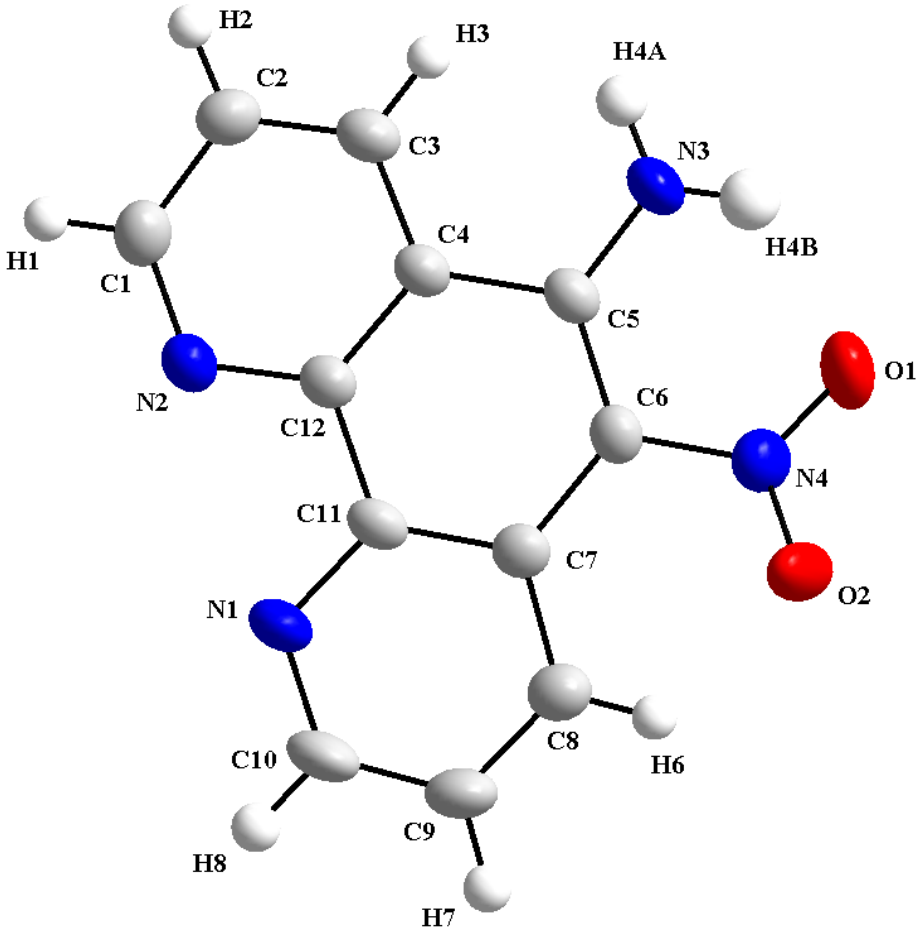

Figure 4.1: Molecular presentation of the crystal structure of 5-amino-6nitro-1,10-phenanthroline.

A summary of the crystal data are given in Table 4.1 and a few selected bond distances and angles of **phen(NH_2)(NO_2)** are reported in Table 4.3.

Table 4.3: Selected bond distances (Å) and angles (°) for the structure phen(NH_2)(NO_2).

Selected Bond lengths (Å)		Selected bond angles (°)	
N1-C10	1.327(3)	C5-N3-H4A	121(2)
N1-C11	1.358(3)	C5-N3-H4B	119(2)
N3-H4A	0.93(4)	H4A-N3-H4B	120(3)
N3-H4B	0.89(3)	O2-N4-O1	120.0(2)
N4-O1	1.244(3)	O2-N4-C6	119.4(2)
N4-O2	1.241(3)	O1-N4-C6	120.5(2)
N2-C12	1.355(3)	C10-N1-C11	118.1(2)
N2-C1	1.331(3)	C1-N2-C12	117.6(2)
C6-N4	1.431(3)		
N3-C5	1.333(3)		

All of the bond distances and angles fall in the same range as for similar molecules.[7]

Phen(NH_2)(NO_2) is basically planar (rms: 0.0389) with O1 and O2 the only atoms significantly out of the plane (C1-C2-C3-C4-C5-C6-C7-C8-C9-C10-C11-C12-N1-N2-N3-N4-H4A-H4B) with the distance between the plane and O1 and O2 being 0.3011 Å and -0.5496 Å respectively.

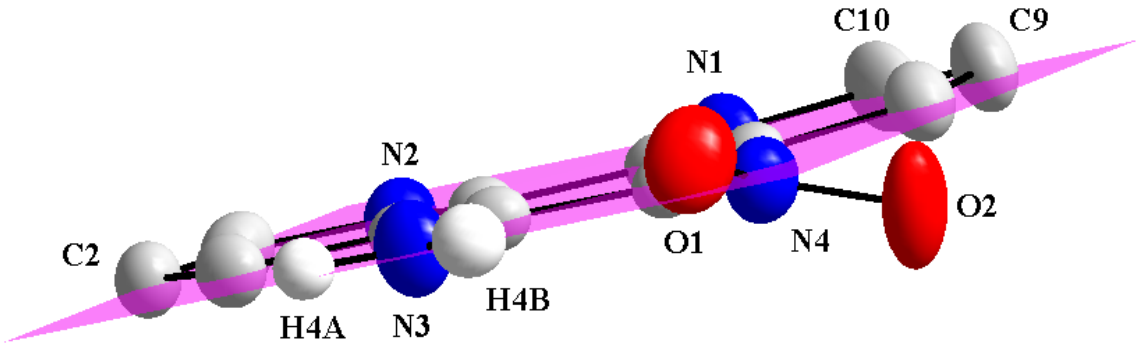

Figure 4.2: Illustration of the plane through N1-N2-C1-C2-C3-C4-C5-C6-C7-C8-C9-C10-C11-C12-N3-H4A-H4B-N4 (pink plane). Hydrogen atoms are omitted for clarity.

There are three N-H…N/O and one C-H…O intermolecular interactions (purple dashed lines) and three intramolecular interactions (green dashed lines). All of the hydrogen bonding interactions of **phen(NH_2)(NO_2)** are illustrated in Figure 4.3. The angles, symmetry operators and distances are given in Table 4.4.

[7] S. F. Haddad, J. A. Marshall, G. A. Crosby and B. Twamley, *Acta Crystallographica*, **2002**, E58, m559-m561.

Table 4.4: A summary of the bonding interactions, bond distances (Å) and angles (°) of phen(NH_2)(NO_2).

D-H…A	d(D-H)	d(H…A)	d(D…A)	<(DHA)
N3-H4A…N1[c]	0.89(3)	2.34(3)	3.092(4)	143(3)
N3-H4A…N2[c]	0.89(3)	2.55(3)	3.111(4)	122(2)
N3-H4B…O1[a]	0.94(4)	1.89(4)	2.571(4)	127(4)
N3-H4B…N4[a]	0.94(4)	2.51(4)	2.841(4)	101(3)
C3-H3…N1[c]	0.95	2.61	3.438(4)	145
C8-H6…O2[a]	0.95	2.12	2.716(4)	119
C9-H7…O1[b]	0.95	2.46	3.395(4)	167

Symmetry code, transformation used to generate equivalent atoms:

[a] x, y, z; [b] x+1/2, -y+3/2, -z+1; [c] x-1/2, y, -z+1/2

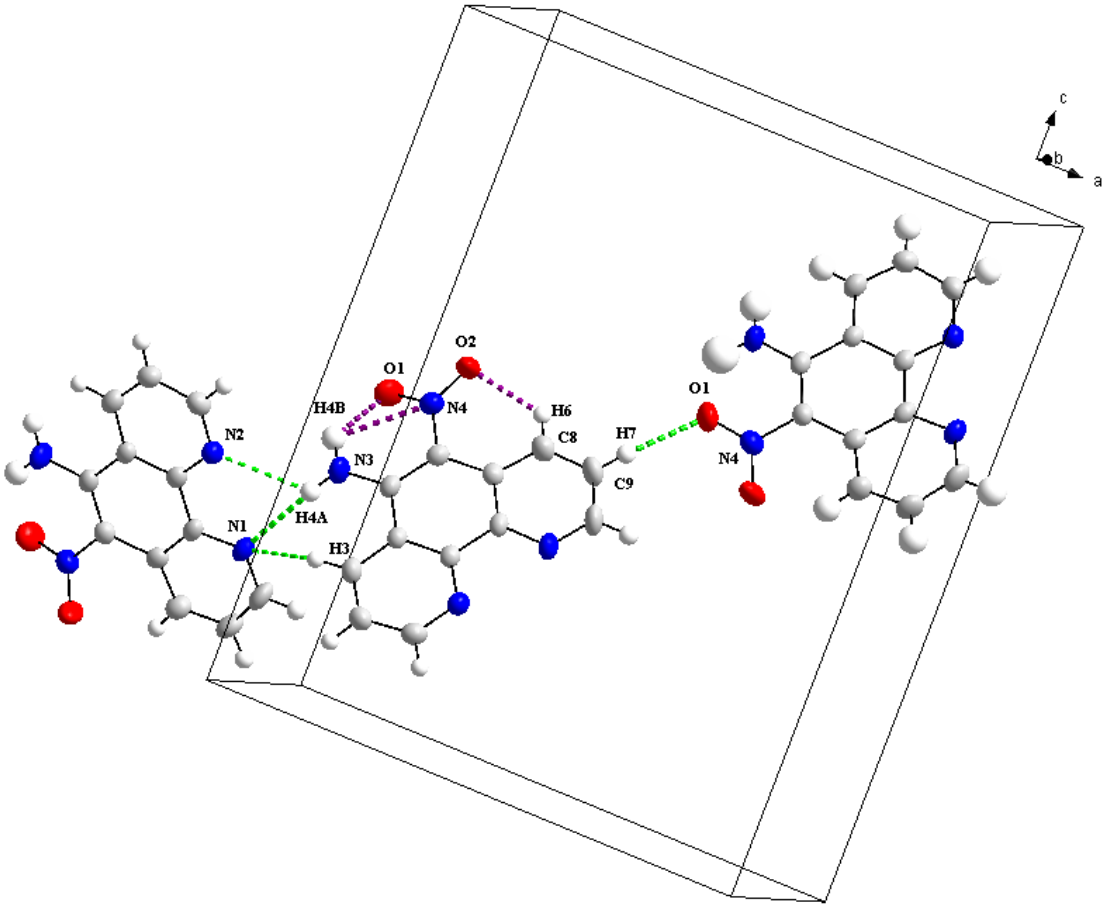

Figure 4.3: Illustration of the intermolecular and intramolecular hydrogen bonding interactions observed in phen(NH_2)(NO_2).

The ligand packs in a column-like fashion 90 ° relative to one another along the *a*-axis when viewed along the *b*,*c*-planes as illustrated in Figure 4.4.

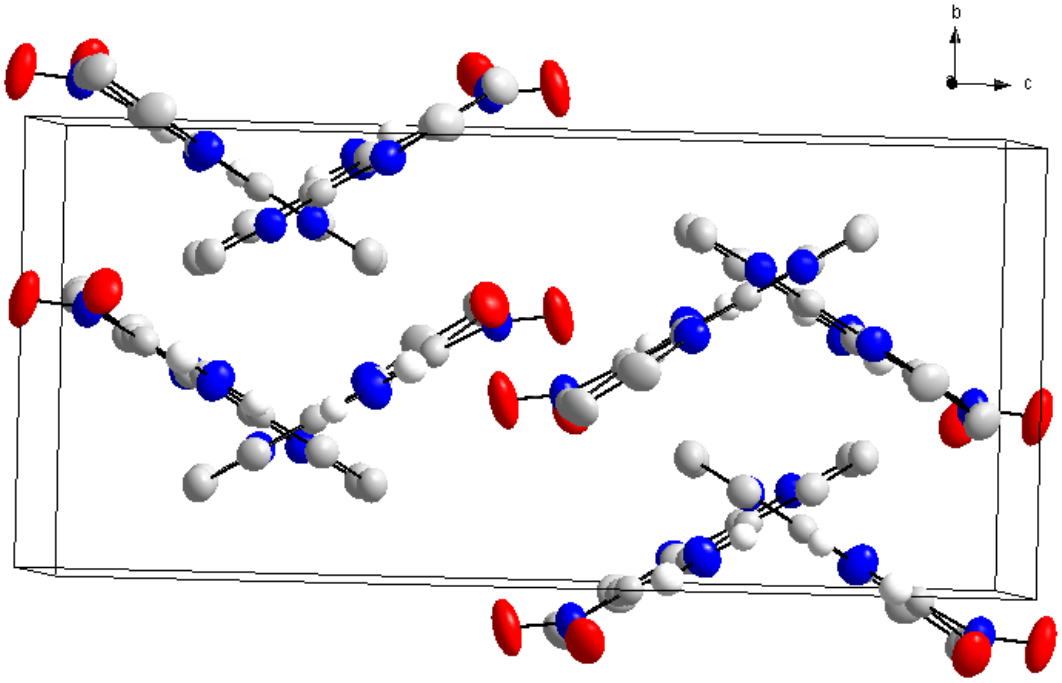

Figure 4.4: Illustration of the packing of phen(NH_2)(NO_2) in the unit cell. Hydrogen atoms are omitted for clarity.

The donor hydrogen atom H4A forms an interaction to two different nitrogen atoms, N1 and N2 forming a symmetrical bifurcated bond (intermolecular interaction **i** and **ii** in Figure 4.5). H4B, the other donor hydrogen atom forms interactions with O1 and N4 within the same molecule (intramolecular interactions **iii** and **iv**). These interactions are part of the infinite chains present in **phen(NH_2)(NO_2)** along the a-axis.

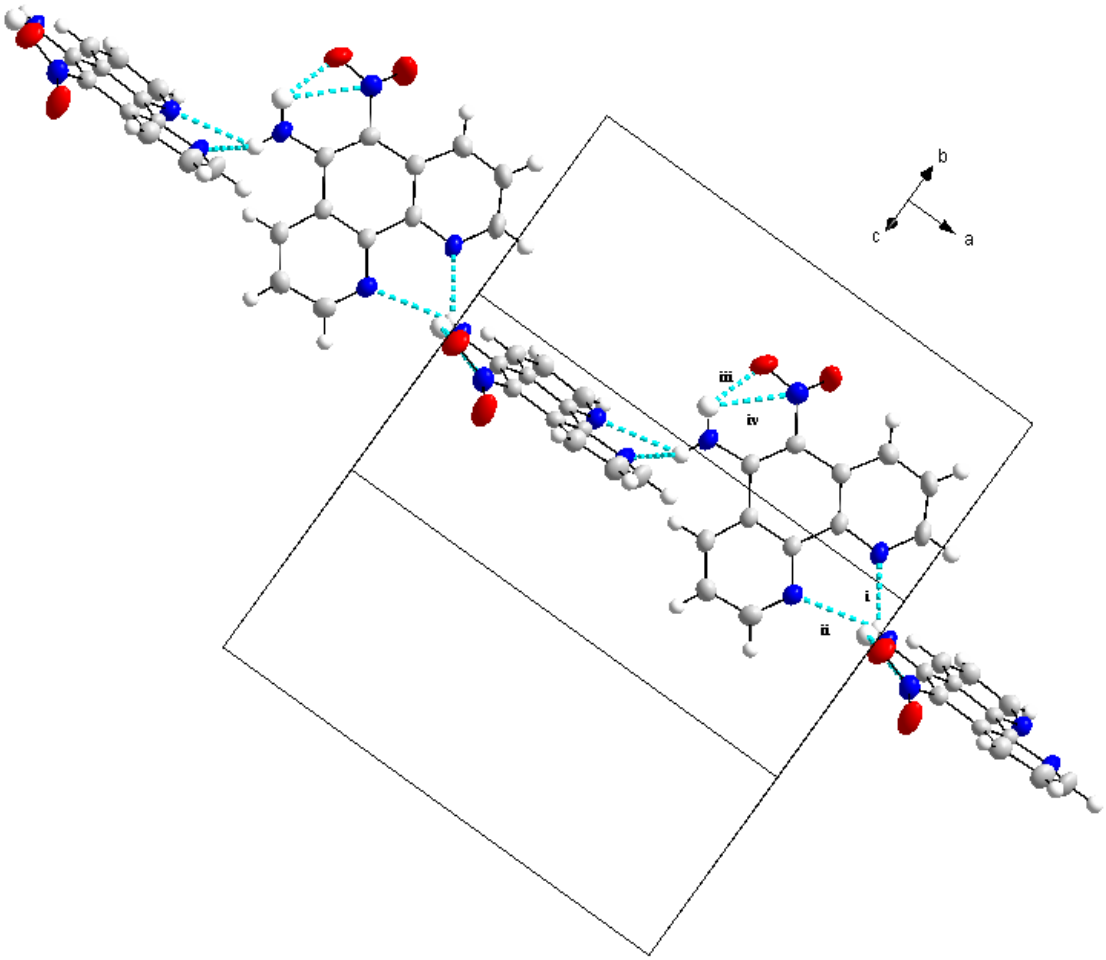

Figure 4.5: Illustration of the infinite chains present in phen(NH_2)(NO_2), with two intramolecular hydrogens bonding interactions and two intermolecular hydrogen bonding interactions along the a-axis.

4.4. Crystal structure of *fac*-[$Re(CO)_3$(phen)(H_2O)][NO_3]·1.5H_2O -(3):

fac-[$Re(CO)_3$(phen)(H_2O)][NO_3]·1.5H_2O was synthesized according to Paragraph 3.5.2.1 as reported in Chapter 3. The compound crystallized in the triclinic $\bar{P}$ 1 space group with a neutral rhenium(I) compound, a nitrate anion and 1.5 solvent water molecules. Two rhenium compounds, two nitrate anions and three water molecules are observed in the asymmetric unit. In the structure of *fac*-[$Re(CO)_3$(phen)(H_2O)][NO_3]·1.5H_2O, the Re(I) centre is surrounded by a N,N′-bidentate ligand (1,10-phenanthroline), three facially coordinated carbonyl ligands and an aqua ligand. The molecular structure of **3** are illustrated in Figure 4.6.

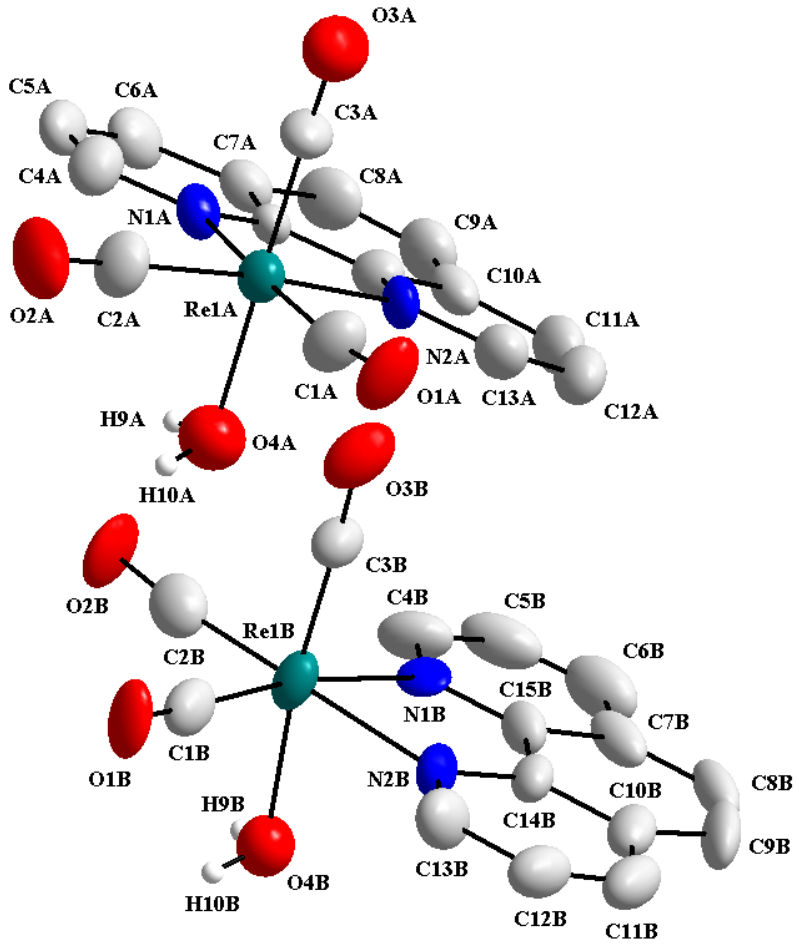

Figure 4.6: Molecular representation of the asymmetric unit of 3, counter ions, solvent molecules and hydrogen atoms are omitted for clarity.

A summary of the general crystal data are given in Table 4.1. The selected bond distances and bond angles are reported in Table 4.5.

Table 4.5: Summary of selected bond distances (Å) and angles (°) of 3.

Selected bond lengths (Å)			
Molecule A		**Molecule B**	
Re1A-C3A	1.866(15)	Re1B-C3B	1.864(15)
Re1A-C2A	1.926(14)	Re1B-C2B	1.906(14)
Re1A-C1A	1.931(12)	Re1B-C1B	1.914(13)
Re1A-N2A	2.166(8)	Re1B-N1B	2.178(8)
Re1A-N1A	2.188(9)	Re1B-N2B	2.180(8)
Re1A-O4A	2.150(11)	Re1B-O4B	2.108(10)
Selected angles (°)			
C3A-Re1A-C2A	90.5(6)	C3B-Re1B-C2B	89.9(6)

C1A-Re1A-C2A	89.8(5)	C2B-Re1B-C1B	89.5(5)
C3A-Re1A-O4A	176.5(5)	C2B-Re1B-N1B	97.3(4)
C1A-Re1A-N1A	171.9(4)	C1B-Re1B-N1B	170.8(4)
C2A-Re1A-N1A	98.0(4)	N1B-Re1B-N2B	76.5(3)
N2A-Re1A-N1A	75.7(3)	C3B-Re1B-O4B	173.6(4)

The bond distances from Re to the carbonyl carbons atoms range from 1.866(15) Å to 1.931(12) Å for molecule A and from 1.864(15) Å to 1.914(13) Å for molecule B and are within the range of similar reported structures.[8, 9, 10,11] The rhenium aqua distances, Re1A-O4A and Re1B-O4B are 2.150(11) Å and 2.108(10) Å respectively, and are similar to previously reported compounds.[9] The distance between the rhenium and the nitrogen atoms are similar to reported values of 2.188(9) Å for Re1A-N1A, 2.166(8) Å for Re1A-N2A and 2.178(8) Å for Re1B-N1B and 2.180(8) Å for Re1B-N2B and corresponds to the distance reported by Haddad and co-workers.[12]

The octahedral geometry around the rhenium metal centre for molecule A are distorted as illustrated by the angles of 171.9(4) ° for C1A-Re1A-N1A and 98.0(4) ° for C2A-Re1A-N1A. Similar distorted angles are illustrated in molecule B, where the angles C1B-Re1B-N1B and C2B-Re1B-N1B are 170.8(4) ° and 97.3(4) ° respectively. Small bite angles of 75.7(3) ° for molecule A (N2A-Re1A-N2A) and 76.5(3) ° for molecule B (N1B-Re1B-N2B) are observed and are within the range reported by Schutte *et al.*[9,10,12]

The planarity of the plane through C1-O1-C2-O2-Re1-N1-N2 is illustrated in the rms value of 0.0633 for molecule A and 0.0407 for molecule B with the largest outliers being C1A at 0.0127 Å and C2A at 0.0119 Å and C1B at 0.0113 Å and C2B at 0.0118 Å. The plane through C4, C5, C6, C7, C8, C9, 10, C11, C12, C13, C14, C15 with a rms value of 0.0390 for molecule A and 0.0296 for molecule B (with no specific outliers) again illustrates the planar nature of the phen entity as illustrated in Appendix A, Figure 1A.

An array of C-H…O and C-H…N hydrogen bonding interactions are observed in **3,** five intramolecular interactions (purple dashed lines) and eight intermolecular interactions (green

[8] I. Chakraborty, J. J. Jimenez, W. M. C. Sameera, M. Kato and P.K. mascharak, *Inorganic Chemistry*, **2017**, 56, 2863-2873.

[9] M. Schutte, H. G. Visser, *Acta Crystallographica*, **2008**, E64, m1226-1227.

[10] M. Schutte, H. G. Visser, G. Steyl, *Acta Crystallograhica*, **2007**, E63, m3195-m3196.

[11] R. Alberto, W.A. Herrmann, P. Kiprof and F. Baumgartner, *Inorganic Chemistry*, **1992**, 31, 895-899.

[12] M. Schutte, H. G. Visser and A. Roodt, *Acta Crystallographica*, **2010**, E66, m859-m860.

dashed lines). Most of these hydrogen bonding interactions were observed between the cation, solvent molecules and the coordinated ligand. All the hydrogen bonding interactions of **3** are illustrated in Figure 4.7 and the distances, angles and symmetry operators are given in Table 4.6.

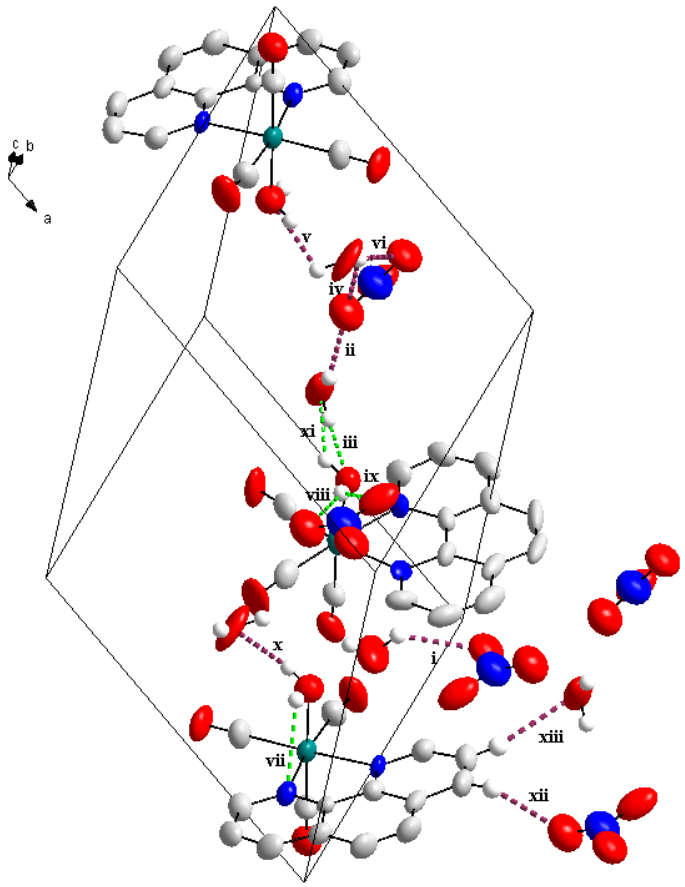

Figure 4.7: Illustration of hydrogen bonding interactions observed in 3. (Intramolecular hydrogen bonding interactions are indicated with green dashed lines while intermolecular hydrogen bonding interactions are indicated with purple dashed lines). Hydrogens atoms not taking part in the hydrogen bonds, are omitted for clarity.

Table 4.6: Summary of the hydrogen bonding interactions' distances (Å) and angles (°) obtained in 3.

Interaction	D-H…A	d(D-H)	d(H-A)	d(D…A)	<(DHA)
i	O7-H1…O1[a]	0.85(2)	2.39(8)	3.30(3)	132(9)
ii	O8-H3…O4[b]	0.87(2)	1.94(8)	2.63(3)	135(10)
iii	08-H4…O4B	0.84(2)	1.89(6)	2.680(16)	155(11)
iv	O9-H5…O4[b]	0.883(14)	2.11(3)	2.71(3)	125.2(19)
v	O9-H6…O4A[c]	0.85(2)	2.32(12)	2.644(17)	103(10)

vi	O9-H5…06[b]	0.883(14)	1.94(2)	2.80(3)	161.6(14)
vii	O4A-H9A…N1A	0.84(2)	2.53(3)	2.890(14)	107(2)
viii	O4B-H9B…O2	0.83(2)	2.20(4)	3.02(3)	167(8)
ix	O4B-H9B…O3	0.83(2)	2.24(5)	2.91(2)	137(7)
x	O4A-H10A…O9[c]	0.84(2)	1.98(5)	2.644(17)	135(6)
xi	O4B-H10B…O8	0.84(2)	2.00(5)	2.680(16)	138(8)
xii	C11A-H6A…O2[d]	0.95	2.45	3.34(3)	157.5
xii	C12A-H17A…O8[d]	0.95	2.60	3.53(2)	166.3

Symmetry codes, transformations used to generate equivalent atoms:

[a] –x + 2, -y + 1, -z + 1; [b] x– 1, y, z; [c] –x + 1, -y + 1, -z + 1; [d] x + 1, y, z.

Two intramolecular C-H…π interactions are observed in **3** with the, H9A to centroid distance of 2.463(9) Å and an angle of 86(6) ° for the O4A-H9A-centroid interaction. The distance of H9B to centroid is 2.97(7) Å and an angle of 54(5) ° for the O4B-H9B-centroid interaction is observed and is illustrated in Figure 4.8.

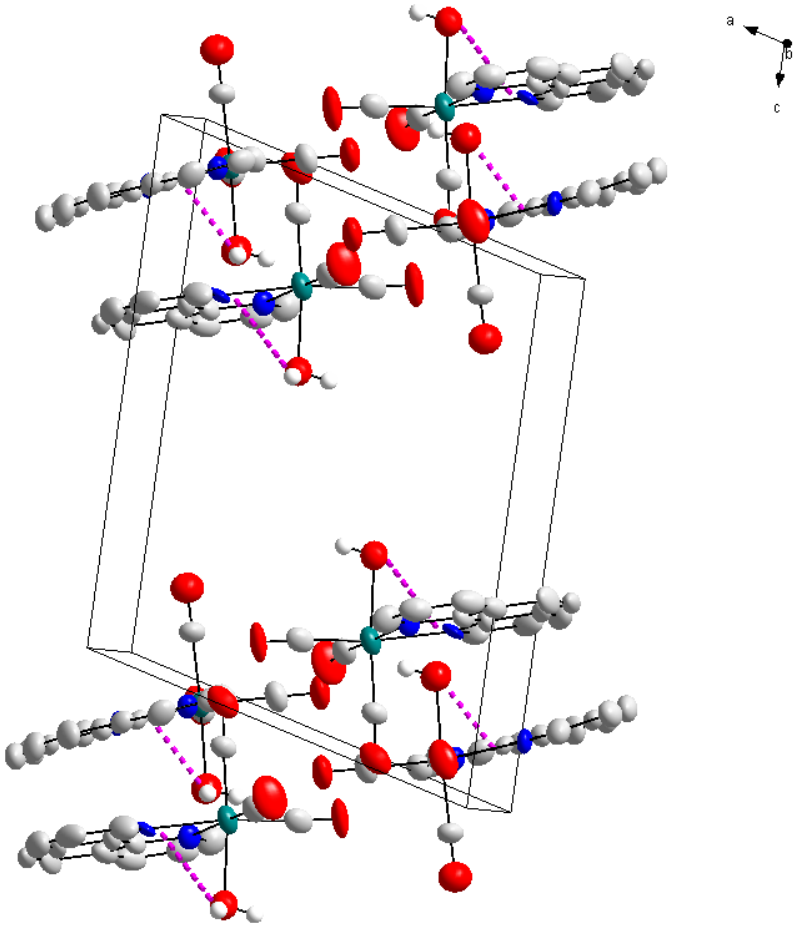

Figure 4.8: Illustration of the two intramolecular *π*interactions between the hydrogen atom of the aqua ligand and the 1,10-phenanthroline ligand. Hydrogen atoms, cations and solvent molecules are omitted for clarity.

As seen in Figure 4.9 **3** packs in a head-to-head fashion along the b-axis in a column-like structure.

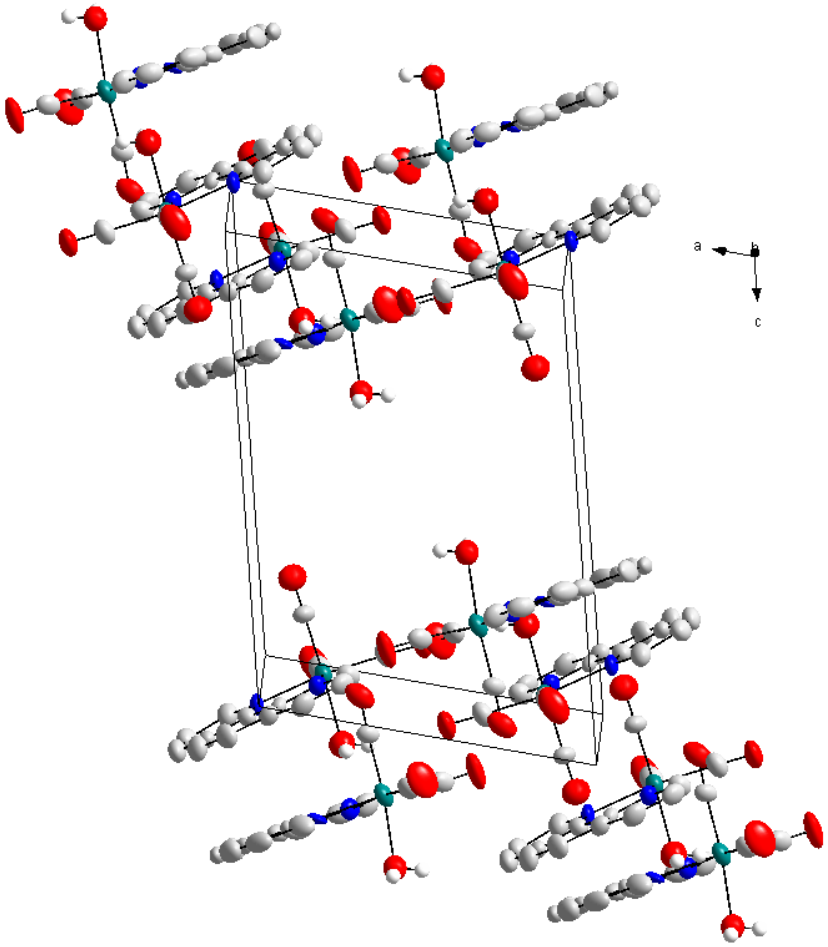

Figure 4.9: Packing of 3 in the unit cell, and hydrogen atoms, cations and solvent molecules are omitted for clarity.

4.5. Crystal structure of *fac*-[Re(CO)$_3$(phen)Br] -(4):

fac-[Re(CO)$_3$(phen)Br] was synthesized according to the synthetic procedure reported in Paragraph 3.5.2.2 in Chapter 3. Yellow cuboidal crystals were obtained from a mixture of chloroform and acetonitrile. The compound crystallized in the $\bar{P}$ 1 space group with two Re-units in the unit cell (Z = 2). The molecular structure of *fac*-[Re(CO)$_3$(phen)Br] is illustrated in Figure 4.10. The Re atom is octahedrally surrounded by a bromido ligand, one bidentate ligand (1,10-phenanthroline) and three facially orientated carbonyl ligands.

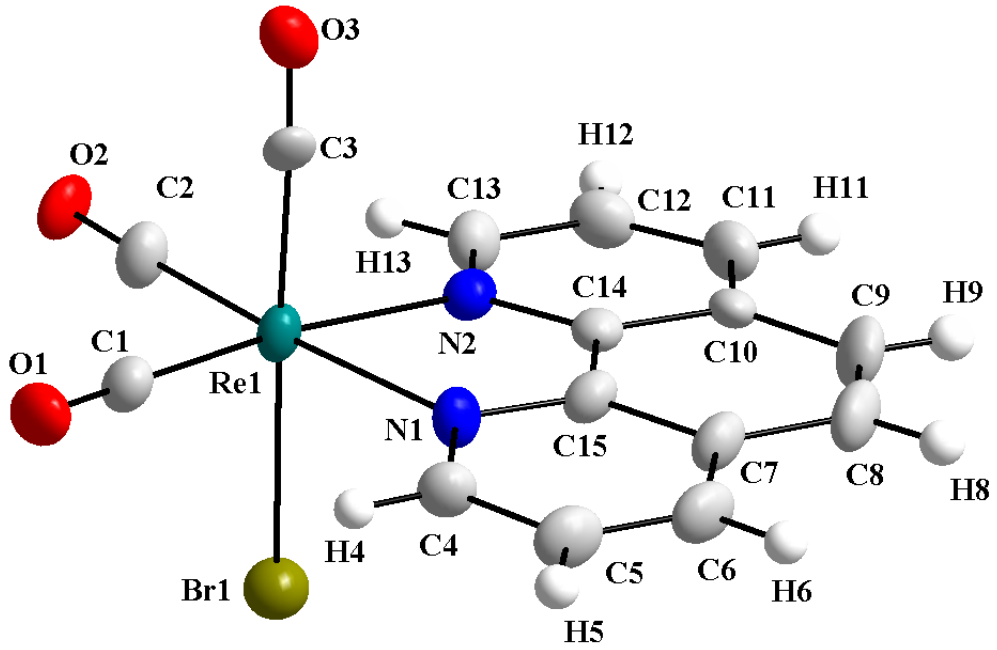

Figure 4.10: Illustration of the molecular presentation of the crystal structure of fac-[Re(CO)3(phen)Br] (4).

A summary of the crystal data are given in Table 4.2 and selected bond angles and bond distances are reported in Table 4.7.

Table 4.7: Selected bond distances (Å) and angles (°) for the structure of 4.

Selected Bond lengths (Å)		Selected bond angles (°)	
Re1-C1	1.934(7)	C3-Re1-C2	88.8(4)
Re1-C2	1.926(7)	C2-Re1-C1	91.5(3)
Re1-C3	1.902(9)	C2-Re1-N1	171.9(3)
Re1-N1	2.183(6)	C1-Re1-N1	96.5(3)
Re1-N2	2.183(6)	N2-Re1-N1	75.8(2)
Re1-Br	2.6318(14)	C3-Re1-Br1	177.7(2)

The bond distances from Re1 to the three carbonyl carbons (C1, C2 and C3) are within the range of similar structures.[81011] The metal to bromido distance of 2.6318(14) Å correspond to the distance reported by Schutte *et al.*[12] Both the distances between the metal and N-atoms of the N,N′-bidentate ligand are the same with a bond distance of 2.183(6) Å. The octahedral arrangement around the rhenium metal centre is distorted as illustrated by the angles of 171.9(3) ° for C2-Re1-N1 and 96.5(3) ° for C1-Re1-N1. The small bite angle (N2-Re1-N1) of 75.8(2) ° are slightly smaller than the bite angle reported by Chakraborty *et al.*[8] with a bite angle of 76.09(18) °.

The planarity of the plane through C1-O1-C2-O2-Re1-N1-N2 is illustrated in the rms value of 0.0117 with the largest outliers being C1 at 0.0072 Å and C2 at 0.0074 Å. The plane through C4-C5-C6-C7-C8-C9-10-C11-C12-C13-C14-C15 with a rms value of 0.0544 (with no specific outliers) again illustrates the planar nature of the phen entity. The dihedral angle between these two planes are calculated as 3.1(3) ° as illustrated in Figure 4.11.

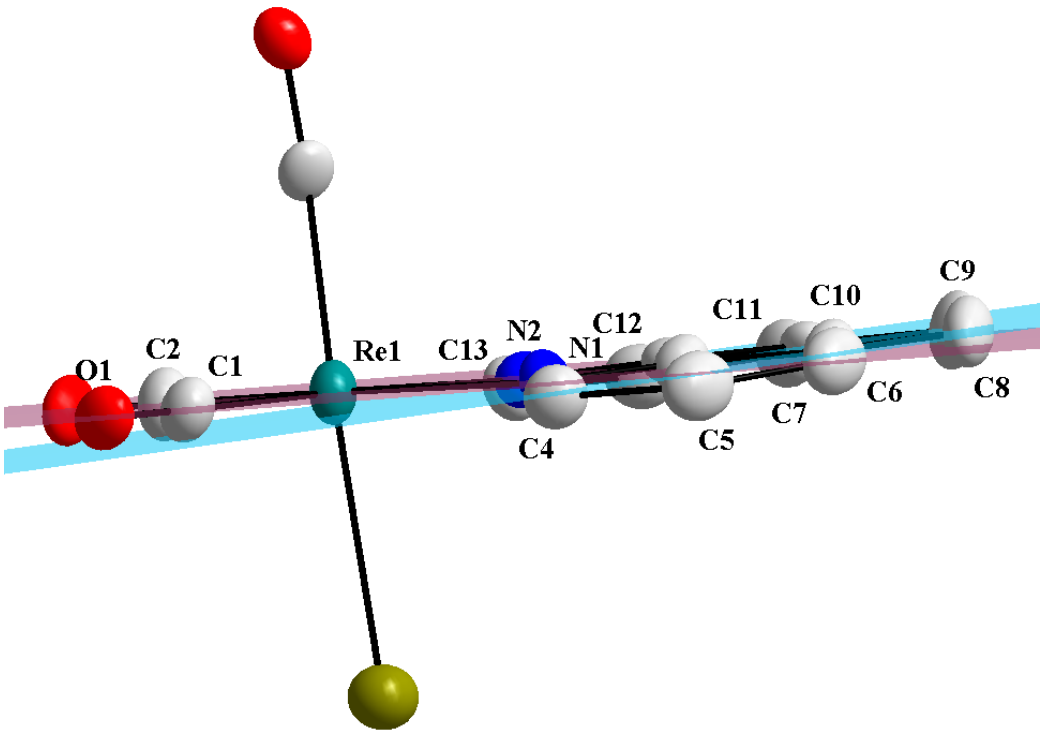

Figure 4.11: Illustration of the planes through the metal, N atoms and carbonyl ligands, purple plane (Re1-N1-N2-C1-O1-C2-O2) and through the 1,10-phenanathroline ligand, blue plane (C4-C5-C6-C7-C8-C9-C10-C11-C12-C13-C14-C15-N1-N2) of 4. The dihedral angle between the two planes are 3.1(3) °. Hydrogen atoms are omitted for clarity.

There are two C-H...O intermolecular hydrogen bonding interactions present in the crystal structure of **4**. This is illustrated in Figure 4.12 with the bond distances, angles and the symmetry operators given in Table 4.8.

Table 4.8: Summary of the hydrogens bonding interactions, distances (Å) and angles (°) observed in 4.

D-H…A	d(D-H)	d(H…A)	d(D…A)	<(DHA)
C6-H6…O1[a]	0.95	2.52	3.411(11)	156.0
C11-H11…O1[b]	0.95	2.52	3.414(11)	156.8

Symmetry code, transformation used to generate equivalent atoms:

[a] x + 1, y – 1, z; [b] x + 1, y, z - 1

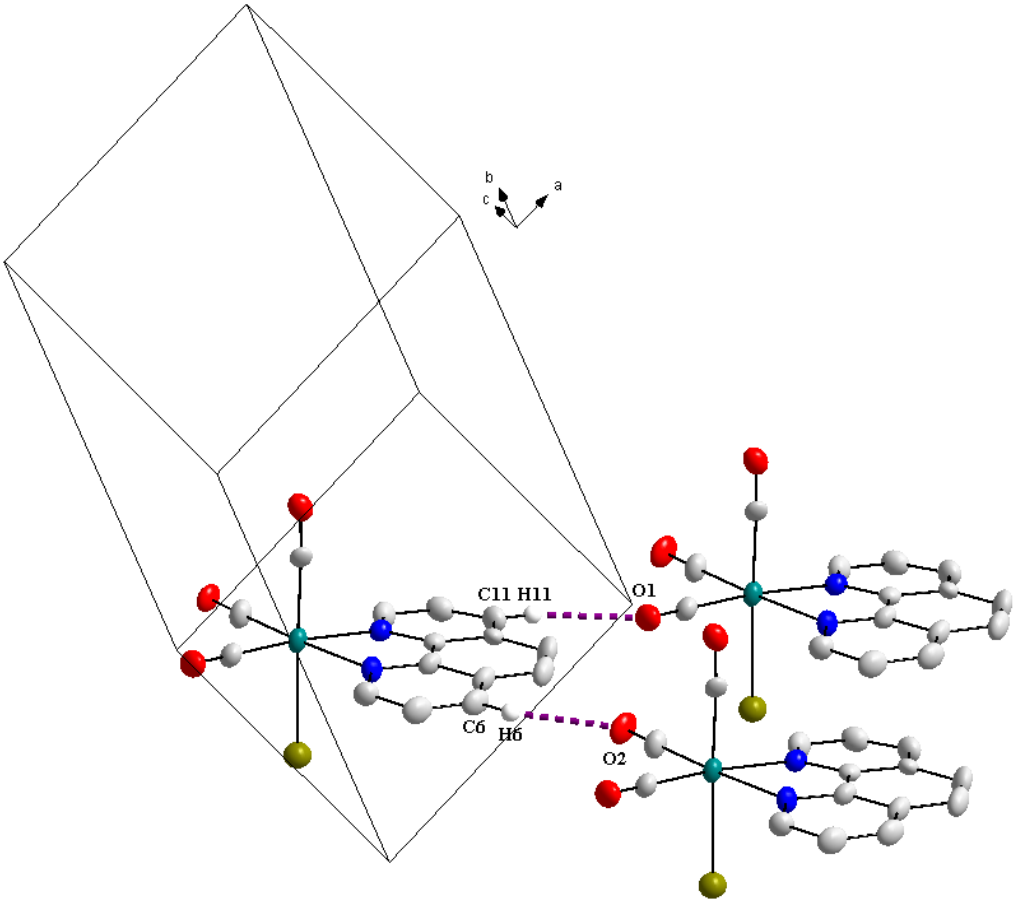

Figure 4.12: Intermolecular hydrogen bonding interactions observed in 4. Hydrogen atoms not taking part in the hydrogen bonding interactions are omitted for clarity.

One weak Br-π interaction is observed in **4** with a Br to centroid distance of 3.859(4) Å and a Re-Br-centroid angle of 163.19(6) ° (symmetry operators: -1 + x, y, z, centroid of C8, C9, C10, C14, C15). This is illustrated in Figure 4.13.

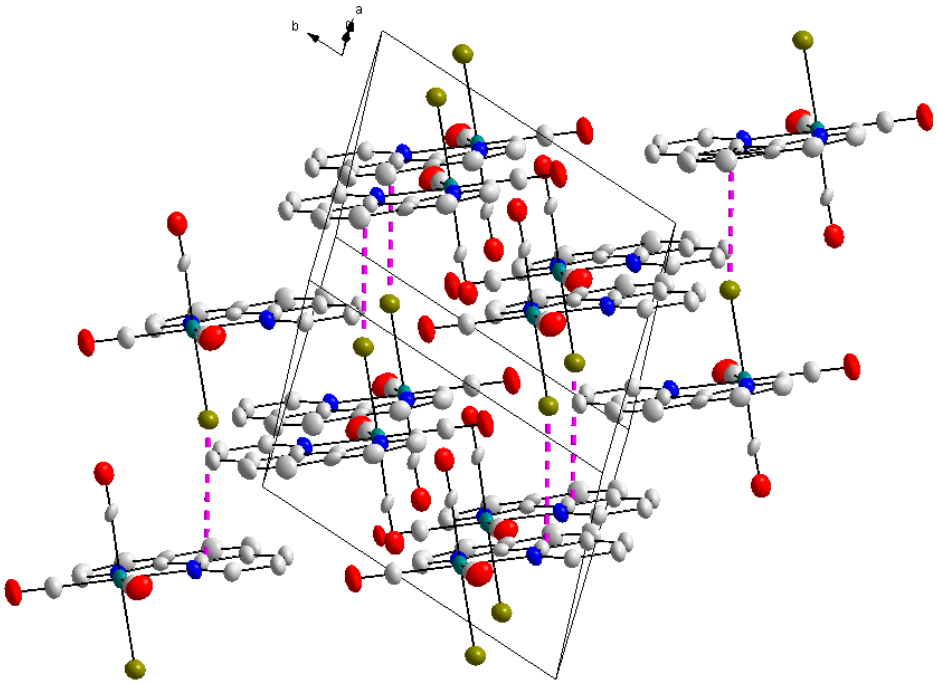

Figure 4.13: Representation of the weak Br-π interaction between the bromido and 1,10-phenanthroline ligand. Hydrogen atoms are omitted for clarity. Symmetry operator: -1 + x, y, z.

The metal complex packs in a head-to-tail fashion when viewed along the *b*,*c*-plane, in alternating layers (180° to the next) as illustrated in Figure 4.14. Hydrogen atoms are omitted for clarity.

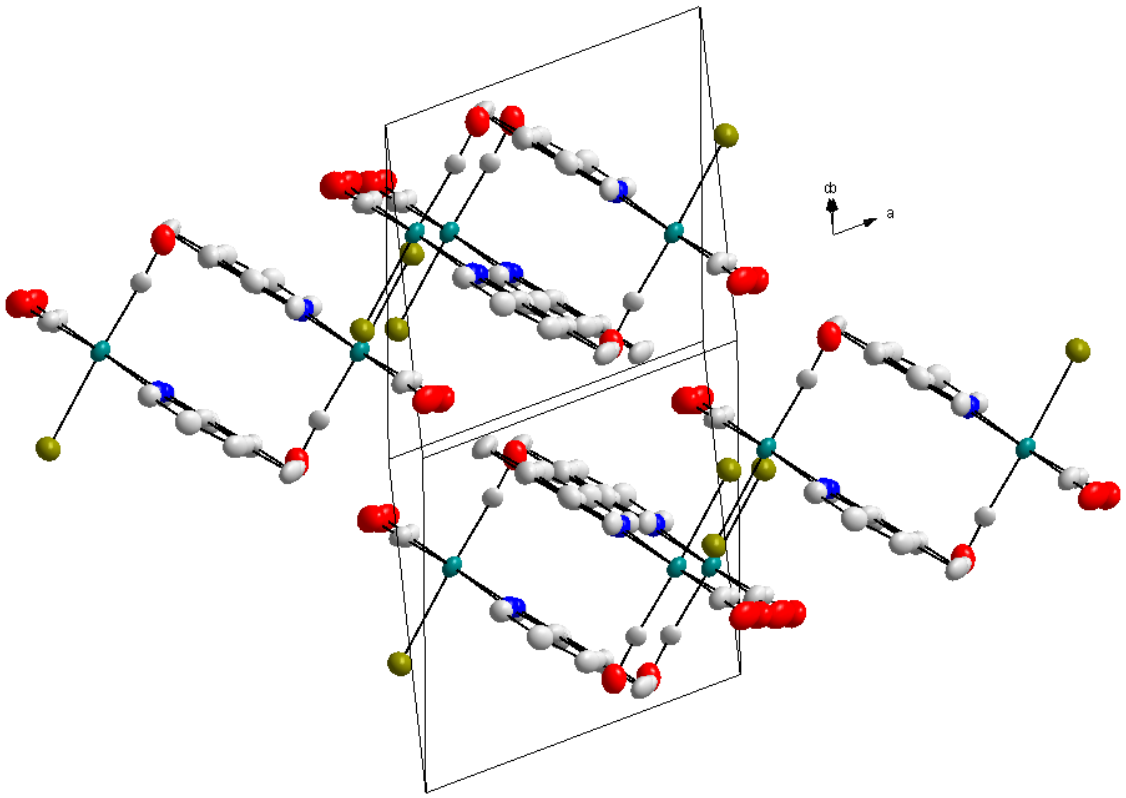

Figure 4.14: Illustration of the packing of 4 in the unit cell and hydrogen atoms are omitted for clarity.

4.6. Summary:

In this Chapter, one N,N′-bidentate ligand and two Rhenium(I) tricarbonyl compounds with a N,N′-bidentate ligand (1,10-phenanthroline) are reported. The reported compounds are:

- 5-amino-6-nitro-1,10-phenanthroline (**phen(NH_2)(NO_2)**),
- *fac*-[Re(CO)$_3$(phen)(H_2O)][NO_3]·1.5H_2O (**3**) and
- *fac*-[Re(CO)$_3$(phen)Br] (**4**).

The crystallographic data of the ligand and the two complexes are reported in Table 4.1 and Table 4.2. The N,N′-bidentate ligand, 5-amino-6-nitro-1,10-phenathroline are compared to previously reported 1,10-phenathroline-5,6-dione containing two carbonyl group (C≡O) on carbon 5 and 6. The C-O bond distances (1.208 Å to 1.213 Å) are smaller than the C-N bond distances (1.333 Å to 1.431 Å) as expected. The angles and selected bond distances of **3** and **4** are summarized in Table 4.9 for comparison. The distances of the three rhenium carbonyl ligands are within the normal range as reported in previous studies.

No variation is observed within these bond distances. The rhenium-bidentate ligand distances (Re-N1, Re-N2) are the distances observed between the Re metal centre and the coordinated N,N′-bidentate ligand and the Re-X distance is the distance from the rhenium centre to the monodentate ligand in the 6th position, O (H_2O) for **3** and Br for **4**. The bite angles are also reported in this table (N1-Re-N2) and the angles between C3-Re-X for **3** and **4**.

The rhenium -carbonyl ligand bond distances are within the range of 1.864(15) Å to 1.931(12) Å for **3** and 1.908(9) Å to 1.934(7) Å for **4**. The distance from rhenium to the nitrogen atoms of the bidentate ligand are 2.188(9) Å and 2.166(8) Å for molecule A and 2.178(8) Å and 2.180(8) Å for molecule B in **3** and 2.183(6) Å and 2.183(6) for **4** as seen in Table 4.9. Re-H_2O distance (2.11 to 2.15 Å) compare well to similar crystal structures with a N,N′-donor ligand with Re-H_2O distances of 2.16 Å and 2.18 Å.[13] The Re-Br distance is comparable to the crystal structure reported by Schutte *el al.*[13]

Table 4.9: Summary of the angles and selected bond distances of 3 and 4.

Re-C1,C2,C3 (Å)	**Re-N1 (Å)**	**Re-N2 (Å)**	**Re-X (Å)**	**N1-Re-N2 (°)**	**C3-Re-X (°)**
***fac*-[Re(CO)$_3$(phen)(H$_2$O)][NO$_3$]·1.5H$_2$O (3)**					
Molecule A					
1.931(12), 1.926(14), 1.866(15)	2.188(9)	2.166(8)	2.150(11)-**O**	75.7(3)	176.5(5)
Molecule B					
1.914(13), 1.906(14), 1.864(15)	2.178(8)	2.180(8)	2.108(10)-**O**	76.5(3)	173.6(4)
***fac*-[Re(CO)$_3$(phen)Br] (4)**					
1.934(7), 1.926(7), 1.902(9)	2.183(6)	2.183(6)	2.6318(14)-**Br**	75.8(2)	177.7(2)

The bite angle for both compounds (N1-Re-N2) are similar and is within the range of 75.7(3) ° to 76.5(3) °.

Overall, the bond distances and angles of **3** and **4** are comparable. Distortions are observed in both crystal structure and it do not obey an octahedral geometry.

[13] M. Schutte, G. Kemp, H.G. Visser and A. Roodt, *Inorganic Chemistry*, **2011**, 50, 12486-12498.

CHAPTER 5: LUMINESCENCE

5.1. Introduction:

Luminescent materials are found in everyday applications such as projection television, X-ray detectors, and fluorescent tubes.[1] The miniaturization, lifetime improvements as well as the spectral stability of fluorescent lamps, brightness, and improvements on the contrast in imaging systems demand luminescent materials.[1] The luminescent materials in plasma display panels (PDP) and field emission display (FED) make use of the high-energy sides of the UV spectrum. Phosphors in light emitting diodes (LED) are excited by UV or blue light.[1]

Rhenium(I) tricarbonyl polypyridine complexes have been designed as cellular imaging reagents and drugs as anticancer agents with large Stokes shifts, high photostability, and long emission lifetimes and can be used as candidates for optical imaging.[2] Interferences caused by cell autofluorescence can be eliminated by long emission lifetimes and improves the sensitivity as stated by Lee *et al.* Rhenium(I) tricarbonyl complexes are used in photodynamic therapy for the treatment of cancer.[2] Therefore rhenium(I) tricarbonyl polypyridine complexes are developed as cellular imaging agents, drugs for cancer treatment and antibacterial agents.[2] According to Striplin and co-workers[3], Re(I) complexes with phenanthroline or substituted phenanthroline ligands are not studied intensively and therefore more focus was placed on these complexes for photoluminescence studies.[3]

Photoluminescence studies were performed on Re(I) tri- and dicarbonyl complexes with 1,10-phenanthroline (phen) and 1,10-phenanthroline-5,6-dione (**phenO_2**) as the bidentate ligands and different phosphine ligands as the monodentate ligands: triphenylphosphine (PPh_3), 1,3,5-triaza-7-phosphaadamantane (PTA) and 3,7-diacetyl-1,3,7-triaza-5-phosphabicyclo[3.3.1]nonane (DAPTA). The complexes studied are illustrated in Scheme 5.1 below.

[1] T. Jüstel, H. Nikol and C. Ronda, *Angewandte Chemie International Edition*, **1998**, 37, 3083-3103.

[2] L. C-C. Lee, K-K. Leung and K. K-W. Lo, *Dalton Transactions*, **2017**, 46, 16357-16380.

[3] D. R. Striplin and G. A. Crosby, *Coordination Chemistry Reviews*, **2001**, 211, 163-175.

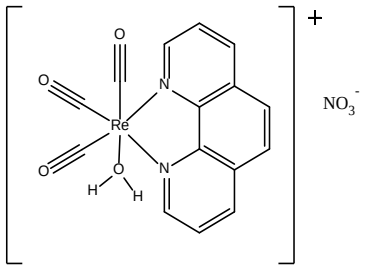

***fac*-[Re(CO)$_3$(phen)(CH$_3$OH)][NO$_3$] (3)**

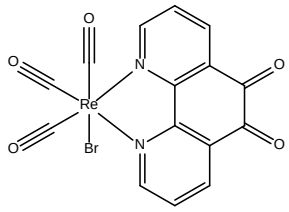

***fac*-[Re(CO)$_3$(phenO$_2$)(Br)] (5)**

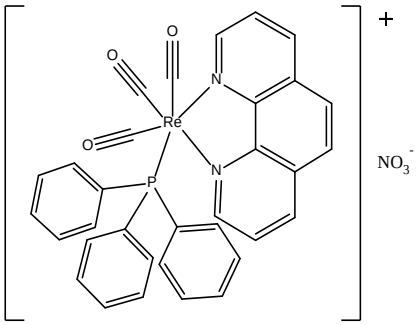

***fac*-[Re(CO)$_3$(phen)(PPh$_3$)][NO$_3$] (6)**

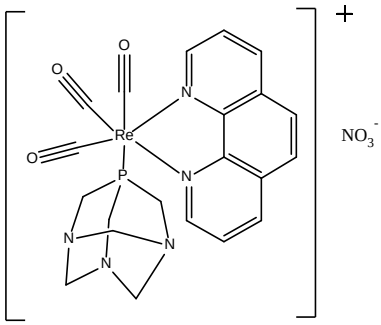

***fac*-[Re(CO)$_3$(phen)(PTA)][NO$_3$] (7)**

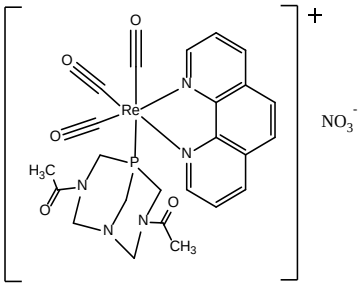

***fac*-[Re(CO)$_3$(phen)(DAPTA)][NO$_3$] (8)**

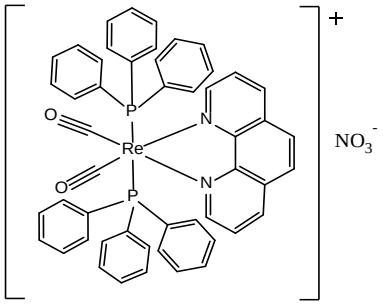

***cis-trans*-[Re(CO)$_2$(phen)(PPh$_3$)$_2$][NO$_3$] (9)**

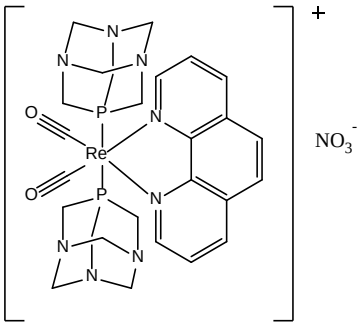

***cis-trans*-[Re(CO)$_2$(phen)(PTA)$_2$][NO$_3$] (10)**

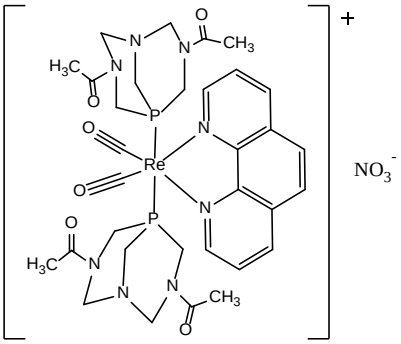

***cis-trans*-[Re(CO)$_2$(phen)(DAPTA)$_2$][NO$_3$] (11)**

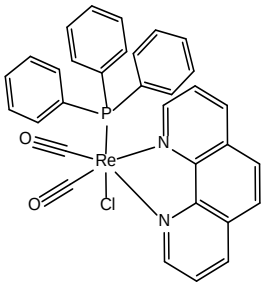

***cis*-[Re(CO)$_2$(phen)(PPh$_3$)(Cl)] (12)**

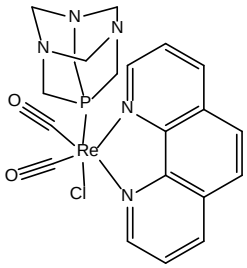

***cis*-[Re(CO)$_2$(phen)(PTA)(Cl)] (13)**

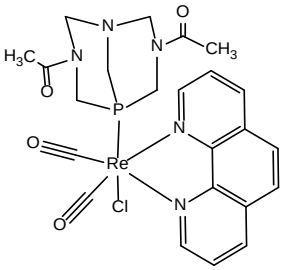

***cis*-[Re(CO)$_2$(phen)(DAPTA)(Cl)] (14)**

Scheme 5.1: Illustration of the Re(I) complexes studied.

5.2. Experimental:

The UV/Vis absorbance was measured in a 1 cm tandem quartz cuvette on a Varian Cary 50 Conc. Spectrophotometer. The absorbance of all the complexes is reported in Chapter 3 with the maximum wavelength. The absorbance was measured in solution with methanol as the solvent. The same samples used for UV/Vis absorption was used for the photoluminescence

analysis. Photoluminescence studies were performed on an Edinburgh Instruments FLS980 photoluminescence spectrometer with a double monochromator. The samples were excited by a 450 W xenon lamp and the excitation and emission spectrums were obtained of the complexes.

5.3. Results:

The results obtained from the photoluminescence (PL) evaluation are presented in Figure 5.1-5.22 below. Each graph has an excitation- (grey) and an emission graph (blue) of the complexes at different wavelengths as indicated on each graph. The methanol (solvent) emission graph (orange) are collected and is negligible.

5.3.1. Excitation, emission, and UV/Vis absorbance of rhenium(I) tricarbonyl complexes:

fac-[Re(CO)$_3$(phen)(CH$_3$OH)][NO$_3$] (**3**) showed a maximum absorbance of photons at a wavelength of 265 nm in methanol at 25.0 °C and is illustrated in Figure 5.1. **3** were synthesized according to the synthetic procedure in Paragraph 3.5.2.1 and the emission and excitation wavelength are collected and illustrated in Figure 5.2. The excitation spectrum (grey) showed 2 peaks, at 236 nm and 270 nm. The excitation peak at 270 nm appears to be more noticeable. This peak gives rise to the maximum emission (blue) at 610 nm as seen in Figure 5.2.

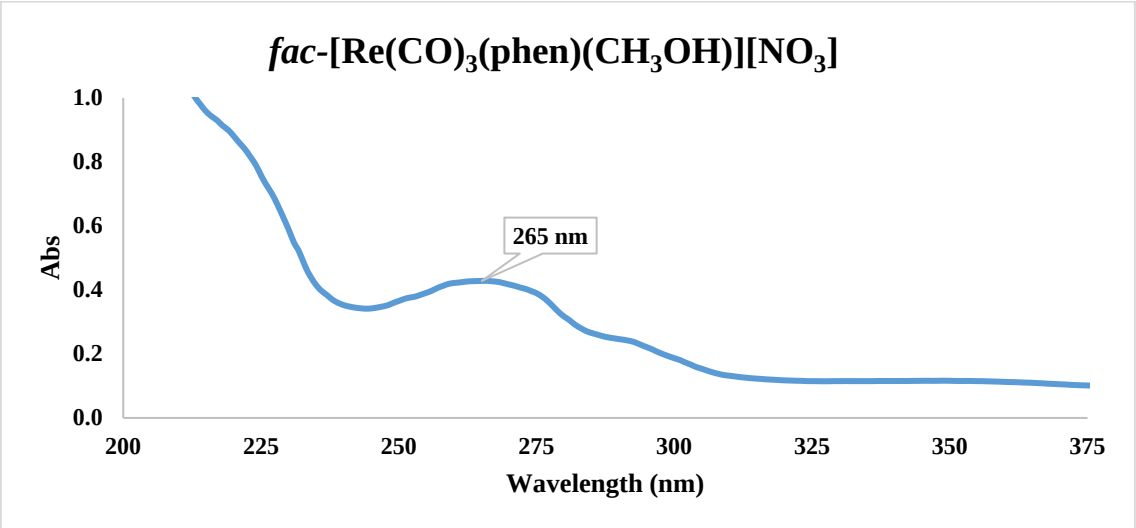

Figure 5.1: Illustration of the UV/Vis absorbance spectra of *fac*-[Re(CO)$_3$(phen)(CH$_3$OH)][NO$_3$] at 25.0 °C in methanol with a concentration of 5.17×10^{-5} M.

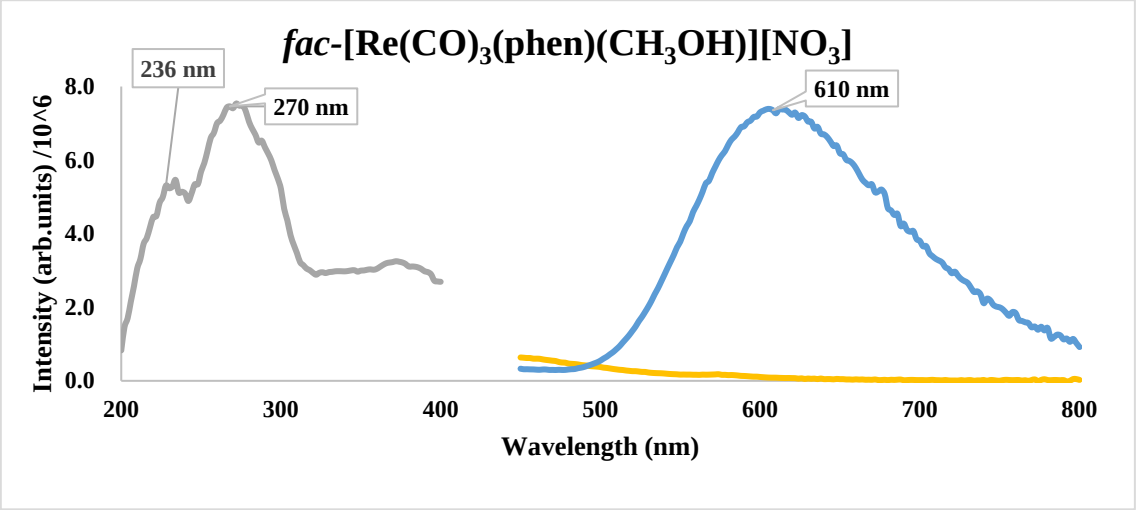

Figure 5.2: Representation of the excitation (grey) and emission (blue) of *fac*-[Re(CO)$_3$(phen)(CH$_3$OH)][NO$_3$] and methanol (orange).

fac-[Re(CO)$_3$(phenO$_2$)(Br)] (**5**) was synthesized according to the synthetic procedure in Paragraph 3.5.3 and the UV/Vis absorption of the complex showed a maximum at wavelength 298 nm (Figure 5.3). The emission and excitation of **5** are illustrated in Figure 5.4. As illustrated in Figure 5.4, **5** showed a range of excitation (grey) wavelengths between 274 - 288 and 330 nm. The wavelength at 330 nm gives rise to the maximum emission (blue) at 648 nm.

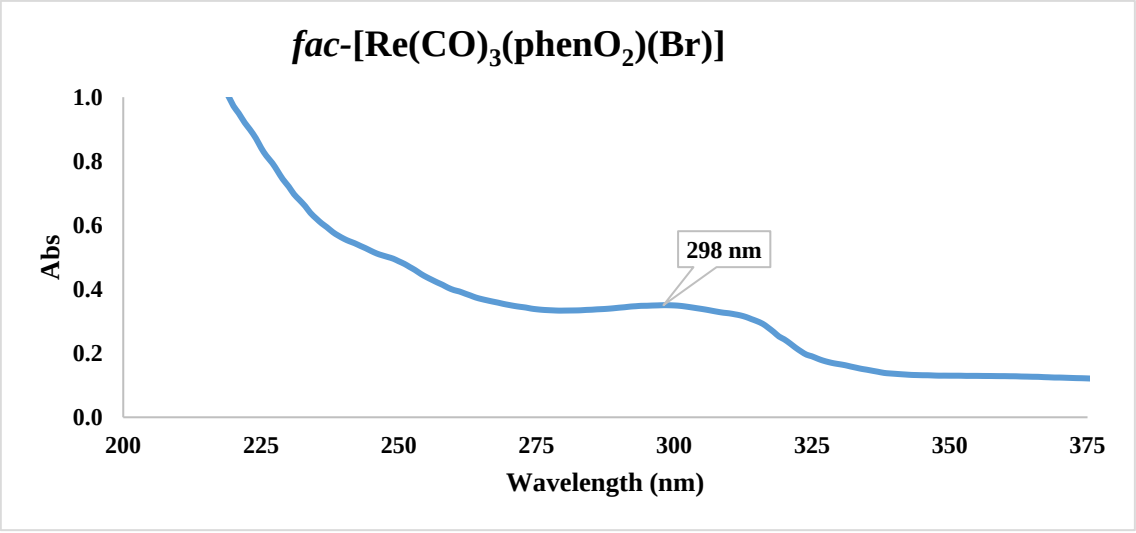

Figure 5.3: Illustration of the UV/Vis absorbance spectra of *fac*-[Re(CO)$_3$(phenO$_2$)(Br)] in methanol at 25.0 °C with a concentration of 5.18×10^{-5} M.

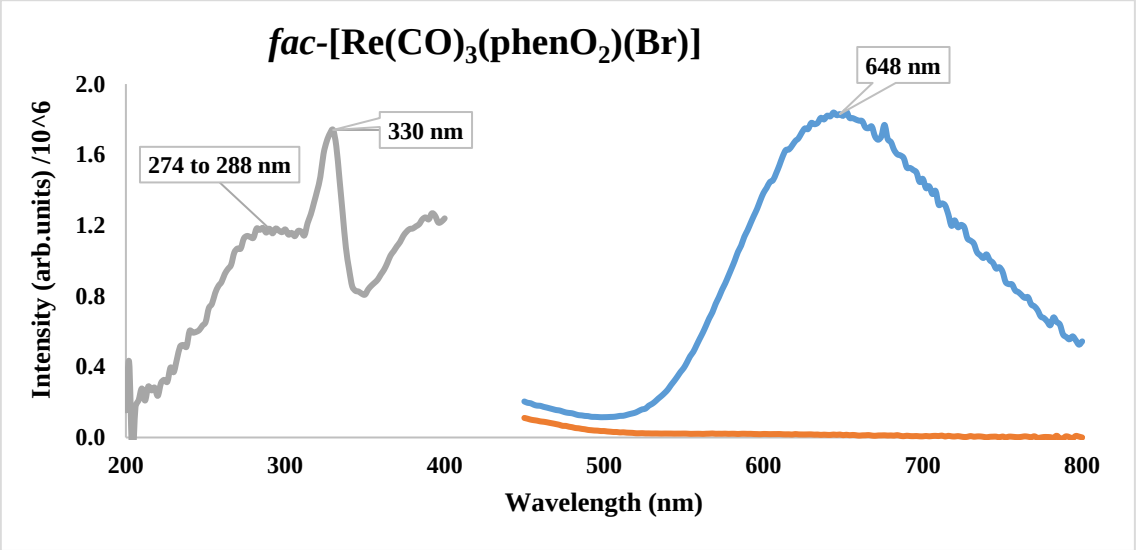

Figure 5.4: Representation of the excitation (grey) and emission (blue) of *fac*-[Re(CO)$_3$(phenO$_2$)(Br)] and methanol (orange).

fac-[Re(CO)$_3$(phen)(PPh$_3$)][NO$_3$] (**6**) was synthesized according to the synthetic procedure in Paragraph 3.5.4 and the maximum absorbance are at 265 nm (Figure 5.5). The emission and excitation graphs were collected. Figure 5.6 showed two excitation wavelengths at 230 nm and 274 nm. The 274 nm peak appears to be the more noticeable excitation peak. This peak gives rise to the maximum emission at 610 nm.

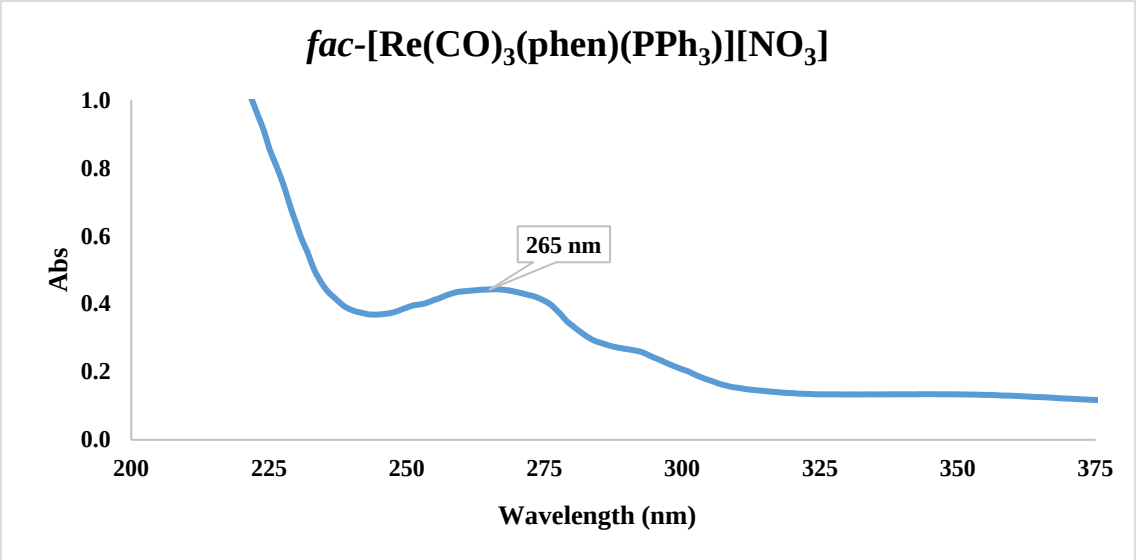

Figure 5.5: Illustration of the UV/Vis absorbance spectra of *fac*-[Re(CO)$_3$(phen)(PPh$_3$)][NO$_3$] in methanol at 25.0 °C with a concentration of 3.86×10^{-5} M.

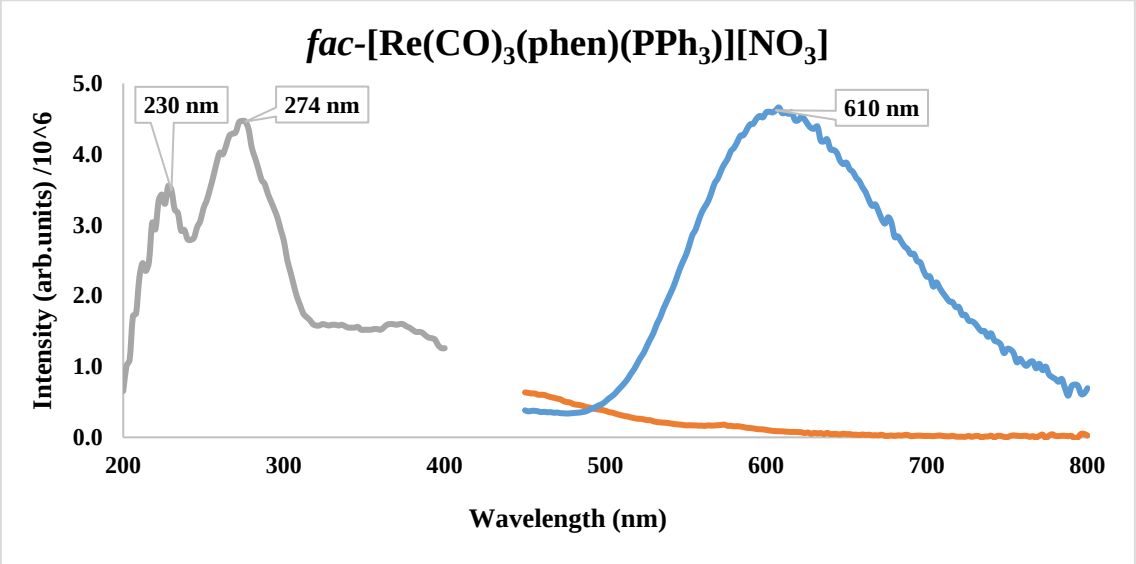

Figure 5.6: Representation of the excitation (grey) and emission (blue) of *fac*-[Re(CO)$_3$(phen)(PPh$_3$)][NO$_3$] and the emission of methanol (orange).

fac-[Re(CO)$_3$(phen)(PTA)][NO$_3$] (**7**) showed an absorption peak at 266 nm. **7** was synthesized according to the synthetic procedure in Paragraph 3.5.5 and has a range of excitation wavelengths between 264 nm to 280 nm as seen in Figure 5.8. 280 nm is more or less the middle of the range and was chosen as the excitation peak to obtain an emission peak. The maximum emission was obtained at 610 nm.

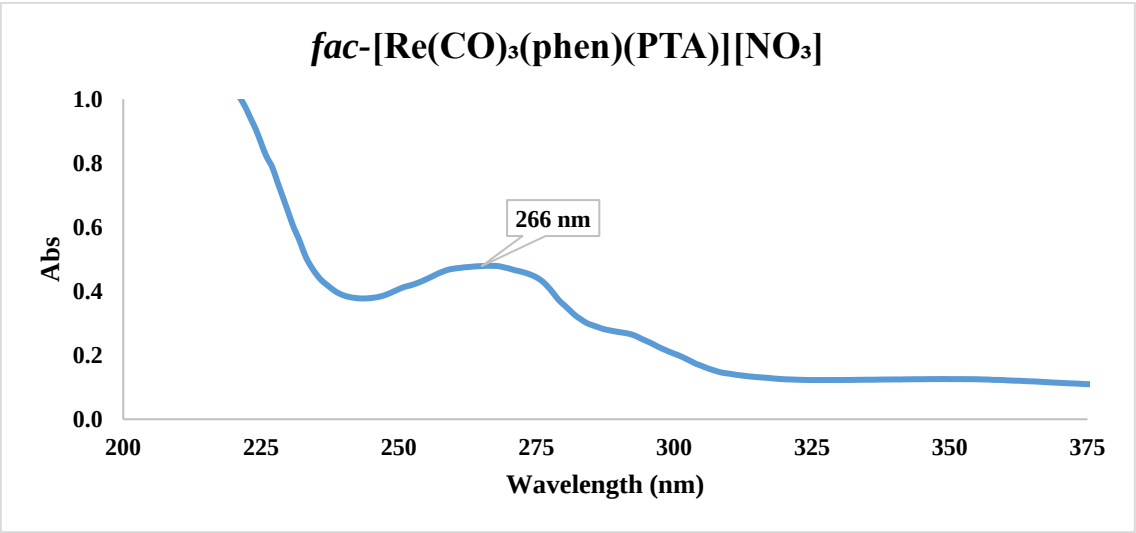

Figure 5.7: Illustration of the UV/Vis absorbance spectra of *fac*-[Re(CO)$_3$(phen)(PTA)][NO$_3$] in methanol at 25.0 °C with a concentration of 3.64×10^{-5} M.

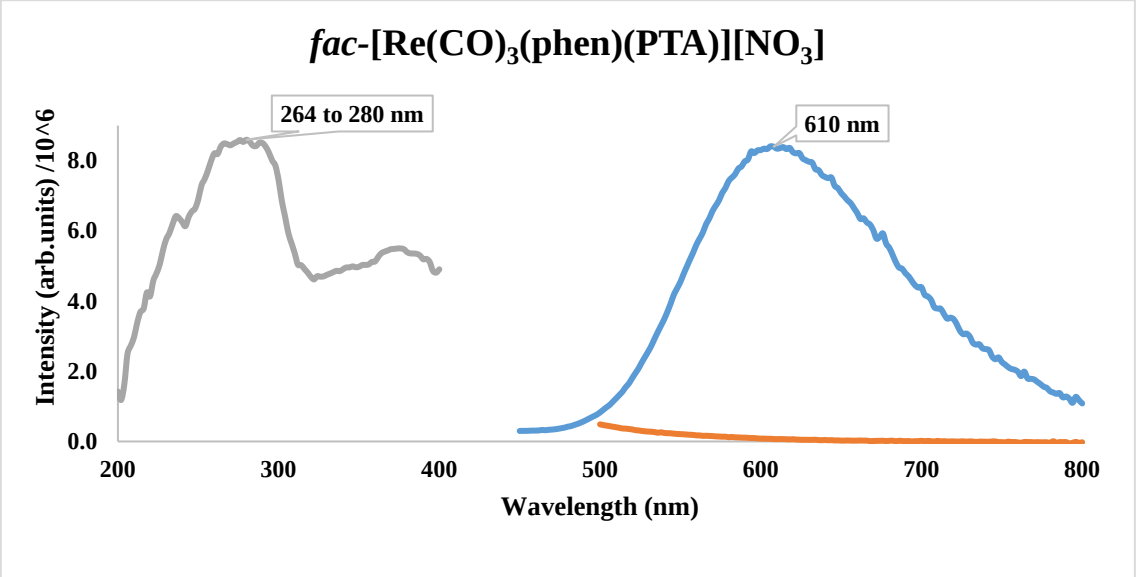

Figure 5.8: Representation of the excitation (grey) and emission (blue) of *fac*-[Re(CO)$_3$(phen)(PTA)][NO$_3$] and methanol (orange).

fac-[Re(CO)$_3$(phen)(DAPTA)][NO$_3$] (**8**) was synthesized according to the synthetic procedure in Paragraph 3.5.6 and electrons were absorbed at a maximum wavelength of 265 nm as seen in Figure 5.9 and the excitation and emission graphs were collected (Figure 5.10). The excitation wavelengths at 228 and 270 nm are observed and the peak at wavelength 270 nm gives rises to the maximum emission at 616 nm.

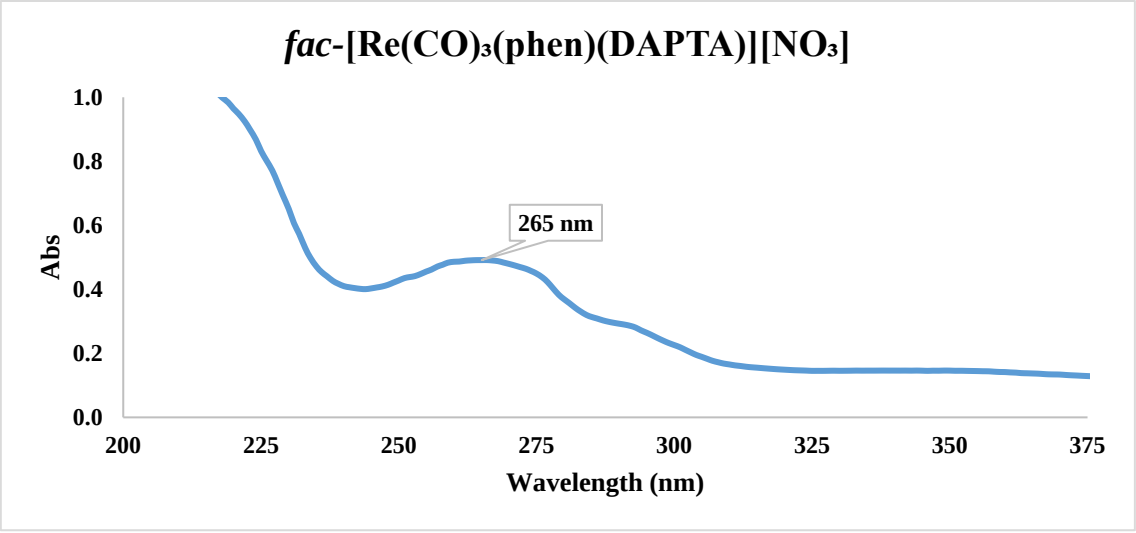

Figure 5.9: Illustration of the UV/Vis absorbance of *fac*-[Re(CO)$_3$(phen)(DAPTA)][NO$_3$] in methanol 25.0 °C with a concentration of 1.58×10^{-5} M.

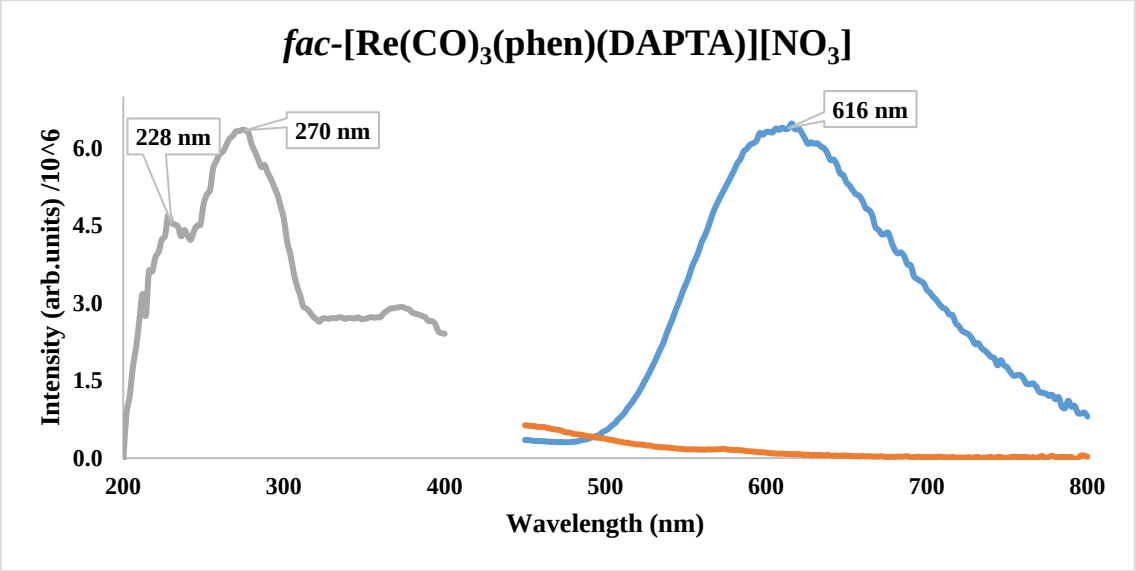

Figure 5.10: Representation of the excitation (grey) and emission (blue) of *fac*-[Re(CO)$_3$(phen)(DAPTA)][NO$_3$] and methanol (orange).

5.3.2. Excitation, emission, and absorbance of rhenium(I) dicarbonyl complexes:

The maximum absorbance of *cis-trans*-[Re(CO)$_2$(phen)(PPh$_3$)$_2$][NO$_3$] (**9**) was at 266 nm and was synthesized according to the procedure in Paragraph 3.5.7. (Figure 5.11). The excitation graph showed more than one excitation wavelength (Figure 5.12) Excitation wavelengths at 236 and 264 - 284 nm is visible. The excitation wavelength at 278 nm gives rise to the maximum emission at 616 nm. The excitation wavelength at 278 nm was the best to obtain the maximum emission wavelength.

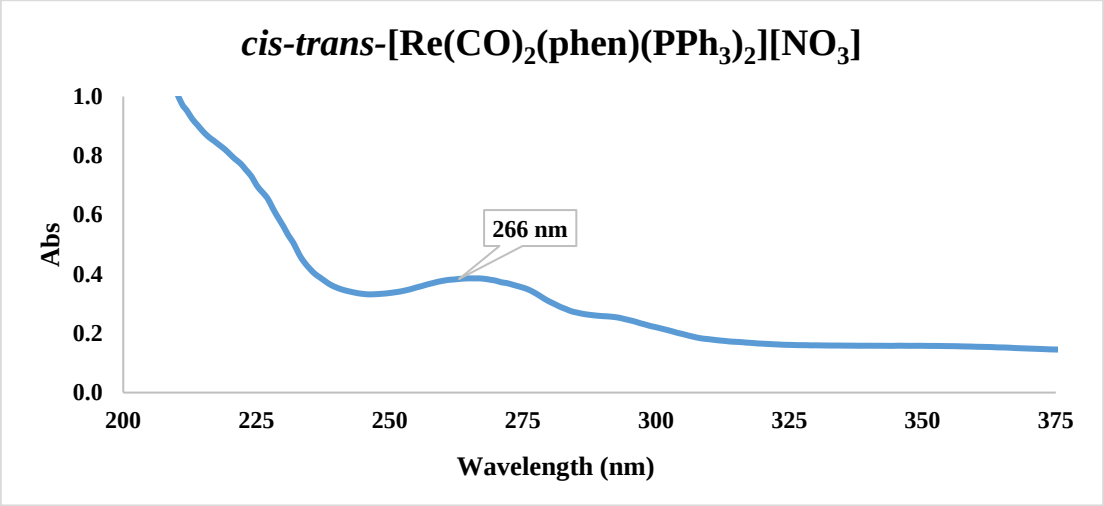

Figure 5.11: Illustration of the UV/Vis absorbance of *cis-trans*-[Re(CO)$_2$(phen)(PPh$_3$)$_2$][NO$_3$] in methanol at 25.0 °C with a concentration of 2.97×10^{-5} M.

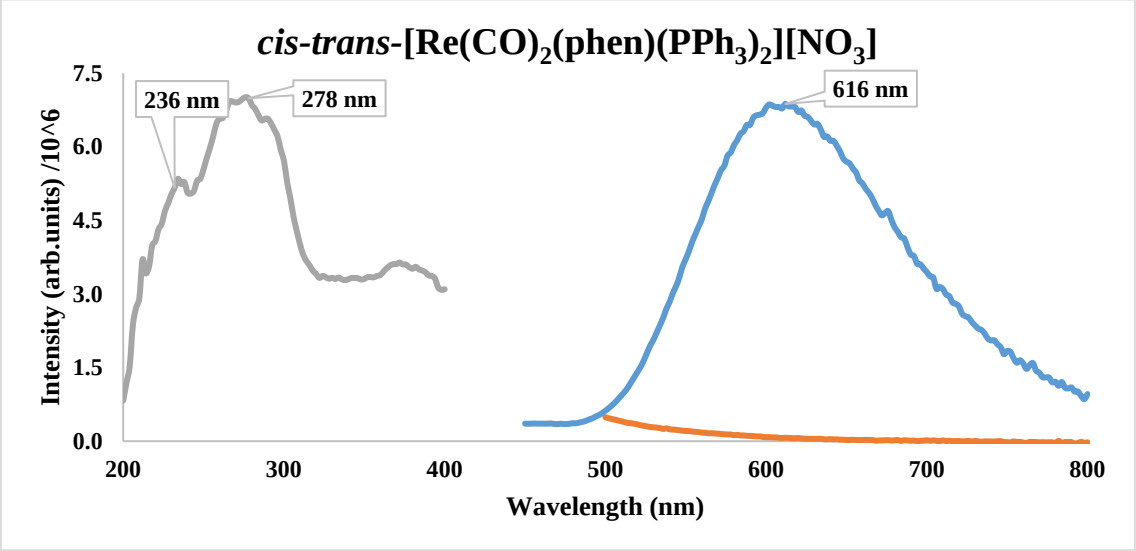

Figure 5.12: Representation of the excitation (grey) and emission (blue) of *cis-trans*-[Re(CO)$_2$(phen)(PPh$_3$)$_2$][NO$_3$] and methanol (orange).

cis-trans-[Re(CO)$_2$(phen)(PTA)$_2$][NO$_3$] (**10**) was synthesised according to the synthetic procedure in Paragraph 3.5.8 and showed a maximum absorption at 262 nm. (Figure 5.13) The excitation spectrum (Figure 5.14) had two excitation wavelengths at 230 nm and 276 nm as seen in Figure 5.14. The 276 nm peak appears to be the more noticeable excitation peak and gives rise to the maximum emission at 610 nm.

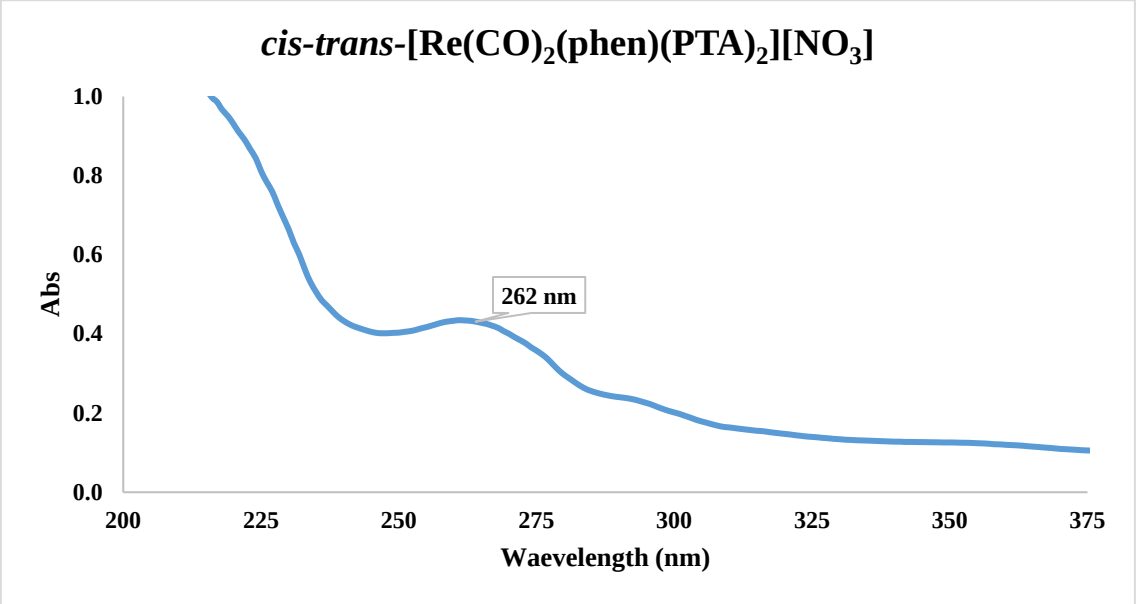

Figure 5.13: Illustration of the UV/Vis absorbance of *cis-trans*-[Re(CO)$_2$(phen)(PTA)$_2$][NO$_3$] at 25.0 °C in methanol with a concentration of 3.00×10^{-5} M.

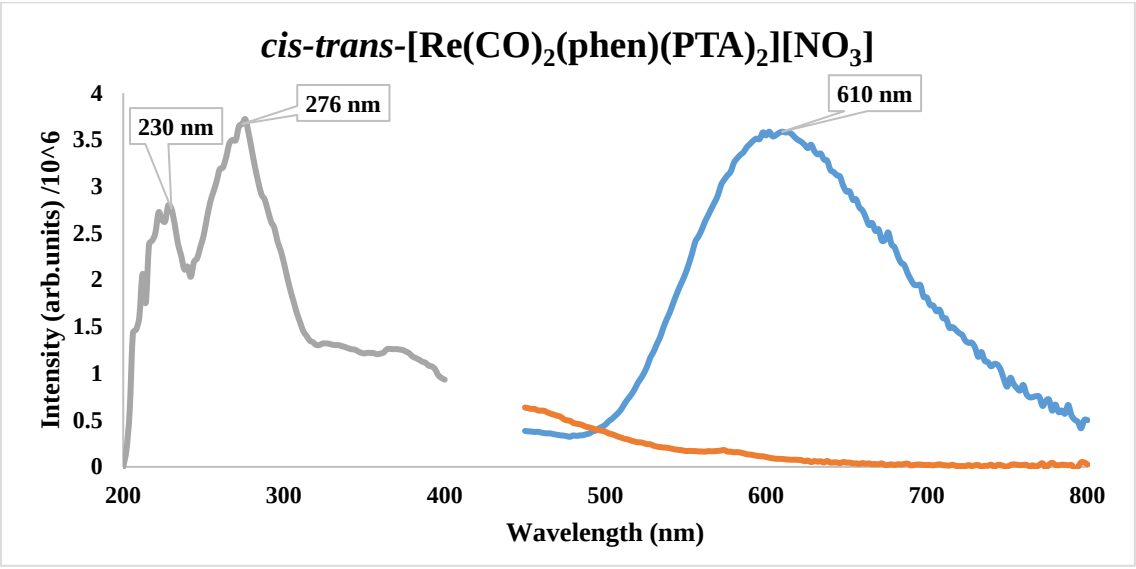

Figure 5.14: Representation of the excitation (grey) and emission (blue) of *cis-trans*-[Re(CO)$_2$(phen)(PTA)$_2$][NO$_3$] and methanol (orange).

cis-trans-[Re(CO)$_2$(phen)(DAPTA)$_2$][NO$_3$] (**11**) was synthesized according to the synthetic procedure in Paragraph 3.5.9 and illustrated the maximum absorption of the electrons at 260 nm. (Figure 5.15) The excitation graph has more than one excitation wavelength at 230 and 274 nm as seen in Figure 5.16. The 274 nm peak appears to be the more noticeable excitation peak. This peak gives rise to the maximum emission at 610 nm.

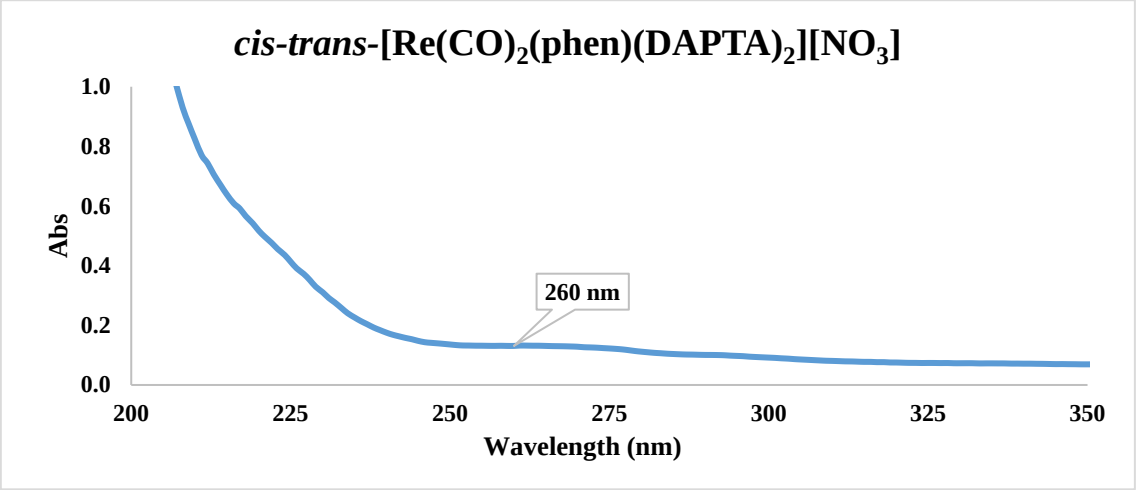

Figure 5.15: Illustration of the UV/Vis absorbance of *cis-trans*-[Re(CO)$_2$(phen)(DAPTA)$_2$][NO$_3$] in methanol at 25.0 °C with a concentration of 1.59×10^{-5} M.

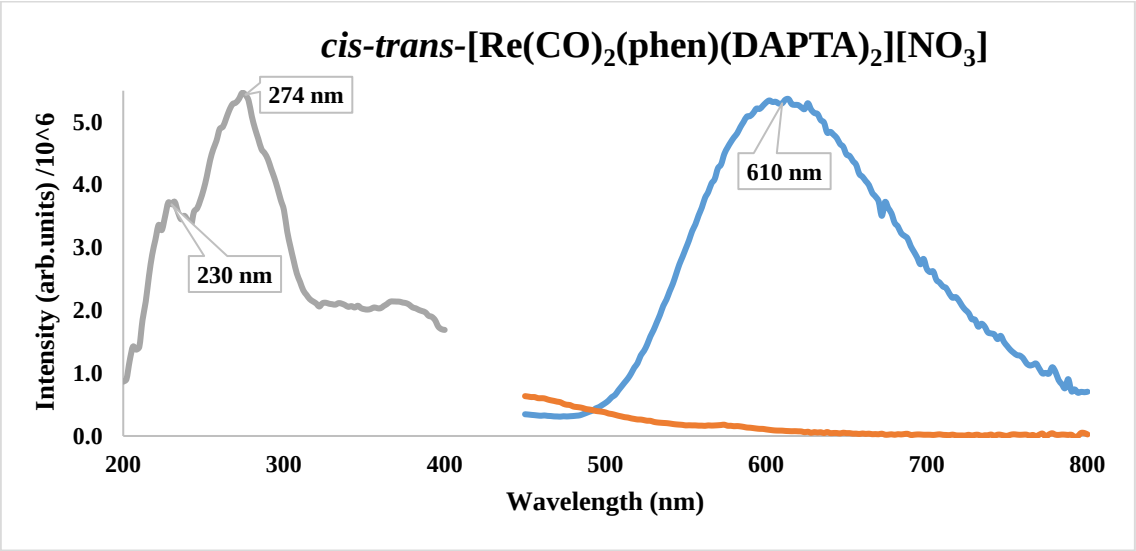

Figure 5.16: Representation of the excitation (grey) and emission (blue) of *cis-trans*-[Re(CO)$_2$(phen)(DAPTA)$_2$][NO$_3$] and methanol (orange).

cis-[Re(CO)$_2$(phen)(PPh$_3$)(Cl)] (**12**) was synthesized according to Paragraph 3.6.1 and the electrons were absorbed at a maximum of 266 nm. (Figure 5.17) The excitation and emission spectrums were obtained and are illustrated in Figure 5.18. The excitation graph has more than one wavelength at 294 and 374 nm. The peak at 374 nm gives rise to the maximum emission at 624 nm.

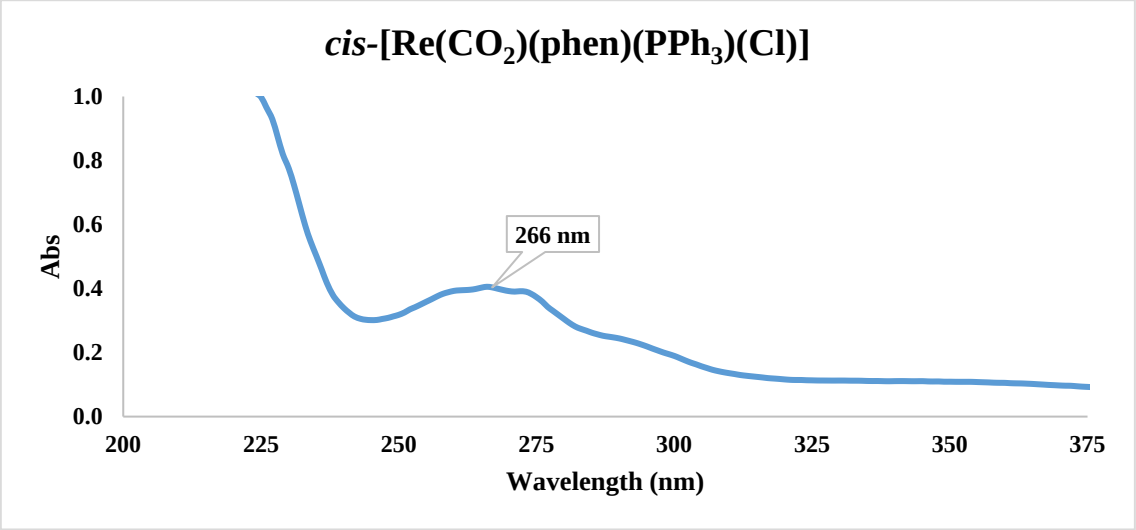

Figure 5.17: Illustration of the UV/Vis absorbance of *cis*-[Re(CO)$_2$(phen)(PPh$_3$)(Cl)] in methanol at 25.0 °C with a concentration of 7.19×10^{-5} M.

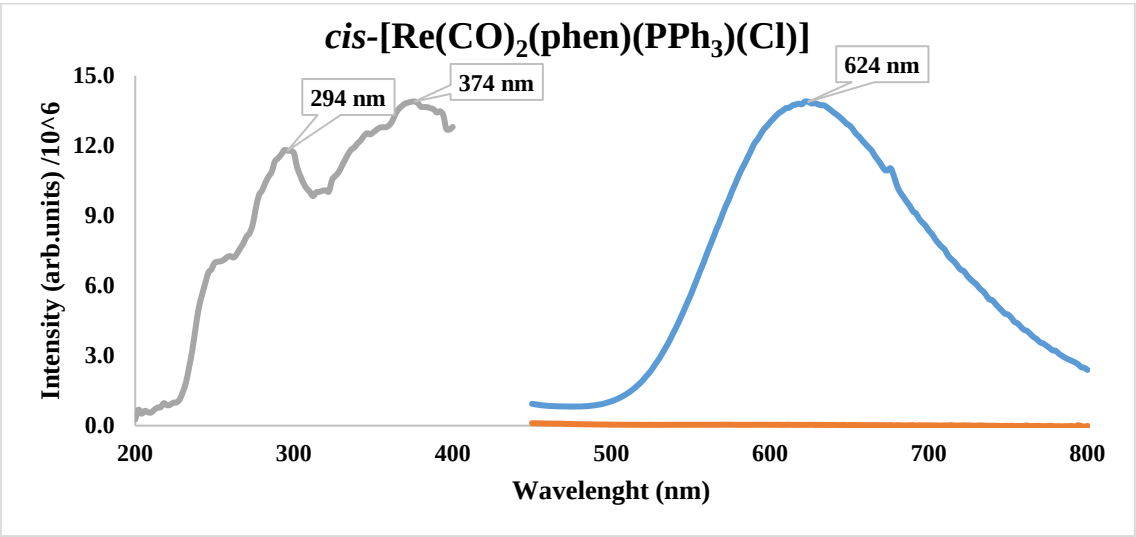

Figure 5.18: Representation of the excitation (grey) and emission (blue) of *cis*-[Re(CO)$_2$(phen)(PPh$_3$)(Cl)] and methanol (orange).

cis-[Re(CO)$_2$(phen)(PTA)(Cl)] (**13**) was synthesized according to the synthetic procedure in Paragraph 3.6.2. The maximum absorption of the electrons by light indicated a peak at wavelength 268 nm (Figure 5.19). The excitation graph showed more than one wavelength at 254 nm and 292 nm as seen in Figure 5.20. The 292 nm peak appears to be the more prominent peak and gives rise to the maximum emission at 630 nm.

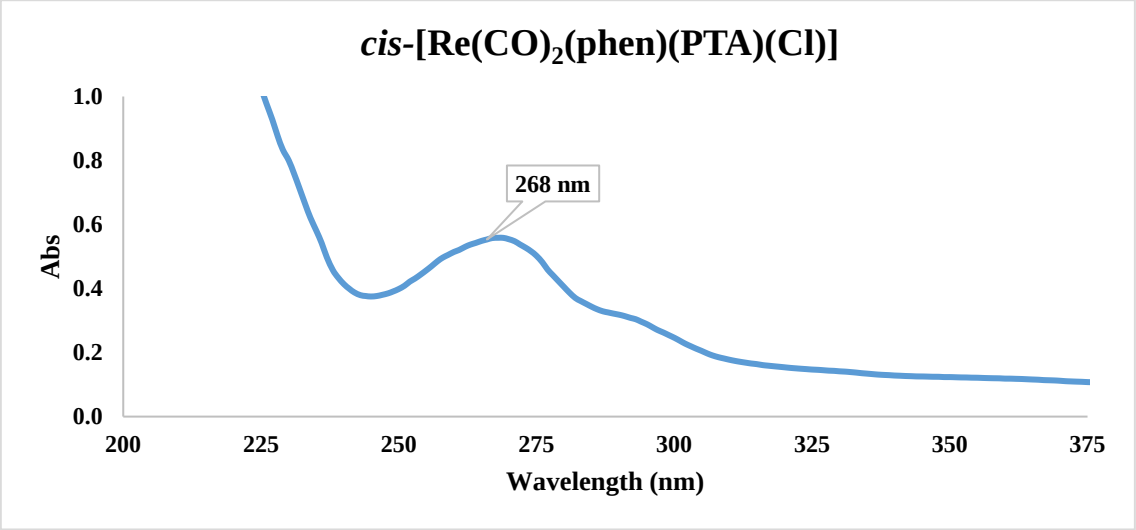

Figure 5.19: Illustration of the UV/Vis absorbance of *cis*-[Re(CO)$_2$(phen)(PTA)(Cl)] at 25.0 °C in methanol with a concentration of 2.33×10^{-4} M.

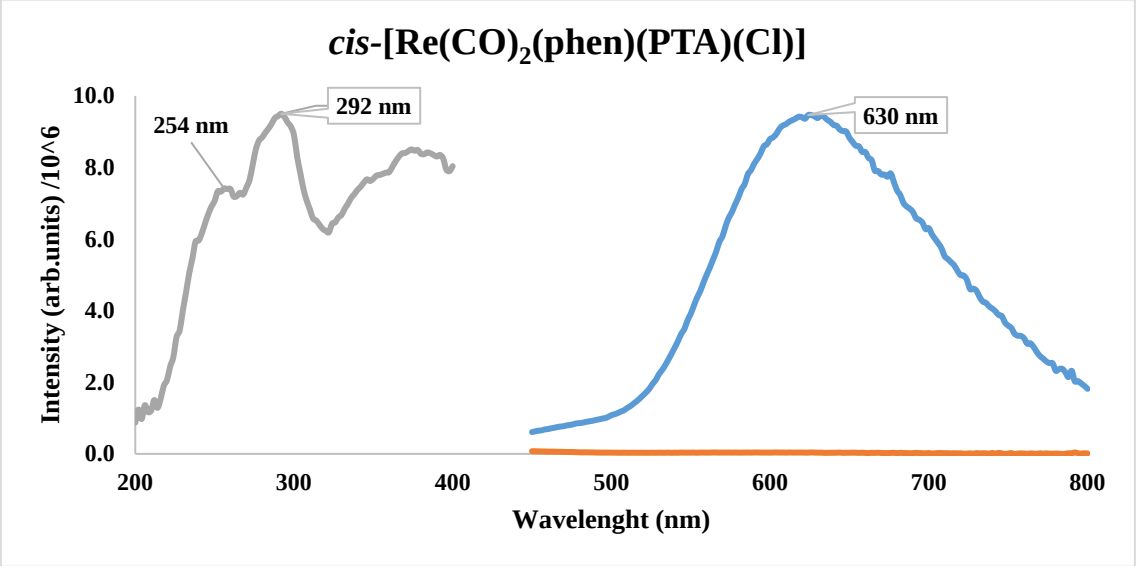

Figure 5.20: Representation of the excitation (grey) and emission (blue) of the *cis*-[Re(CO)$_2$(phen)(PTA)(Cl)] and methanol (orange).

cis-[Re(CO)$_2$(phen)(DAPTA)(Cl)] (**14**) was synthesized according to the synthetic procedure in Paragraph 3.6.3 and has an absorption peak at 269 nm. (Figure 5.21.) The excitation wavelength at 370 nm was chosen as the maximum excitation wavelength and the peak gives rise to the maximum emission at 620 nm as seen in Figure 5.22.

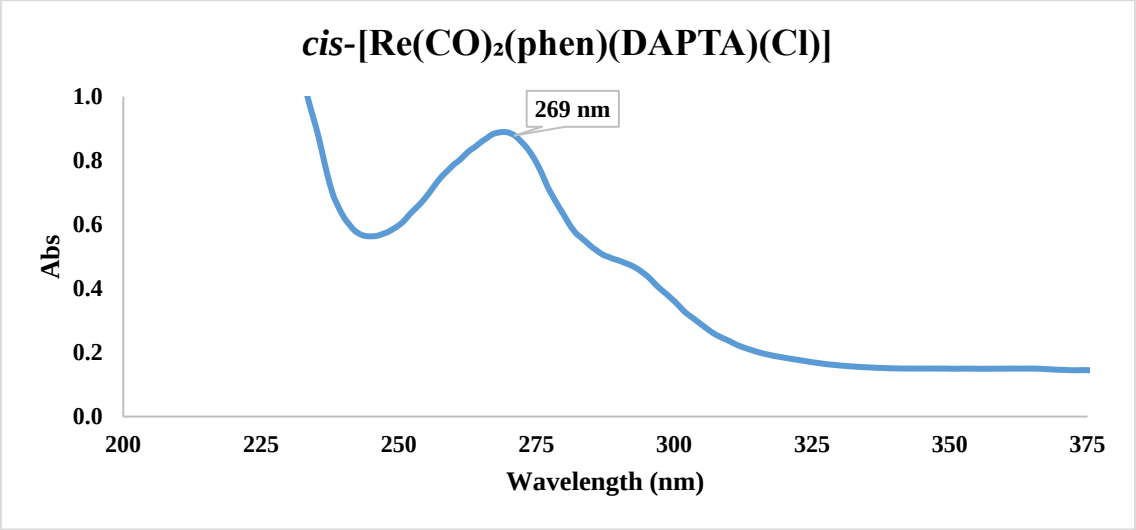

Figure 5.21: Illustration of the UV/Vis absorbance spectra of *cis*-[Re(CO)$_2$(phen)(DAPTA)(Cl)] at 25.0 °C in methanol with a concentration of 2.20×10^{-4} M.

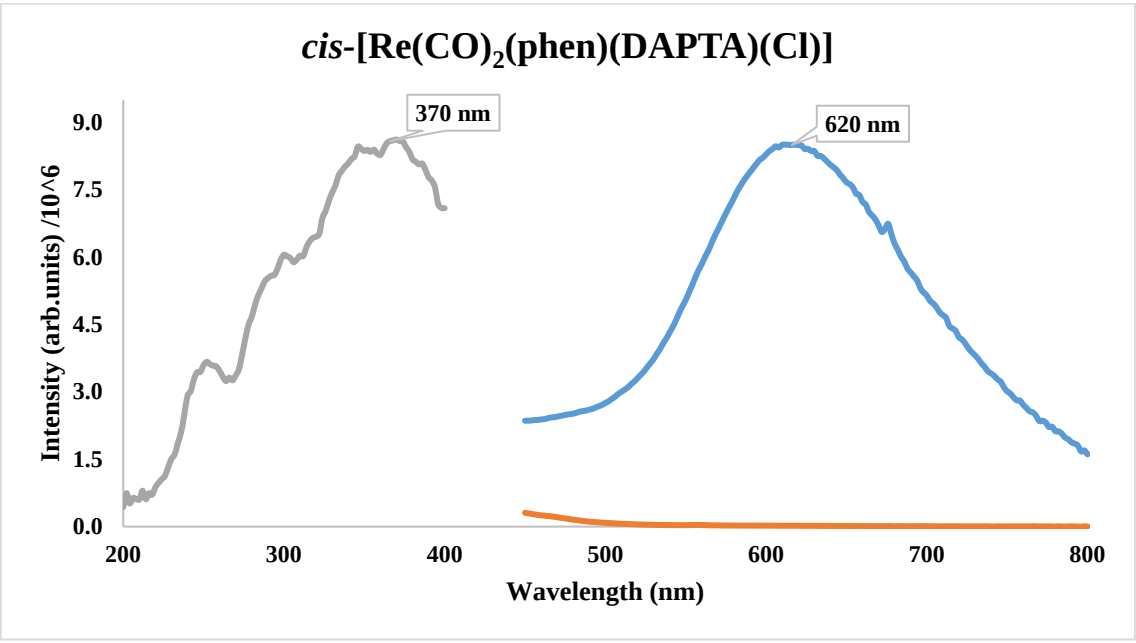

Figure 5.22: Representation of the excitation (grey) and emission (blue) of *cis*-[Re(CO)$_2$(phen)(DAPTA)(Cl)] and methanol (orange).

5.4. Discussion:

Photoluminescence is one of the more sensitive characterization methods.[4] All of the Re(I) tri- and dicarbonyl complexes tested in this study showed luminescent properties. The excitation and absorption wavelengths were recorded with UV/Vis absorbance and PL studies

[4] M. Koós, M. Veres, M. Füle and I. Pocsik, *Diamond and Related Materials*, **2002**, 11, 53-58.

respectively. It is expected that the maximum wavelengths obtained from the UV/Vis absorbance studies to be similar to the wavelengths obtained from the excitation graph, which is not the case here. The wavelengths obtained from the excitation graphs are slightly higher in each case.

Table 5.1: Summary of the molar absorptivity and the wavelengths of the absorbance, emission, and excitation of all the studied complexes.

	Complex Name	Molar absorptivity (ε) (M^{-1} cm^{-1})	Wavelengths		
			Absobance (λ_{max})	Emission (nm)	Excitation (nm)
3	*fac*-[$Re(CO)_3(phen)(CH_3OH)][NO_3$]	32595	265	610	270
5	*fac*-[$Re(CO)_3(phenO_2)(Br)$]	6766	298	648	330
6	*fac*-[$Re(CO)_3(phen)(PPh_3)][NO_3$]	11490	265	610	270
7	*fac*-[$Re(CO)_3(phen)(PTA)][NO_3$]	13146	266	610	280
8	*fac*-[$Re(CO)_3(phen)(DAPTA)][NO_3$]	31185	265	610	270
9	*cis-trans*[$Re(CO)_2(phen)(PPh_3)_2][NO_3$]	12961	266	616	280
10	*cis-trans*[$Re(CO)_2(phen)(PTA)_2][NO_3$]	14465	262	610	270
11	*cis-trans*-[$Re(CO)_2(phen)(DAPTA)_2][NO_3$]	8279	260	610	270
12	*cis*-[$Re(CO)_2(phen)(PPh_3)(Cl)$]	5641	266	624	297, 374
13	*cis*-[$Re(CO)_2(phen)(PTA)(Cl)$]	2399	268	630	292
14	*cis*-[$Re(CO)_2(phen)(DAPTA)(Cl)$]	4041	269	620	370

All the complexes studied display characteristic UV/Vis spectra of the low-spin d^6 Re(I) di- and tricarbonyl metal centre. As stated by Beer's Law, molar absorptivity is constant, while the absorbance is proportional to the concentration and measures how strongly compounds absorbs light at a specific wavelength. A difference between the calculated molar absorptivity coefficients (ε) of each complex are observed due to the specificity of every solution or sample with a change only in the absorbance measurement. As seen in Table 5.1, the molar absorptivity, absorbance, emission and excitation wavelengths are reported of the Re(I) tri- and dicarbonyl complexes.

A few luminescent Re(I) dicarbonyl compounds were synthesized by Smithback and co-workers with a general formula of *cis*-$[Re(CO)_2(P\text{-}P)(N\text{-}N)]^+$, where P-P is a chelating

diphosphine and N-N a polypyridine ligand. [5] These complexes (*cis-trans*-$[Re(CO)_2(PPh_3)(bpy)]^+$, *cis-trans*-$[Re(CO)_2(P(OPh)_3)_2(bpy)]^+$, *cis-trans*-$[Re(CO)_2(P(OPh)_3)_2)(phen)]^+$ and *cis-trans*-$[Re(CO)_2(P(OCH_3)_3)_2)(bpy)]^+$) exhibit yellow-orange colorations in solid state as well as in solution state because of the MLCT transitions within the range of 380 nm to 560 nm. The luminescence of these compounds occurred in the range of 600 nm to 700 nm. The emission wavelengths of these compounds are 620 nm, 568 nm, 556 nm and 614 nm for *cis-trans*-$[Re(CO)_2(PPh_3)(bpy)]^+$, *cis-trans*-$[Re(CO)_2(P(OPh)_3)_2(bpy)]^+$, *cis-trans*-$[Re(CO)_2(P(OPh)_3)_2)(phen)]^+$ and *cis-trans*-$[Re(CO)_2(P(OCH_3)_3)_2)(bpy)]^+$ respectively.[5] The emission wavelengths of **9**, **10** and **11**, the dicarbonyl bisphosphine compounds as seen in Table 5.1, are greater than the wavelengths reported by Smithback *et al*. accept for *cis-trans*-$[Re(CO)_2(PPh_3)(bpy)]^+$ (emission wavelength: 620 nm). Similar compounds, $[Re(CO)_3(pbt)(PTA)]CF_3SO_3$ and $[Re(CO)_3(phen)(PTA)]CF_3SO_3$ were synthesized by Chakraborty *et al.*[6] and have an orange luminescence at a wavelength of 550 nm and an excitation at 345 nm. When these complexes are exposed to low UV light, a diminution of the luminescence are reported and the dicarbonyl species had no fluorescence. [6] Fifteen water-soluble Re(I) tricarbonyl compounds were synthesized by Marker *et al.*[7] with the same general formula as Smithback *et al.*[5] for luminescence studies. These compounds undergo photosubstitution of the CO ligand when irradiated with 365 nm light and showed to be emissive except for the compound with the PTA ligand which did not undergo photosubstitution when irradiated with light at 365 nm. The maximum absorbance wavelengths for the Re(I) PTA complex were at 226, 274 and 368 nm while the Re(I) complex with the DAPTA ligand showed a maximum absorbance at wavelengths of 225, 275 and 367 nm.

As seen in Table 5.1, **13** (PTA) and **14** (DAPTA) has a maximum absorbance of 268 nm and 269 nm respectively and are within the range of the absorbance wavelengths obtained from Marker and co-workers.[7] All of the complexes synthesized by Marker *et al*. were evaluated as photoactivated anticancer agents in HeLa (human cervical), cisplatin-resistant ovarian

[5] J. L. Smithback, J. B. Helms, E. Schutte, S. M. Woessner and B. P. Sullivan, *Inorganic Chemistry*, **2006**, 5(45), 2163-2174.

[6] I. Chakraborty, S. J. Carrington, G. Roseman and P. K. Mascharak¸ *Inorganic Chemistry*, **2017**, 56, 1534-1545.

[7] S. C. Marker, S. N. MacMillan, W. R. Zipfel, Z. Li, P. C. Ford and J. J. Wilson, *Inorganic Chemistry*, **2018**, 57, 1311-1331.

(A2780CP70) as well as ovarian (A2780) cancer cell lines and the DAPTA complex with 1,10-phenanthroline resulted in a cytotoxic response. When the DAPTA complex was irradiated with light, the results showed that the compound is very phototoxic to HeLa cells (IC_{50} value of 6 μM).[7] The phototoxic response is obtained from the release of the CO ligands and production of $^1O_2$.

5.5: Conclusion:

UV/Vis absorption spectra were obtained in methanol solutions and were characterized by the presence of the overlapping of the strong absorption bands at very low wavelengths (below 300 nm) and resulted in broad low-energy bands in the range of 260 to 390 nm. The emission spectra are broad with a visible maximum peak present and are dependent on the nature of the N,N′-ligand in the complex. N,N′-ligands with better electron acceptor properties, result in lower energy of emission.[8] The electronic excitation localized within the rhenium(I) ion or the ligands refers to the existence of the excited metal-to-ligand charge transfer and are linked with the charge transfer fragments coordinated to the α-diimine ligands. This type of phenomenon affects the properties of the excited species. The excited metal charge states (MC) are above the ligand states (LC) and are due to the large splitting of the rhenium(I) d-orbitals caused by the presence of the three CO ligands which have a strong ligand field.[8] The energy gap between the two excited states of the *MLCT and *LC are smaller and allow an electronic interaction between them. In metal/ligand combinations that contain any strong π-acid such as CO and/or aromatic phosphines, the auxiliary ligand is used as the model system and result in a large energy splitting of the d-orbitals of the metal ion. The increased energy splitting between the d sublevels leads to an * MC state with high energy.

[8] A. Kamecka, K. Prachnio and A. Kapturkiewicz, *Journal of Luminescence*, **2018**, 203, 409-419.

CHAPTER 6: CYTOTOXICITY OF BIMETALLIC COMPOUNDS

6.1. Introduction:

Cytotoxic drugs are used to destroy cancer cells and inhibit cell division. These drugs are transported in the bloodstream through the body.[1] Cytotoxicity can be defined as a biological evaluation or screening test making use of tissue cells *in vitro* for the observation of cell growth and reproduction by medical devices. [2] The cytotoxicity tests are preliminary tests performed on different cell lines such as HeLa, HepG2 or PT45 to determine whether the compounds could be used as potential PDT (photodynamic therapy) agents. PDT is the administration of non-toxic drugs or dyes also known as photosensitizers (PS) to patients.[3] In the presence of oxygen in a wavelength range of 620 nm to 690 nm, cytotoxicity is generated and can lead to cell death or the damage of tissue. PDT, only one of the different therapeutic options, is used as a treatment for various cancer types and has the ability to be selective and specific.[3] Different types of cytotoxic drugs are also used in cancer therapy and have several different effects. The effectiveness of chemotherapy is dependent on the tumour type as well as the proportion of the cells in the distribution stage.[1]

During the last few years, more attention is given to transition metal complexes for the use as chemotherapeutics as well as antiviral drugs. Cisplatin and its analogs are very effective chemotherapeutic agents and are in clinical use. Cisplatin is intravenously administrated because of the insolubility in water and is highly toxic.[4]

6.2. Cytotoxicity of monometallic compounds:

Organometallic compounds such as Re(I) complexes showed to be toxic to a few cancer cell lines, but lack the property of being selective towards cancer cells for the use as novel

[1] Y. Zhang, *Clinical and Translational Medicine*, **2018**, 7(34), 1-6.

[2] W. Li, J. Zhou and Y. Xu, *Biomedical Reports*, **2015**, 3, 617-620.

[3] C. A. Robertson, D. Hawkins Evans and H. Abrahamse, *Journal of Photochemistry and Photobiology*, **2009**, 29, 1-8.

[4] A. F. Tikum, Y. J. Jean, J. H. Lee, M. H. Park, I. Y. Bae, S. H. Kim, H. J. Lee and J. Kim, *Journal of Inorganic Biochemistry*, **2018**, 180, 204-210.

chemotherapeutic agents.[5] Leonidova and co-workers showed that Re-COOH (Re(I) tricarbonyl [N,N′-bis(quinolin-2-ylmethyl)amino]-5-valeric acid) and Re-NH_2 (Re(I) tricarbonyl [N,N′-bis(quinolin-2-ylmethyl)amino]-4-butane-1-amine) have the potential of being PDT photosensitizes. These compounds can be improved to be more selective when conjugated to peptides such as nuclear localization signal (NLS) and neuropeptide bombesin.[5] The cytotoxicity for PDT applications of these Re(I) complexes coordinated to the peptides is increased upon the irradiation of light.[5]

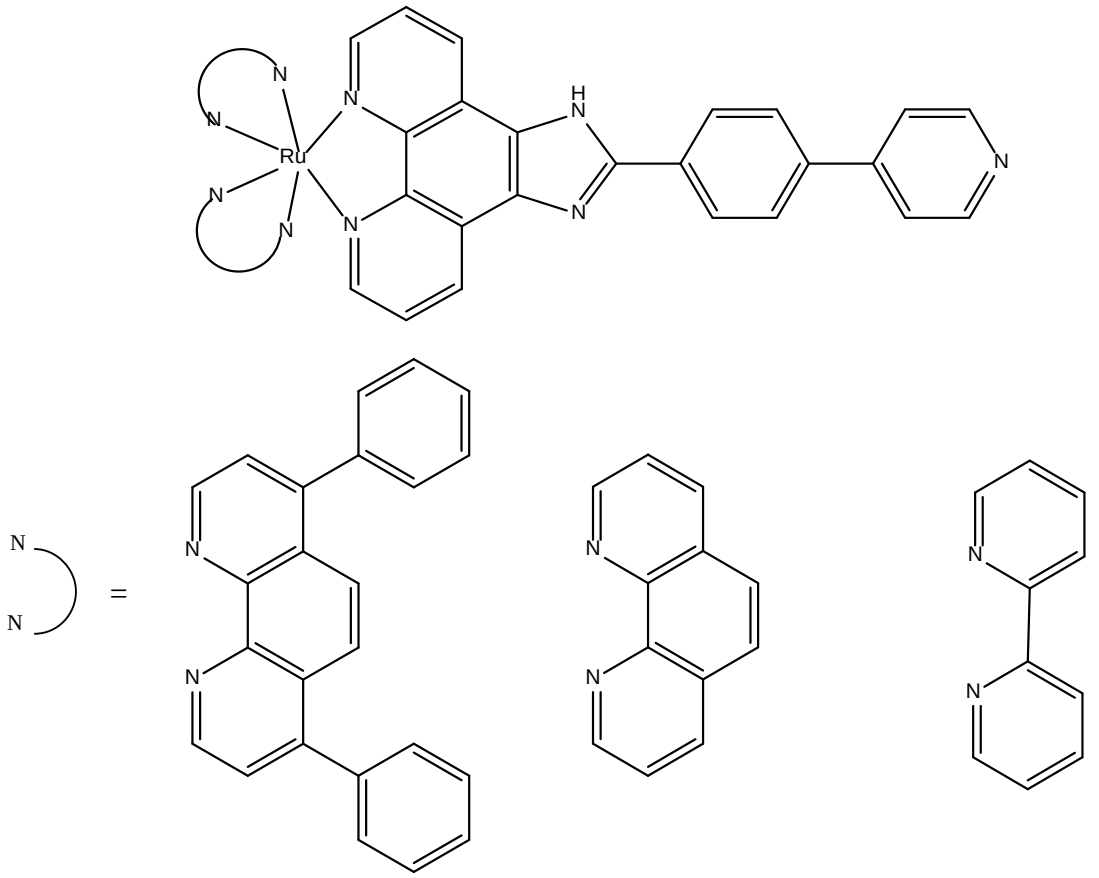

4,7-diphenyl-1,10-phenanthroline **1,10-phenanthroline** **2,2′-bipyridine**

Figure 6.1: Ruthenium metal complex with the auxiliary ligand, phenylisoquiolinate, and one of the three chelating ligands, 4,7-diphenyl-1,10-phenanthroline, 1,10-phenanthroline and 2,2′-bipyridine. [4]

During the study by Tikum *et al*. they discovered that ruthenium showed to be one of the most promising transition metals with a low toxicity and had the ability to mimic iron in the

[5] A. Leonidova, V. Pierroz, R. Rubbiani, J. Heier, S. Ferrari and G. Gasser, *Dalton Transactions*, **2014**, 43, 4287-4294.

binding to biomolecules.[4] They studied the interactions between a variety of metal complexes and the biomolecules, with the aim of developing new cell imaging agents. They synthesized three ruthenium complexes with piq (phenylisoquinolinate) as the auxiliary ligand and different chelating ligands as seen in Figure 6.1.[4]

6.3. The cytotoxicity of bimetallic compounds:

Multimetallic compounds were synthesized with the main aim of increasing the cytotoxicity of metallodrugs.[6]

Dicobalt hexacarbonyl complexes were synthesized with alkyne ligands by Gross *et al.*[7] These cobalt-alkyne complexes have antitumor activity and revealed that the dicobalt hexacarbonyl complex with a propargylic ester of acetylsalicylic acid (Figure 6.2) also showed cytotoxicity against various cell lines.[7]

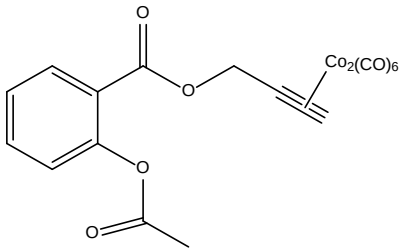

Figure 6.2: Schematic representation of the dicobalt hexacarbonyl complex.[8]

Most of the chemotherapeutic agents lack the property of being tumor-specific and to obtain specificity, the cytotoxic agents are linked to biomolecules like peptides. Neurotensin (NT) is one example of many peptides and are found in various tumors such as breast- and prostate cancer.[7] Gross and co-workers combined the tumor-specific property of the NT with the cytotoxic effect of the cobalt compound. To ensure enhancement of the cellular uptake, they combined a ruthenocene moiety to the cobalt compound, forming a bimetallic peptide biconjugate.[7] The newly synthesized complex was tested against three cell lines. The ruthenocene cobalt carbonyl NT peptide complex (Figure 6.3) showed to be cytotoxic against HeLa, PT45 and HepG2 cells.

[6] M. Wenzel, E. bigaeva, P. Richard, P. Le Gendre, M. Picquet, A. Casini and E. Bodio, *Journal of Inorganic Biochemistry*, **2014**, 141, 10-16.

[7] A. Gross, M. Neukamm and N. Metzler-Nolte, *Dalton Transactions*, **2011**, 40, 1382-1386.

[8] I. Zanellato, I. Bonarrigo, M. B. Ravera, E. Gabano, R. Gust and D. Osella, *The Royal Society of Chemistry,* **2013**, 5, 1604-1613.

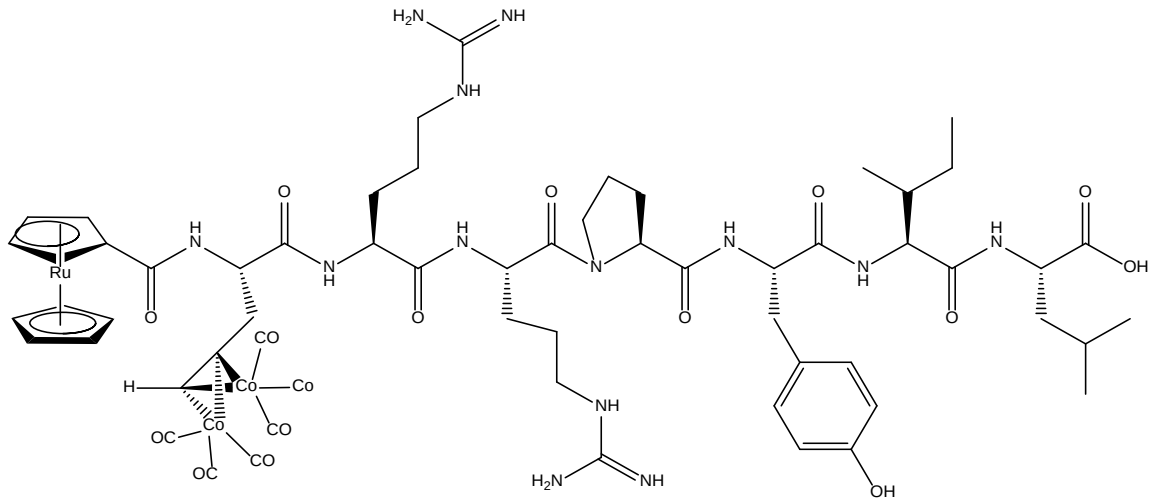

Figure 6.3: Structure of the ruthenocene cobalt carbonyl NT peptide complex.[7]

This bimetallic compound showed to be selective towards cancer cells and less toxic to the normal cell when tested against different cell lines.[9]

6.4. *In vitro* testing of novel synthesized bimetallic complexes:

During the study of the cytotoxicity of bimetallic complexes, three bimetallic- and one dinuclear complex were synthesized and the synthetic procedures were reported in Chapter 3 and are illustrated in Figure 6.4.

The four compounds tested for *in vitro* cytotoxicity were:

- $[Re_2(CO)_6(\mu\text{-phenO}_2)Br_2]$ – (**Re-Re**),
- $[Ru(phen)_2(N,N'\text{-phenO}_2\text{-}O,O')\text{-}Re(CO)_3Br][PF_6]_3$ – (**Ru-Re**),
- $[Ru(phen)_2(N,N'\text{-phenO}_2\text{-}O,O')\text{-}PtCl_2][PF_6]_3$ – (**Ru-Pt**) and
- $[Re(CO)_3(N,N'\text{-phenO}_2\text{-}O,O')\text{-}PtCl_2]Br$ – (**Re-Pt**).

[9] L. Massai, J. Fernandez-Gallardo, A. Guerri, A. Arcangeli, S. Pillozzi, M. Contal and L. Messori, *Dalton Transactions*, **2015**, 44, 11067-11076.

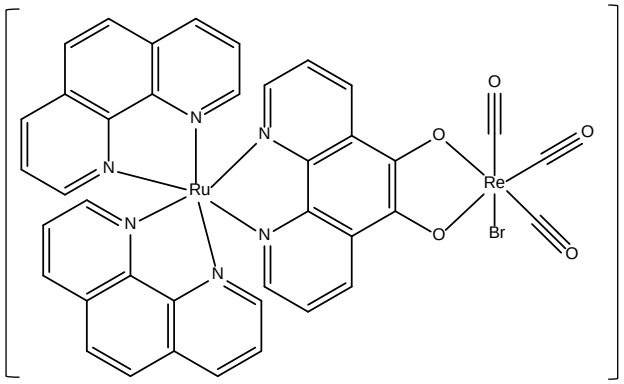

[Ru(phen)$_2$(*N,N′*-phenO$_2$-*O,O′*)-Re(CO)$_3$Br][PF$_6$]$_3$

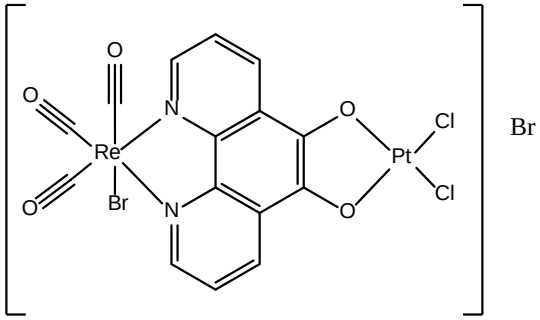

[Re(CO)$_3$(*N,N′*-phenO$_2$-*O,O′*)-PtCl$_2$]Br

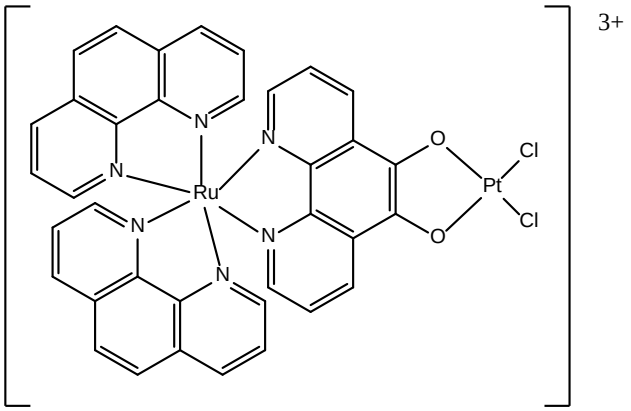

[Ru(phen)$_2$(*N,N′*-phenO$_2$-*O,O′*)-PtCl$_2$][PF$_6$]$_3$

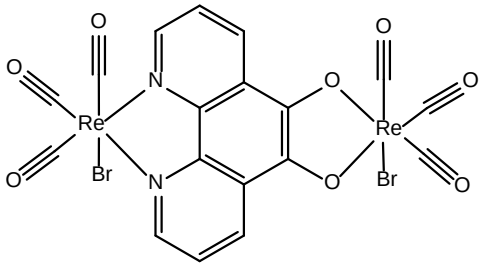

[Re$_2$(CO)$_6$(μ-phenO$_2$)Br$_2$]

Figure 6.4: Illustration of the compounds tested for *in vitro* cytotoxicity.

The four compounds were tested against the following cell lines:

- HeLa: *Homo sapiens* cervix adenocarcinoma cell line
- hTERT: Immortalized retinal pigmented epithelial cells
- RPE-1: *Homo sapiens* retinal pigmented epithelial cell line

These complexes were screened for photoactivated *in vitro* anticancer activity and the results are reported in Paragraph 6.6.

6.5. Experimental:

2500 µM stock solutions of each compound were prepared in DMSO.The stock solutions were then diluted with media starting from the highest DMSO concentration of 2 %. The final concentration of DMSO was superior to 1 %.

Cell culture:

- HeLa cell lines were cultured in DMEM (Gibco, Life Technologies, USA) supplemented with 10 % of fetal calf serum (Gibco).
- RPE-1 cell lines were cultured in DMEM/F-12 (Gibco) supplemented with 10 % of fetal calf serum.
- All cell lines were complemented with 100 U/ml penicillin-streptomycin mixture (Gibco) and maintained in a humidified atmosphere at 37 °C and 5 % of CO_2.

Cytotoxicity was assessed by fluorometric cell viability assay using resazurin (ACROS Organics). HeLa and RPE-1 cells were seeded in triplicates in 96 well plates at a density of 4000 cells per well in 100µl, 24 h prior to treatment. Cells were then treated with an increasing concentration of the compounds for 48 h. After that time, the medium was replaced by fresh complete medium containing resazurin (0.2 mg ml^{-1} final concentration). After 4 h incubation at 37 °C, the fluorescence signal of the resorufin product was read by SpectraMax M5 microplate reader (ex: 540 nm em: 590 nm). IC_{50} values were calculated using GraphPad Prism software[10].

6.6. Results and Discussion:

The four bimetallic complexes were evaluated for *in vitro* cytotoxicity against HeLa and RPE-1 cell lines.

Table 6.1: IC_{50} values (in µM) of the bimetallic compounds against HeLa and RPE-1 cell lines.

Compounds / Cell line	Re-Pt	Ru-Pt	Ru-Re	Re-Re
HeLa	7.31 ± 0.07	> 100	non soluble	> 100
RPE-1	10.92 ± 0.13	> 100		> 100

[10] GraphPad Prism version 7.00 for Windows, GraphPad software, La Jolla California USA.

Compounds with the ability for metal coordination with slow metal-ligand exchange rates are comparable to the cell divisions processes and appears to be very active in killing cancer cells.[11] This may be present in platinum, rhenium and ruthenium complexes.

As seen in Table 6.1, only **Re-Pt** showed to be cytotoxic against HeLa cells, while the other compounds were outside the concentration range used for the testing or not soluble. According to Gross *et al.*[12] cisplatin showed a cytotoxic effect against the HeLa cell line with an IC_{50} value of 1.3 ± 0.2 µM therefore **Re-Pt** has a lower cytotoxicity than cisplatin against the HeLa cell line. $[Pt(C_6H_{13}N)I_2]_2$ was prepared by Zhang and co-workers[13] and tested against a few other cell lines such as HCT-8, BGC-823, HL-60, and MCF-7. This compound showed to have better cytotoxicity than cisplatin in previously mentioned cell lines with IC_{50} values of 1.02 ± 0.21, 4.00 ± 0.35, 0.02 ± 0.009 and 1.70 ± 0.21 respectively.[13]

6.7. Conclusion:

The four bimetallic compounds were successfully synthesized and characterized as reported in Chapter 3. These compounds were tested against cervical cancer cells (HeLa cells) and retinal pigmented epithelial cells (RPE-1 cells) and the results were obtained. $[Re(CO)_3(N,N'\text{-phen}O_2\text{-}O,O')\text{-}PtCl_2]Br$ is the only complex that showed cytotoxic effects against HeLa cell lines and shows a cytotoxicity of 7.31 ± 0.07 µM which is slightly lower than cisplatin (1.3 ± 0.2 µM).

[11] J. Reedijk, *Platinum Metals Review,* **2008**, 52(1), 2-11.

[12] A. Gross, M. Neukamm and N. Metzler-Nolte, *Dalton Transactions*, **2011**, 40, 1382-1386.

[13] J. Zhang, L. Lu, Y. Gang, X. Zheng, M. Yang, J. Cui and S. Shen, *European Journal of Medical Chemistry,* **2009**, 44, 2322-2327.

CHAPTER 7: EVALUATION OF THIS STUDY

7.1. Introduction:

As shown by Leonidova and co-workers, Re(I) compounds have the ability to be toxic to different cancer cell lines and can act as chemotherapeutic agents.[1] However, during this study more focus was given to Re(I) tri- and dicarbonyl complexes and their luminescent properties for its use as diagnostic and therapeutic agents. Dinuclear complexes with polypyridyl fragments and conjugated bridging ligands have been studied before for three reasons:

i) their photophysical properties of being multi-chromophores due to their relevance to solar energy and artificial synthesis,

ii) the redox properties with mixed-valance compounds and

iii) for the separation of diastereoisomers to determine how isomerisation affects the chemical properties of these complexes.[2]

7.2. Results obtained:

One of the main aims of this study was the synthesis of two *N*,*N*′-bidentate ligands: 1,10-phenanthroline-5,6-dione (**phenO_2**) and 1,10-phenanthroline-5,6-diamine (**phen(NH_2)$_2$**). Both these ligands were successfully synthesized and characterized with IR, UV/Vis and NMR. These ligands were coordinated to **ReAA** for the formation of two novel dinuclear complexes where both these ligands act as the bridging ligand. **PhenO_2** act as a *N*,*N*′- and an *O*,*O*′-bidentate ligand for the use as a bridging ligand forming the bimetallic compounds, while **phen(NH_2)$_2$** has two *N*,*N*′-bidentate binding sites.

Re(I) tri- and dicarbonyl complexes were synthesized and characterized successfully by NMR, IR and UV/Vis. Photoluminescence studies were performed on these complexes and are reported in Chapter 5. The crystal structures of 5-amino-6-nitro-1,10-phenanthroline (**phen(NH_2)(NO_2)**), *fac*-[Re(CO)$_3$(phen)(H_2O)][NO_3]·1.5H_2O (**3**) and *fac*-

[1] A. Leonidova, V. Pierroz, R. Rubbiani, J. Heier, S. Ferrari and G. Gasser, *Dalton Transactions*, **2014**, 43, 4287-4294.

[2] N. C. Fletcher, T. C. Robinson, A. Behrendt, J. C. Jeffery, Z. R. Reeves and M. D. Ward¸ *Journal of the Chemical Society, Dalton Transactions*, **1999**, 2999-3006.

$[Re(CO)_3(phen)(Br)]$ (4) were obtained and reported in Chapter 4. $[Ru(phen)_2(phenO_2)][PF_6]_3$, the precursor of the bimetallic compounds were successfully synthesized and characterized as well as coordinated to other metal centres such as Pt(II) and Re(I). The bimetallic compounds were characterized by IR, NMR and elemental analysis. There were a few difficulties for obtaining the ^{13}C NMR of these bimetallic compounds. Three bimetallic complexes, $Ru(phen)_2(N,N'\text{-}phenO_2\text{-}O,O')\text{-}Re(CO)_3Br][PF_6]_3$, $[Ru(phen)_2(N,N'\text{-}phenO_2\text{-}O,O')\text{-}PtCl_2][PF_6]_3$ and $[Re(CO)_3(N,N'\text{-}phenO_2\text{-}O,O')\text{-}PtCl_2]Br$ and one dinuclear complex $[Re_2(CO)_6(\mu\text{-}phenO_2)Br_2]$ were successfully synthesized and characterized by NMR , IR and elemental analysis. Cytotoxicity studies were performed on the three bimetallic complexes $Ru(phen)_2(N,N'\text{-}phenO_2\text{-}O,O')\text{-}Re(CO)_3Br][PF_6]_3$, $[Ru(phen)_2(N,N'\text{-}phenO_2\text{-}O,O')\text{-}PtCl_2][PF_6]_3$ and $[Re(CO)_3(N,N'\text{-}phenO_2\text{-}O,O')\text{-}PtCl_2]Br$ and the dinuclear compound $[Re_2(CO)_6(\mu\text{-}phenO_2)Br_2]$ at Chimie ParisTech in Paris France and resulted that only one complex, $[Re(CO)_3(N,N'\text{-}phenO_2\text{-}O,O')\text{-}PtCl_2]Br$ showed to be cytotoxic against HeLa and RPE-1 cell lines as seen in Chapter 6.

7.3. Future research:

Future research will be performed on the following topics stated below:

- **$Phen(NH_2)_2$** , the *N,N′*-bidentate ligand have two coordinating abilities for the formation of new bimetallic as well as dinuclear compounds. A crystallographic study on the ligand as well as a variety of metal complexes will be performed.
- The Re(I) tri- and dicarbonyl complexes with watersoluble monodentate phosphine ligands will be synthesized with a different *N,N′*-bidentate ligand, changing the electronic properties of the complex. The solution and solid state effects will be evaluated.
- Synthesis of the $^{99/99m}Tc$ counterparts of the Re(I) tri- and dicarbonyl complexes as well as ^{186}Re and ^{188}Re radiolabelling.
- More research on bimetallic compounds with unique properties for future use as photosensitizers in photodynamic therapy.
- Kinetic studies on synthesized complexes to evaluate the reactivity as well as the stability of the compounds.

APPENDIX

APPENDIX A

Table 1A: Atomic coordinates ($x10^4$) and equivalent isotropic displacement parameters ($Å^2x10^3$) for 5-amino-6-nitro-1,10-phenanthroline (phen(NH_2)(NO_2)). U(eq) is defined as one third of the trace of the orthogonalized U^{ij} tensor.

	x	y	z	U(eq)
N(1)	4083(1)	4435(3)	3324(1)	38(1)
C(12)	2658(2)	3587(3)	2716(1)	29(1)
C(6)	1578(2)	5134(3)	3877(1)	31(1)
C(7)	2596(2)	5190(3)	3924(1)	30(1)
C(11)	3131(2)	4415(3)	3344(2)	31(1)
C(4)	1672(2)	3585(3)	2673(1)	28(1)
N(2)	3209(2)	2864(3)	2183(1)	36(1)
N(3)	173(2)	4325(3)	3197(2)	45(1)
C(5)	1103(2)	4399(3)	3262(2)	31(1)
O(1)	200(1)	6244(3)	4366(1)	56(1)
N(4)	1033(2)	5857(3)	4476(1)	42(1)
C(9)	4077(2)	6088(4)	4449(2)	46(1)
C(8)	3119(2)	6052(4)	4481(2)	40(1)
C(1)	2786(2)	2137(4)	1596(2)	39(1)
C(3)	1257(2)	2785(3)	2050(2)	36(1)
C(2)	1816(2)	2063(4)	1510(2)	38(1)
C(10)	4533(2)	5254(4)	3868(2)	47(1)
O(2)	1385(2)	6016(4)	5118(1)	79(1)

Table 1B: Bond lengths (Å) and angles (°) for 5-amino-6-nitro-1,10-phenanthroline (phen(NH_2)(NO_2)).

Bond	Bond distance	Bond angle	Angle
N(1)-C(10)	1.327(3)	C(10)-N(1)-C(11)	118.1(2)
N(1)-C(11)	1.358(3)	N(2)-C(12)-C(4)	122.8(2)
C(12)-N(2)	1.355(3)	N(2)-C(12)-C(11)	116.9(2)
C(12)-C(4)	1.409(3)	C(4)-C(12)-C(11)	120.3(2)
C(12)-C(11)	1.455(3)	C(5)-C(6)-N(4)	118.3(2)
C(6)-C(5)	1.406(4)	C(5)-C(6)-C(7)	122.5(2)
C(6)-N(4)	1.431(3)	N(4)-C(6)-C(7)	119.2(2)
C(6)-C(7)	1.456(3)	C(8)-C(7)-C(11)	115.5(2)
C(7)-C(8)	1.413(4)	C(8)-C(7)-C(6)	125.6(2)
C(7)-C(11)	1.418(4)	C(11)-C(7)-C(6)	118.9(2)
C(4)-C(3)	1.402(4)	N(1)-C(11)-C(7)	123.5(2)
C(4)-C(5)	1.469(4)	N(1)-C(11)-C(12)	116.7(2)

N(2)-C(1)	1.331(3)	C(7)-C(11)-C(12)	119.8(2)
N(3)-C(5)	1.333(3)	C(3)-C(4)-C(12)	117.6(2)
N(3)-H(4A)	0.89(3)	C(3)-C(4)-C(5)	121.5(2)
N(3)-H(4B)	0.93(4)	C(12)-C(4)-C(5)	120.9(2)
O(1)-N(4)	1.244(3)	C(1)-N(2)-C(12)	117.6(2)
N(4)-O(2)	1.241(3)	C(5)-N(3)-H(4A)	121(2)
C(9)-C(8)	1.368(4)	C(5)-N(3)-H(4B)	119(2)
C(9)-C(10)	1.384(4)	H(4A)-N(3)-H(4B)	120(3)
C(9)-H(7)	0.95	N(3)-C(5)-C(6)	124.4(3)
C(8)-H(6)	0.95	N(3)-C(5)-C(4)	118.0(3)
C(1)-C(2)	1.393(4)	C(6)-C(5)-C(4)	117.5(2)
C(1)-H(1)	0.95	O(2)-N(4)-O(1)	120.0(2)
C(3)-C(2)	1.369(4)	O(2)-N(4)-C(6)	119.4(2)
C(3)-H(3)	0.95	O(1)-N(4)-C(6)	120.5(2)
C(2)-H(2)	0.95	C(8)-C(9)-C(10)	119.3(3)
C(10)-H(8)	0.95	C(8)-C(9)-H(7)	120.4
		C(10)-C(9)-H(7)	120.4
		C(9)-C(8)-C(7)	120.6(3)
		C(9)-C(8)-H(6)	119.7
		C(7)-C(8)-H(6)	119.7
		N(2)-C(1)-C(2)	123.6(3)
		N(2)-C(1)-H(1)	118.2
		C(2)-C(1)-H(1)	118.2
		C(2)-C(3)-C(4)	119.4(2)
		C(2)-C(3)-H(3)	120.3
		C(4)-C(3)-H(3)	120.3
		C(3)-C(2)-C(1)	119.1(3)
		C(3)-C(2)-H(2)	120.5
		C(1)-C(2)-H(2)	120.5
		N(1)-C(10)-C(9)	123.0(3)
		N(1)-C(10)-H(8)	118.5
		C(9)-C(10)-H(8)	118.5

Table 1C: Anisotropic displacement parameters ($Å^2x10^3$) for 5-amino-6-nitro-1,10-phenanthroline (phen(NH_2)(NO_2)). The anisotropic displacement factor exponent takes the form: $-2p^2[h^2a^{*2}U^{11} + ... + 2 h k a^* b^* U^{12}]$.

	U11	U22	U33	U23	U13	U12
N(1)	25(1)	45(1)	45(2)	-1(1)	-6(1)	-1(1)
C(12)	27(1)	28(1)	32(2)	4(1)	-2(1)	0(1)
C(6)	30(1)	32(2)	31(2)	2(1)	2(1)	3(1)
C(7)	31(1)	29(1)	30(2)	4(1)	-3(1)	1(1)
C(11)	24(1)	32(1)	36(2)	6(1)	-5(1)	-2(1)
C(4)	25(1)	30(1)	31(2)	5(1)	-2(1)	-1(1)
N(2)	29(1)	42(1)	36(1)	0(1)	1(1)	2(1)
N(3)	24(1)	59(2)	50(2)	-10(1)	-1(1)	3(1)
C(5)	25(1)	34(1)	35(2)	4(1)	1(1)	-1(1)
O(1)	42(1)	73(2)	54(2)	-9(1)	7(1)	20(1)
N(4)	38(1)	53(2)	35(2)	-3(1)	5(1)	-2(1)
C(9)	40(2)	50(2)	48(2)	-9(2)	-13(1)	-6(1)
C(8)	39(2)	41(2)	42(2)	-5(1)	-5(1)	-1(1)
C(1)	40(2)	45(2)	33(2)	0(1)	4(1)	4(1)
C(3)	29(1)	40(2)	41(2)	1(1)	-5(1)	-2(1)
C(2)	39(2)	42(2)	33(2)	-1(1)	-4(1)	-4(1)
C(10)	27(1)	53(2)	61(2)	-5(2)	-12(1)	-6(1)
O(2)	52(2)	142(3)	42(2)	-29(1)	5(1)	-14(2)

Table 1D: Hydrogen bond distances (Å) and angles (°) of 5-amino-6-nitro-1,10-phenanthroline (phen(NH_2)(NO_2)).

D-H…A	d(D-H)	d(H…A)	d(D…A)	<(DHA)
N3-H4A…N1[c]	0.89(3)	2.34(3)	3.092(4)	143(3)
N3-H4A…N2[c]	0.89(3)	2.55(3)	3.111(4)	122(2)
N3-H4B…O1[a]	0.94(4)	1.89(4)	2.571(4)	127(4)
N3-H4B…N4[a]	0.94(4)	2.51(4)	2.841(4)	101(3)
C3-H3…N1[c]	0.95	2.61	3.438(4)	145
C8-H6…O2[a]	0.95	2.12	2.716(4)	119
C9-H7…O1[b]	0.95	2.46	3.395(4)	167

Symmetry code, transformation used to generate equivalent atoms:

[a] x, y, z; [b] x+1/2, -y+3/2, -z+1; [c] x-1/2, y, -z+1/2

Table 2A: Atomic coordinates ($x10^4$) and equivalent isotropic displacement parameters ($Å^2 x\ 10^3$) for *fac*-$[Re(CO)_3(phen)(H_2O)][NO_3]\cdot 1.5H_2O$ (3). U(eq) is defined as one third of the trace of the orthogonalized U^{ij} tensor.

	x	y	z	U(eq)
Re(1B)	6644(1)	6545(1)	2156(1)	40(1)
Re(1A)	8385(1)	2582(1)	476(1)	39(1)
O(2A)	5322(9)	1414(9)	-661(8)	74(3)
O(1B)	3831(9)	6387(8)	1287(9)	75(4)
C(10A)	12019(11)	2696(11)	2314(10)	43(3)
C(5A)	7736(13)	-1029(10)	214(11)	47(3)
O(2B)	5375(11)	3854(7)	1386(9)	84(4)
O(3A)	9092(11)	2313(8)	-1500(9)	71(3)
N(2A)	10457(8)	3256(7)	1444(7)	36(2)
C(9A)	12289(13)	1792(12)	2437(12)	57(4)
O(4B)	6472(9)	6866(7)	3702(8)	57(3)
C(13A)	11395(12)	4406(11)	1901(10)	52(4)
O(1A)	8693(11)	4996(8)	561(9)	83(4)
N(2B)	7748(9)	8453(7)	2794(8)	38(2)
C(13B)	7272(14)	9217(10)	2727(11)	53(4)
C(7A)	10034(11)	357(10)	1313(10)	40(3)
C(12A)	12658(13)	4734(12)	2610(11)	57(4)
C(2B)	5834(13)	4883(12)	1726(11)	54(4)
C(4B)	9154(14)	6159(13)	3066(11)	58(4)
C(5B)	10488(15)	6480(15)	3617(11)	63(4)
C(6B)	11393(15)	7632(15)	4039(12)	71(4)
N(1A)	8532(9)	1025(8)	561(8)	38(2)
C(4A)	7557(13)	-100(10)	111(11)	49(3)
C(11B)	9420(15)	10874(11)	3685(11)	59(4)
N(1B)	8707(9)	6915(8)	2948(7)	36(2)
O(4A)	7969(10)	2759(8)	1921(8)	69(3)
C(1A)	8505(14)	4076(12)	545(11)	59(4)
C(12B)	8090(14)	10419(10)	3139(11)	52(3)
C(15A)	9742(10)	1257(8)	1173(9)	29(3)
C(11A)	12964(12)	3925(12)	2802(11)	59(4)
C(3A)	8824(13)	2395(10)	-754(11)	45(3)
C(8A)	11357(13)	673(12)	1942(11)	55(4)
C(2A)	6448(13)	1839(11)	-251(11)	54(4)
C(1B)	4868(13)	6431(9)	1644(10)	46(3)
C(15B)	9623(11)	8076(10)	3404(9)	43(3)
C(7B)	11009(12)	8524(13)	3985(10)	53(3)
C(8B)	11858(12)	9706(14)	4403(11)	63(4)
C(9B)	11359(13)	10462(13)	4301(11)	68(4)
C(10B)	9985(13)	10124(10)	3750(10)	50(3)

C(14B)	9128(11)	8915(9)	3326(9)	40(3)
C(14A)	10756(11)	2440(10)	1649(9)	39(3)
C(3B)	6982(12)	6417(9)	899(11)	40(3)
O(3B)	7140(10)	6306(7)	99(8)	60(3)
N(1)	7210(20)	5000	4610(16)	227(6)
O(2)	6240(20)	4599(19)	3842(17)	237(6)
O(1)	7740(20)	4462(16)	4962(16)	222(6)
O(3)	7784(18)	6079(12)	5047(15)	203(7)
O(7)	9428(14)	3579(13)	3773(10)	115(5)
O(9)	4543(14)	8079(18)	7887(18)	196(10)
C(6A)	8953(13)	-829(10)	825(11)	49(3)
O(5)	15010(20)	10140(20)	5942(17)	203(7)
N(2)	15120(20)	9560(20)	6477(19)	227(6)
O(4)	14780(20)	8430(20)	6137(19)	237(6)
O(6)	15660(20)	10080(20)	7439(15)	222(6)
O(8)	4711(14)	7715(16)	4206(15)	162(9)

Table 2B: Bond lengths (Å) and angles (°) for *fac*-[Re(CO)$_3$(phen)(H$_2$O)][NO$_3$]·1.5H$_2$O (3).

Bond	Bond distance	Bond angle	Angle
Re(1B)-C(3B)	1.864(15)	C(3B)-Re(1B)-C(2B)	89.9(6)
Re(1B)-C(2B)	1.906(14)	C(3B)-Re(1B)-C(1B)	91.2(6)
Re(1B)-C(1B)	1.914(13)	C(2B)-Re(1B)-C(1B)	89.5(5)
Re(1B)-N(1B)	2.178(8)	C(3B)-Re(1B)-N(1B)	95.0(4)
Re(1B)-N(2B)	2.180(8)	C(2B)-Re(1B)-N(1B)	97.3(4)
Re(1B)-O(4B)	2.180(10)	C(1B)-Re(1B)-N(1B)	170.8(4)
Re(1A)-C(3A)	1.866(15)	C(3B)-Re(1B)-N(2B)	93.5(4)
Re(1A)-C(1A)	1.926(14)	C(2B)-Re(1B)-N(2B)	173.1(4)
Re(1A)-C(2A)	1.931(12)	C(1B)-Re(1B)-N(2B)	96.4(4)
Re(1A)-O(4A)	2.150(11)	N(1B)-Re(1B)-N(2B)	76.5(3)
Re(1A)-N(2A)	2.166(8)	C(3B)-Re(1B)-O(4B)	173.6(4)
Re(1A)-N(1A)	2.188(9)	C(2B)-Re(1B)-O(4B)	95.0(5)
O(2A)-C(2A)	1.119(13)	C(1B)-Re(1B)-O(4B)	92.9(5)
O(1B)-C(1B)	1.152(14)	N(1B)-Re(1B)-O(4B)	80.3(3)
C(10A)-C(9A)	1.404(18)	N(2B)-Re(1B)-O(4B)	81.2(4)
C(10A)-C(14A)	1.419(15)	C(3A)-Re(1A)-C(1A)	88.3(6)
C(10A)-C(11A)	1.440(16)	C(3A)-Re(1A)-C(2A)	90.5(6)
C(5A)-C(6A)	1.370(17)	C(1A)-Re(1A)-C(2A)	89.8(5)
C(5A)-C(4A)	1.377(16)	C(3A)-Re(1A)-O(4A)	176.5(5)
C(5A)-H(2A)	0.95	C(1A)-Re(1A)-O(4A)	94.2(6)
O(2B)-C(2B)	1.178(14)	C(2A)-Re(1A)-O(4A)	92.0(5)
O(3A)-C(3A)	1.137(15)	C(3A)-Re(1A)-N(2A)	96.6(5)
N(2A)-C(14A)	1.351(14)	C(1A)-Re(1A)-N(2A)	96.3(4)
N(2A)-C(13A)	1.361(14)	C(2A)-Re(1A)-N(2A)	170.8(5)

C(9A)-C(8A)	1.335(17)	O(4A)-Re(1A)-N(2A)	80.7(4)
C(9A)-H(5A)	0.95	C(3A)-Re(1A)-N(1A)	93.6(5)
O(4B)-H(9B)	0.83(2)	C(1A)-Re(1A)-N(1A)	171.9(4)
O(4B)-H(10B)	0.84(2)	C(2A)-Re(1A)-N(1A)	98.0(4)
C(13A)-C(12A)	1.419(17)	O(4A)-Re(1A)-N(1A)	83.6(4)
C(13A)-H(8A)	0.95	N(2A)-Re(1A)-N(1A)	75.7(3)
O(1A)-C(1A)	1.160(15)	C(9A)-C(10A)-C(14A)	120.8(11)
N(2B)-C(13B)	1.337(14)	C(9A)-C(10A)-C(11A)	124.9(11)
N(2B)-C(14B)	1.389(13)	C(14A)-C(10A)-C(11A)	114.3(11)
C(13B)-C(12B)	1.385(15)	C(6A)-C(5A)-C(4A)	119.7(11)
C(13B)-H(8B)	0.95	C(6A)-C(5A)-H(2A)	120.1
C(7A)-C(15A)	1.421(14)	C(4A)-C(5A)-H(2A)	120.1
C(7A)-C(8A)	1.424(15)	C(14A)-N(2A)-C(13A)	119.7(10)
C(7A)-C(6A)	1.441(15)	C(14A)-N(2A)-Re(1A)	114.6(7)
C(12A)-C(11A)	1.339(19)	C(13A)-N(2A)-Re(1A)	125.5(8)
C(12A)-H(7A)	0.95	C(8A)-C(9A)-C(10A)	120.8(12)
C(4B)-N(1B)	1.324(15)	C(8A)-C(9A)-H(5A)	119.6
C(4B)-C(5B)	1.392(17)	C(10A)-C(9A)-H(5A)	119.6
C(4B)-H(1B)	0.95	Re(1B)-O(4B)-H(9B)	104(2)
C(5B)-C(6B)	1.35(2)	Re(1B)-O(4B)-H(10B)	103(2)
C(5B)-H(2B)	0.95	H(9B)-O(4B)-H(10B)	109(3)
C(6B)-C(7B)	1.43(2)	N(2A)-C(13A)-C(12A)	119.4(12)
C(6B)-H(3B)	0.95	N(2A)-C(13A)-H(8A)	120.3
N(1A)-C(15A)	1.348(13)	C(12A)-C(13A)-H(8A)	120.3
N(1A)-C(4A)	1.350(13)	C(13B)-N(2B)-C(14B)	116.9(10)
C(4A)-H(1A)	0.95	C(13B)-N(2B)-Re(1B)	128.4(8)
C(11B)-C(12B)	1.351(18)	C(14B)-N(2B)-Re(1B)	114.7(7)
C(11B)-C(10B)	1.385(18)	N(2B)-C(13B)-C(12B)	123.2(13)
C(11B)-H(6B)	0.95	N(2B)-C(13B)-H(8B)	118.4
N(1B)-C(15B)	1.366(13)	C(12B)-C(13B)-H(8B)	118.4
O(4A)-H(9A)	0.84(2)	C(15A)-C(7A)-C(8A)	118.6(10)
O(4A)-H(10A)	0.84(2)	C(15A)-C(7A)-C(6A)	117.6(10)
C(12B)-H(7B)	0.95	C(8A)-C(7A)-C(6A)	123.7(11)
C(15A)-C(14A)	1.415(14)	C(11A)-C(12A)-C(13A)	121.0(12)
C(11A)-H(6A)	0.95	C(11A)-C(12A)-H(7A)	119.5
C(8A)-H(4A)	0.95	C(13A)-C(12A)-H(7A)	119.5
C(15B)-C(7B)	1.418(14)	O(2B)-C(2B)-Re(1B)	174.1(13)
C(15B)-C(14B)	1.448(16)	N(1B)-C(4B)-C(5B)	124.0(13)
C(7B)-C(8B)	1.371(19)	N(1B)-C(4B)-H(1B)	118
C(8B)-C(9B)	1.36(2)	C(5B)-C(4B)-H(1B)	118
C(8B)-H(4B)	0.95	C(6B)-C(5B)-C(4B)	118.2(13)
C(9B)-C(10B)	1.425(18)	C(6B)-C(5B)-H(2B)	120.9
C(9B)-H(5B)	0.95	C(4B)-C(5B)-H(2B)	120.9
C(10B)-C(14B)	1.400(15)	C(5B)-C(6B)-C(7B)	122.5(13)

C(3B)-O(3B)	1.159(15)	C(5B)-C(6B)-H(3B)	118.8
N(1)-O(2)	1.224(17)	C(7B)-C(6B)-H(3B)	118.8
N(1)-O(3)	1.236(14)	C(15A)-N(1A)-C(4A)	117.9(9)
N(1)-O(1)	1.250(17)	C(15A)-N(1A)-Re(1A)	114.1(6)
O(7)-H(2)	0.85(2)	C(4A)-N(1A)-Re(1A)	127.9(8)
O(7)-H(1)	0.85(2)	N(1A)-C(4A)-C(5A)	124.0(12)
O(9)-H(6)	0.85(2)	N(1A)-C(4A)-H(1A)	118
O(9)-H(5)	0.883(14)	C(5A)-C(4A)-H(1A)	118
C(6A)-H(3A)	0.95	C(12B)-C(11B)-C(10B)	119.2(11)
O(5)-N(2)	1.271(17)	C(12B)-C(11B)-H(6B)	120.4
N(2)-O(6)	1.272(17)	C(10B)-C(11B)-H(6B)	120.4
N(2)-O(4)	1.319(17)	C(4B)-N(1B)-C(15B)	117.1(10)
O(8)-H(3)	0.87(2)	C(4B)-N(1B)-Re(1B)	128.0(9)
O(8)-H(4)	0.84(2)	C(15B)-N(1B)-Re(1B)	114.9(7)
		Re(1A)-O(4A)-H(9A)	105(2)
		Re(1A)-O(4A)-H(10A)	105(2)
		H(9A)-O(4A)-H(10A)	107(3)
		O(1A)-C(1A)-Re(1A)	173.4(13)
		C(11B)-C(12B)-C(13B)	120.1(12)
		C(11B)-C(12B)-H(7B)	120
		C(13B)-C(12B)-H(7B)	120
		N(1A)-C(15A)-C(14A)	117.6(9)
		N(1A)-C(15A)-C(7A)	122.2(9)
		C(14A)-C(15A)-C(7A)	120.1(9)
		C(12A)-C(11A)-C(10A)	121.5(12)
		C(12A)-C(11A)-H(6A)	119.3
		C(10A)-C(11A)-H(6A)	119.3
		O(3A)-C(3A)-Re(1A)	177.9(12)
		C(9A)-C(8A)-C(7A)	121.4(12)
		C(9A)-C(8A)-H(4A)	119.3
		C(7A)-C(8A)-H(4A)	119.3
		O(2A)-C(2A)-Re(1A)	179.1(15)
		O(1B)-C(1B)-Re(1B)	175.4(12)
		N(1B)-C(15B)-C(7B)	124.8(12)
		N(1B)-C(15B)-C(14B)	117.7(9)
		C(7B)-C(15B)-C(14B)	117.5(11)
		C(8B)-C(7B)-C(15B)	120.6(13)
		C(8B)-C(7B)-C(6B)	126.0(12)
		C(15B)-C(7B)-C(6B)	113.4(13)
		C(9B)-C(8B)-C(7B)	120.0(12)
		C(9B)-C(8B)-H(4B)	120
		C(7B)-C(8B)-H(4B)	120
		C(8B)-C(9B)-C(10B)	124.8(12)
		C(8B)-C(9B)-H(5B)	117.6

C(10B)-C(9B)-H(5B)	117.6
C(11B)-C(10B)-C(14B)	119.0(12)
C(11B)-C(10B)-C(9B)	126.1(12)
C(14B)-C(10B)-C(9B)	114.7(13)
N(2B)-C(14B)-C(10B)	121.4(11)
N(2B)-C(14B)-C(15B)	116.2(9)
C(10B)-C(14B)-C(15B)	122.4(11)
N(2A)-C(14A)-C(15A)	117.9(9)
N(2A)-C(14A)-C(10A)	124.1(10)
C(15A)-C(14A)-C(10A)	118.0(10)
O(3B)-C(3B)-Re(1B)	177.3(11)
O(2)-N(1)-O(3)	115.5(16)
O(2)-N(1)-O(1)	128.0(15)
O(3)-N(1)-O(1)	116.3(18)
H(2)-O(7)-H(1)	105(3)
H(6)-O(9)-H(5)	101(3)
C(5A)-C(6A)-C(7A)	118.4(11)
C(5A)-C(6A)-H(3A)	120.8
C(7A)-C(6A)-H(3A)	120.8
O(5)-N(2)-O(6)	120(2)
O(5)-N(2)-O(4)	127(2)
O(6)-N(2)-O(4)	114(2)
H(3)-O(8)-H(4)	105(3)

Table 2C: Anisotropic displacement parameters ($Å^2x10^3$) for *fac*-$[Re(CO)_3(phen)(H_2O)][NO_3]\cdot 1.5H_2O$ (3). The anisotropic displacement factor exponent takes the form: $-2p^2[h^2a^{*2}U^{11} + ... + 2 h k a^* b^* U^{12}]$.

	U^{11}	U^{22}	U^{33}	U^{23}	U^{13}	U^{12}
Re(1B)	32(1)	30(1)	45(1)	10(1)	-3(1)	9(1)
Re(1A)	29(1)	42(1)	40(1)	13(1)	5(1)	14(1)
O(2A)	32(5)	103(8)	72(8)	39(6)	0(5)	17(5)
O(1B)	32(5)	64(6)	111(10)	37(6)	-15(5)	12(4)
C(10A)	27(5)	66(6)	32(8)	20(5)	10(5)	17(5)
C(5A)	49(6)	38(5)	48(8)	20(5)	21(5)	9(5)
O(2B)	88(8)	23(4)	113(10)	18(5)	0(7)	14(5)
O(3A)	77(7)	63(6)	68(9)	25(6)	25(6)	26(5)
N(2A)	17(4)	39(5)	41(7)	12(4)	4(4)	7(4)
C(9A)	37(6)	70(6)	65(10)	25(6)	14(6)	27(5)
O(4B)	52(5)	53(5)	59(7)	19(5)	15(5)	21(4)
C(13A)	40(7)	54(7)	53(10)	12(6)	14(6)	20(6)
O(1A)	83(7)	41(5)	107(10)	16(5)	-10(6)	33(5)
N(2B)	34(5)	27(4)	44(7)	15(4)	9(4)	6(4)
C(13B)	58(8)	40(6)	61(11)	25(6)	24(7)	16(6)

C(7A)	38(5)	50(6)	43(8)	25(5)	17(5)	24(4)
C(12A)	42(7)	59(7)	44(9)	9(6)	5(6)	8(6)
C(2B)	44(7)	70(9)	45(10)	28(7)	6(6)	22(6)
C(4B)	67(7)	79(8)	45(9)	18(7)	20(6)	52(7)
C(5B)	70(8)	110(8)	49(10)	42(8)	29(6)	68(7)
C(6B)	48(7)	124(9)	55(11)	39(8)	17(7)	47(6)
N(1A)	29(5)	44(5)	40(7)	21(4)	9(4)	11(4)
C(4A)	50(7)	47(5)	44(9)	21(5)	8(6)	16(5)
C(11B)	75(7)	39(6)	42(9)	12(6)	20(6)	9(5)
N(1B)	36(5)	54(5)	10(5)	7(4)	0(4)	20(4)
O(4A)	66(3)	73(3)	68(3)	24(2)	22(2)	31(2)
C(1A)	54(8)	53(8)	60(11)	10(7)	6(7)	26(7)
C(12B)	74(7)	40(6)	45(9)	19(6)	24(6)	24(6)
C(15A)	24(5)	30(5)	31(7)	9(4)	12(4)	10(4)
C(11A)	32(6)	74(6)	47(9)	11(6)	5(6)	12(5)
C(3A)	48(7)	49(7)	33(9)	17(6)	16(6)	15(6)
C(8A)	43(6)	75(6)	56(9)	25(6)	9(5)	37(5)
C(2A)	42(7)	54(7)	53(10)	19(7)	-1(6)	17(6)
C(1B)	55(8)	32(6)	41(9)	18(5)	11(6)	9(5)
C(15B)	24(5)	60(7)	30(8)	15(6)	3(5)	9(5)
C(7B)	28(6)	97(7)	29(8)	27(6)	8(5)	23(5)
C(8B)	23(6)	104(8)	31(9)	20(7)	6(5)	3(5)
C(9B)	36(6)	71(8)	44(9)	11(7)	-1(6)	-17(5)
C(10B)	48(6)	48(7)	30(8)	11(6)	9(5)	3(5)
C(14B)	33(6)	39(6)	28(8)	6(5)	5(5)	2(5)
C(14A)	35(6)	48(6)	33(8)	12(5)	8(5)	20(5)
C(3B)	48(7)	36(6)	32(9)	15(6)	9(6)	14(5)
O(3B)	76(7)	44(5)	53(7)	13(5)	-3(5)	32(5)
N(1)	245(13)	243(12)	153(12)	49(10)	41(9)	97(10)
O(2)	250(13)	239(12)	178(12)	60(10)	27(9)	95(11)
O(1)	240(13)	249(12)	134(11)	38(10)	36(9)	101(10)
O(3)	215(15)	320(20)	240(20)	208(17)	136(14)	179(15)
O(7)	99(11)	134(12)	57(9)	10(8)	14(8)	21(8)
O(9)	64(10)	290(20)	280(30)	190(20)	79(12)	57(12)
C(6A)	53(6)	50(6)	60(9)	35(6)	27(5)	23(5)
O(5)	215(15)	320(20)	240(20)	208(17)	136(14)	179(15)
N(2)	245(13)	243(12)	153(12)	49(10)	41(9)	97(10)
O(4)	250(13)	239(12)	178(12)	60(10)	27(9)	95(11)
O(6)	240(13)	249(12)	134(11)	38(10)	36(9)	101(10)
O(8)	46(8)	124(11)	226(19)	-36(15)	12(11)	38(7)

Table 2D: Hydrogen bond distances (Å) and angles (°) obtained in *fac*-[Re(CO)$_3$(phen)(H$_2$O)][NO$_3$]·1.5H$_2$O (3).

D-H…A	d(D-H)	d(H-A)	d(D…A)	<(DHA)
O7-H1…O1[a]	0.85(2)	2.39(8)	3.30(3)	132(9)
O8-H3…O4[b]	0.87(2)	1.94(8)	2.63(3)	135(10)
08-H4…O4B	0.84(2)	1.89(6)	2.680(16)	155(11)
O9-H5…O4[b]	0.883(14)	2.11(3)	2.71(3)	125.2(19)
O9-H6…O4A[c]	0.85(2)	2.32(12)	2.644(17)	103(10)
O9-H5…06[b]	0.883(14)	1.94(2)	2.80(3)	161.6(14)
O4A-H9A…N1A	0.84(2)	2.53(3)	2.890(14)	107(2)
O4B-H9B…O2	0.83(2)	2.20(4)	3.02(3)	167(8)
O4B-H9B…O3	0.83(2)	2.24(5)	2.91(2)	137(7)
O4A-H10A…O9[c]	0.84(2)	1.98(5)	2.644(17)	135(6)
O4B-H10B…O8	0.84(2)	2.00(5)	2.680(16)	138(8)
C11A-H6A…O2[d]	0.95	2.45	3.34(3)	157.5
C12A-H17A…O8[d]	0.95	2.60	3.53(2)	166.3

Symmetry codes, transformations used to generate equivalent atoms:

[a] –x + 2, -y + 1, -z + 1; [b] x– 1, y, z; [c] –x + 1, -y + 1, -z + 1; [d] x + 1, y, z.

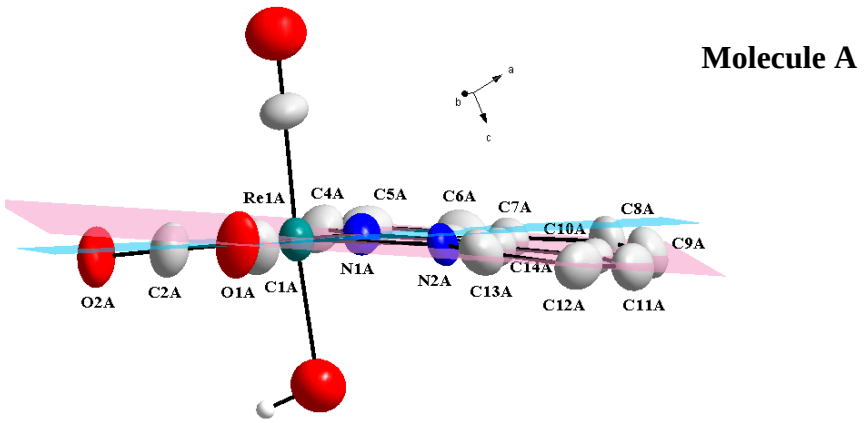

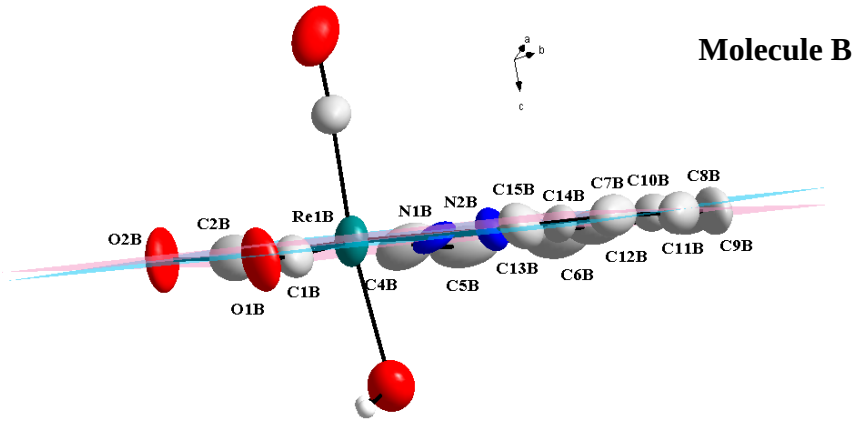

Figure 1A: Illustration of the planes through Re1-N1-N2-C1-C2 (pink plane) and through the 1,10-phenanathroline ligand, C4-C5-C6-C7-C8-C9-C10-C11-C12-C13-C14-C15-N1-N2 (blue plane) for molecule A and B.

Table 3A: Atomic coordinates ($x10^4$) and equivalent isotropic displacement parameters ($Å^2 x\ 10^3$) for *fac*-[$Re(CO)_3$(phen)(Br)] (4). U(eq) is defined as one third of the trace of the orthogonalized U^{ij} tensor.

	x	y	z	U(eq)
Re(1)	1239(1)	3169(1)	3169(1)	25(1)
Br(1)	-570(1)	2030(1)	2032(1)	38(1)
O(1)	-1007(9)	2426(8)	6138(7)	50(2)
O(2)	-989(9)	6143(7)	2418(7)	51(2)
O(3)	3396(9)	4464(7)	4446(6)	42(2)
N(1)	3025(8)	1124(7)	3360(6)	27(2)
N(2)	3007(8)	3361(6)	1120(6)	26(1)
C(1)	-200(10)	2718(8)	5028(8)	31(2)
C(2)	-183(11)	5028(8)	2722(8)	33(2)
C(3)	2631(10)	3949(7)	3957(8)	24(2)
C(4)	2925(10)	-25(8)	4441(8)	30(2)
C(5)	4151(11)	-1277(9)	4473(9)	37(2)
C(6)	5515(11)	-1373(8)	3356(8)	35(2)
C(7)	5638(10)	-206(8)	2167(8)	30(2)
C(8)	6984(11)	-224(9)	913(9)	38(2)
C(9)	6963(11)	923(9)	-217(8)	38(2)
C(10)	5644(9)	2179(8)	-203(8)	26(2)
C(11)	5504(11)	3349(9)	-1361(8)	34(2)
C(12)	4138(11)	4472(9)	-1277(8)	34(2)
C(13)	2925(10)	4445(8)	-21(8)	31(2)
C(14)	4342(9)	2221(8)	1030(7)	24(2)
C(15)	4335(10)	1027(8)	2220(7)	27(2)

Table 3B: Bond distances (Å) and bond angles (°) for *fac*-[$Re(CO)_3$(phen)(Br)] (4).

Bond	Bond distance	Bond angle	Angle
Re(1)-C(3)	1.902(9)	C(3)-Re(1)-C(2)	88.8(4)
Re(1)-C(2)	1.926(7)	C(3)-Re(1)-C(1)	89.0(4)
Re(1)-C(1)	1.934(7)	C(2)-Re(1)-C(1)	91.5(3)
Re(1)-N(2)	2.183(6)	C(3)-Re(1)-N(2)	93.3(3)
Re(1)-N(1)	2.183(6)	C(2)-Re(1)-N(2)	96.2(3)
Re(1)-Br(1)	2.6318(14)	C(1)-Re(1)-N(2)	172.0(3)
O(1)-C(1)	1.141(9)	C(3)-Re(1)-N(1)	92.7(3)
O(2)-C(2)	1.144(9)	C(2)-Re(1)-N(1)	171.9(3)

O(3)-C(3)	1.141(11)	C(1)-Re(1)-N(1)	96.5(3)
N(1)-C(4)	1.340(9)	N(2)-Re(1)-N(1)	75.8(2)
N(1)-C(15)	1.363(9)	C(3)-Re(1)-Br(1)	177.7(2)
N(2)-C(13)	1.336(9)	C(2)-Re(1)-Br(1)	92.9(3)
N(2)-C(14)	1.371(8)	C(1)-Re(1)-Br(1)	92.5(3)
C(4)-C(5)	1.391(10)	N(2)-Re(1)-Br(1)	85.0(2)
C(4)-H(4)	0.95	N(1)-Re(1)-Br(1)	85.3(2)
C(5)-C(6)	1.371(11)	C(4)-N(1)-C(15)	118.1(6)
C(5)-H(5)	0.95	C(4)-N(1)-Re(1)	127.1(5)
C(6)-C(7)	1.415(10)	C(15)-N(1)-Re(1)	114.8(4)
C(6)-H(6)	0.95	C(13)-N(2)-C(14)	117.9(6)
C(7)-C(15)	1.415(9)	C(13)-N(2)-Re(1)	127.5(5)
C(7)-C(8)	1.447(10)	C(14)-N(2)-Re(1)	114.6(4)
C(8)-C(9)	1.364(12)	O(1)-C(1)-Re(1)	178.0(7)
C(8)-H(8)	0.95	O(2)-C(2)-Re(1)	177.8(7)
C(9)-C(10)	1.435(10)	O(3)-C(3)-Re(1)	176.7(6)
C(9)-H(9)	0.95	N(1)-C(4)-C(5)	122.7(7)
C(10)-C(11)	1.399(10)	N(1)-C(4)-H(4)	118.7
C(10)-C(14)	1.416(9)	C(5)-C(4)-H(4)	118.7
C(11)-C(12)	1.373(10)	C(6)-C(5)-C(4)	119.8(7)
C(11)-H(11)	0.95	C(6)-C(5)-H(5)	120.1
C(12)-C(13)	1.390(10)	C(4)-C(5)-H(5)	120.1
C(12)-H(12)	0.95	C(5)-C(6)-C(7)	119.6(6)
C(13)-H(13)	0.95	C(5)-C(6)-H(6)	120.2
C(14)-C(15)	1.428(9)	C(7)-C(6)-H(6)	120.2
		C(6)-C(7)-C(15)	117.0(7)
		C(6)-C(7)-C(8)	123.7(6)
		C(15)-C(7)-C(8)	119.3(6)
		C(9)-C(8)-C(7)	120.1(6)
		C(9)-C(8)-H(8)	120
		C(7)-C(8)-H(8)	120
		C(8)-C(9)-C(10)	121.9(7)
		C(8)-C(9)-H(9)	119.1
		C(10)-C(9)-H(9)	119.1
		C(11)-C(10)-C(14)	117.3(6)
		C(11)-C(10)-C(9)	124.2(7)
		C(14)-C(10)-C(9)	118.5(6)
		C(12)-C(11)-C(10)	120.1(7)
		C(12)-C(11)-H(11)	120
		C(10)-C(11)-H(11)	120
		C(11)-C(12)-C(13)	119.3(7)
		C(11)-C(12)-H(12)	120.4
		C(13)-C(12)-H(12)	120.4
		N(2)-C(13)-C(12)	123.1(6)

N(2)-C(13)-H(13)	118.5
C(12)-C(13)-H(13)	118.5
N(2)-C(14)-C(10)	122.4(6)
N(2)-C(14)-C(15)	117.2(6)
C(10)-C(14)-C(15)	120.4(6)
N(1)-C(15)-C(7)	122.7(6)
N(1)-C(15)-C(14)	117.5(5)
C(7)-C(15)-C(14)	119.8(6)

Table 3C: Anisotropic displacement parameters ($Å^2x10^3$) for *fac*-[$Re(CO)_3$(phen)(Br)] (4). The anisotropic displacement factor exponent takes the form: $-2p^2[h^2a^{*2}U^{11} + ... + 2\,h\,k\,a^*\,b^*\,U^{12}]$.

	U^{11}	U^{22}	U^{33}	U^{23}	U^{13}	U^{12}
Re(1)	24(1)	22(1)	25(1)	-7(1)	-3(1)	3(1)
Br(1)	37(1)	38(1)	40(1)	-10(1)	-12(1)	-6(1)
O(1)	50(4)	57(4)	41(3)	-15(3)	9(3)	-21(3)
O(2)	56(4)	34(3)	58(4)	-13(3)	-21(3)	14(3)
O(3)	38(3)	37(3)	43(3)	0(3)	-5(3)	-6(3)
N(1)	24(3)	26(3)	25(3)	-4(2)	-5(2)	2(3)
N(2)	27(3)	24(3)	27(3)	-7(2)	-7(2)	-3(3)
C(1)	32(4)	29(4)	32(4)	-13(3)	-1(3)	-4(3)
C(2)	33(4)	29(4)	31(4)	-9(3)	-4(3)	3(3)
C(3)	29(3)	12(3)	29(3)	-2(3)	-2(3)	-6(3)
C(4)	33(4)	24(4)	30(3)	-3(3)	-6(3)	-6(3)
C(5)	43(4)	25(4)	42(4)	-3(3)	-18(4)	0(3)
C(6)	36(4)	25(4)	45(4)	-10(3)	-18(3)	6(3)
C(7)	31(4)	24(4)	34(4)	-12(3)	-11(3)	5(3)
C(8)	29(4)	40(5)	45(4)	-22(4)	-11(3)	11(4)
C(9)	37(4)	44(5)	32(4)	-19(3)	2(3)	2(4)
C(10)	20(3)	27(4)	34(3)	-14(3)	0(3)	-10(3)
C(11)	31(4)	39(4)	30(4)	-10(3)	3(3)	-11(3)
C(12)	36(4)	35(4)	29(4)	-1(3)	-6(3)	-13(4)
C(13)	25(3)	29(4)	34(4)	-7(3)	-8(3)	3(3)
C(14)	21(3)	25(4)	28(3)	-9(3)	-7(3)	-5(3)
C(15)	29(4)	22(3)	29(3)	-9(3)	-9(3)	1(3)

Table 3D: Hydrogen coordinates ($x10^4$) and isotropic displacement parameters ($Å^2x\ 10^3$) for *fac*-[$Re(CO)_3$(phen)(Br)] (4).

	x	y	z	U(eq)
H(4)	1978	17	5218	36
H(5)	4045	-2063	5266	44
H(6)	6371	-2217	3380	42
H(8)	7884	-1036	878	45

H(9)	7847	889	-1037	46
H(11)	6354	3366	-2206	41
H(12)	4023	5259	-2068	41
H(13)	1995	5234	27	37

Table 3E: Torsion angles (°) for *fac*-[Re(CO)$_3$(phen)(Br)] (4).

Torsion angle	Angle
C(15)-N(1)-C(4)-C(5)	3.4(13)
Re(1)-N(1)-C(4)-C(5)	-178.9(7)
N(1)-C(4)-C(5)-C(6)	-1.0(14)
C(4)-C(5)-C(6)-C(7)	-1.4(14)
C(5)-C(6)-C(7)-C(15)	1.3(13)
C(5)-C(6)-C(7)-C(8)	-177.4(9)
C(6)-C(7)-C(8)-C(9)	176.8(10)
C(15)-C(7)-C(8)-C(9)	-1.8(14)
C(7)-C(8)-C(9)-C(10)	0.9(15)
C(8)-C(9)-C(10)-C(11)	-176.1(10)
C(8)-C(9)-C(10)-C(14)	0.5(14)
C(14)-C(10)-C(11)-C(12)	-0.4(13)
C(9)-C(10)-C(11)-C(12)	176.3(9)
C(10)-C(11)-C(12)-C(13)	1.4(14)
C(14)-N(2)-C(13)-C(12)	-0.9(13)
Re(1)-N(2)-C(13)-C(12)	179.1(7)
C(11)-C(12)-C(13)-N(2)	-0.8(14)
C(13)-N(2)-C(14)-C(10)	1.9(12)
Re(1)-N(2)-C(14)-C(10)	-178.0(6)
C(13)-N(2)-C(14)-C(15)	-175.3(8)
Re(1)-N(2)-C(14)-C(15)	4.7(9)
C(11)-C(10)-C(14)-N(2)	-1.3(12)
C(9)-C(10)-C(14)-N(2)	-178.1(8)
C(11)-C(10)-C(14)-C(15)	175.9(8)
C(9)-C(10)-C(14)-C(15)	-1.0(12)
C(4)-N(1)-C(15)-C(7)	-3.5(13)
Re(1)-N(1)-C(15)-C(7)	178.5(7)
C(4)-N(1)-C(15)-C(14)	175.1(8)
Re(1)-N(1)-C(15)-C(14)	-2.8(10)
C(6)-C(7)-C(15)-N(1)	1.2(13)
C(8)-C(7)-C(15)-N(1)	179.9(8)
C(6)-C(7)-C(15)-C(14)	-177.4(8)
C(8)-C(7)-C(15)-C(14)	1.3(13)
N(2)-C(14)-C(15)-N(1)	-1.3(12)
C(10)-C(14)-C(15)-N(1)	-178.6(7)
N(2)-C(14)-C(15)-C(7)	177.4(8)
C(10)-C(14)-C(15)-C(7)	0.1(13)

Table 3F: Hydrogen bonding interactions for *fac*-[Re(CO)$_3$(phen)(Br)] (4).

D-H...A	d(D-H)	d(H...A)	d(D...A)	<(DHA)
C(6)-H(6)...O(2)#1	0.95	2.52	3.408(9)	156
C(11)-H(11)...O(1)#2	0.95	2.52	3.414(10)	156.8

Symmetry transformations used to generate equivalent atoms:

#1: x+1,y-1,z

#2 x+1,y,z-1